Identification and Functional Characterisation

of Enzymes in the Glycosylation Pathway

of *Leishmania major*

Dem Fachbereich Chemie
der Universität Hannover
zur Erlangung des Grades

Doktorin der Naturwissenschaften
Dr. rer. nat.

genehmigte Dissertation

von

Dipl.-Biochem. Anne-Christin Lamerz

geboren am 25.12.1974 in Bad Gandersheim

2005

Abstract

The protozoan parasite *Leishmania* of the family Trypanosomatidae is the causative organism of Leishmaniasis. *Leishmania* species are spread in tropical regions and in countries surrounding the Mediterranean Sea. Over 12 million people are infected world wide (WHO). Depending on the *Leishmania* species the disease can range from self-healing cutaneous lesions to mucocutaneous lesions destroying mucocutanous membranes in nose, mouth and throat. In the visceral Leishmaniasis, the parasites invade the spleen, liver and bone marrow and ultimatively cause death. Until today there are no vaccines or effective drugs available that protect or specifically heal Leishmaniasis.

Leishmania are transmitted by the female sand fly of the genus *Phlebotomus* and *Lutzomyia*. Upon the bite of an infected sand fly, the parasites are inoculated into the mammalian host and enter mononuclear phagocytes like macrophages, dendritic- or Langerhanscells. The parasites proliferate within these cells until lyses of the host cells occurs. The released parasites invade new host cells. During the next blood meal, a sand fly takes up the parasites that undergo a specific life cycle within the fly. Afterwards, the *Leishmania* can be again transmitted into the mammalian host.

It is known that various glycoconjugates are essential for parasite virulence: they form a dense cell surface glycocalyx allowing the survival and proliferation of the parasite in the very hostile environments of the sand fly vector and the mammalian host. Among other protective functions, they shield the parasite against complement lyses and prevent the activation of macrophages. The major components of the glycoconjugates are mannose, galactose, glucose and arabinose. Potential drug targets are therefore enzymes that are involved in the synthesis of these glycoconjugates.

The aim of this study was the identification of enzymes essential for the biosynthesis of galactose containing glycoconjugates. A complementation cloning strategy has been used and unexpectedly identified the enzyme UDP-glucose pyrophosphorylase (UGP). UGP catalyses the formation of UDP-glucose from glucose-1-phosphate and UTP. The activation of glucose to the nucleotide sugar is crucial for the entry in biosynthetic pathways and UDP-glucose is required for the synthesis of UDP-galactose. Thus, the isolated enzyme provides a key function in the biosynthesis pathways involving glucose and galactose and should be an optimal target for disturbing glycoconjugate synthesis in *Leishmania*.

The activity of the *L. major* UGP was proven by an *in vivo* complementation assay using UGP negative *E .coli* mutant strains and by an *in vitro* assay system using recombinant protein. In addition, the recombinant UGP was kinetically characterised and its oligmerisation status was determined. Despite the high sequence homology to the mammalian counterparts, these data showed that differences in the regulation of these enzymes

exist.

Crystallisation trials have been carried out and generated well diffracting crystals that are presently used to resolve the 3-dimensional structure. Finally, the role of the UGP in the pathomechanism of *Leishmania* has been investigated by gene deletion. The obtained clone demonstrated drastically reduced virulence in a mouse infection model, indicating the importance of this gene for pathogen development in the host.

Zusammenfassung

Leishmanien sind einzellige Parasiten der Familie der Trypanosomatidae und verursachen die Krankheit Leishmaniose, die besonders in den tropischen Regionen und im Mittelmeerraum verbreitet ist. Laut WHO sind weltweit 12 Millionen Menschen infiziert. Bei einer Infektion entstehen je nach Art der *Leishmanien* Hautgeschwüre und Knoten (Orientbeule), mucokutane Läsionen, die zum Auflösen der Schleimhäute der Nase, Mund und Rachen führen, oder viszerale Leishmaniosen (Kala-Azar), die die Milz, Leber und das Knochenmark befallen und tödlich sind. Bis heute gibt es weder eine spezifische medikamentöse Behandlungsmöglichkeit noch eine Impfung, die vor Leishmaniose schützt.

Leishmanien werden durch die weiblichen Schmetterlingsmücken der Gattung *Phlebotomus* sowie *Lutzomyia* übertragen. Durch den Stich einer infizierten Mücke werden *Leishmanien* auf den Wirt übertragen und von Phagozyten wie z.B. Makrophagen, dendritischen Zellen oder Langerhans-Zellen aufgenommen. Die Parasiten vermehren sich in der Wirtszelle bis zu dessen Lyse. Die freien Parasiten befallen nun erneut Phagozyten. Bei der Blutmahlzeit einer Schmetterlingsmücke werden *Leishmanien* aufgenommen, die nach ihrem Lebenszyklus in der Fliege wieder auf den Wirt übertragen werden.

Um in der feindlichen Umgebung des Vektors und des Wirtes überleben und proliferieren zu können, besitzen *Leishmanien* eine dichte Glykokalyx. Die verschiedenen Komponenten der Glykokalyx schützen den Parasiten z.B. vor der Lyse durch das Komplementsystem und verhindern die Aktivierung der Makrophagen. Die Hauptkomponenten der Glykokonjugate sind Mannose, Galactose, Glucose und Arabinose. Enzyme, die am Aufbau dieser Strukturen beteiligt sind, stellen daher potentielle Angriffsziele bei der Entwicklung von Medikamenten zur Behandlung der Leishmaniose dar.

Ziel dieser Arbeit war es, Enzyme zu identifizieren, die für den Aufbau Galactose-haltiger Glykokonjugate essential wichtig sind. Der Einsatz einer Komplementations-Klonierungsstrategie führte unerwartet zur Identifizierung des Enzyms UDP-Glucose Pyrophosphorylase (UGP). UGP katalysiert die Bildung von UDP-Glucose aus Glucose-1 Phosphat und UTP. Die Aktivierung der Glucose zu dem Zuckernukleotid ist substantiell wichtig für den Eintritt in die biosynthetischen Stoffwechselwege. Außerdem wird UDP-Glucose für die Synthese von UDP-Galactose benötigt. Somit hat das isolierte Enzym eine Schlüsselfunktion für biosynthetische Stoffwechselwege, bei denen Glucose und Galactose eine Rolle spielen und sollte ein optimales *target* für die Störung der Glykokonjugat-Synthese in *Leishmanien* darstellen.

Die Aktivität der *L. major* UGP wurde durch *in vivo* Komplementations-Assays mit einem UGP-negativem *E. coli*-Stamm als auch durch ein *in vitro* Assay-System mit rekombinantem Protein bewiesen. Außerdem wurde die rekombinante UGP kinetisch charakterisiert und der Oligomerisationsstatus bestimmt. Trotz hoher Sequenzhomologie zu den mammalia UGPs zeigten diese Daten, dass Unterschiede in der Regulation der Enzyme bestehen.

Die Kristallisierung der rekombinanten UGP wurde erfolgreich durchgeführt, und gut streuende Kristalle werden momentan zur Auflösung der dreidimensionalen Struktur herangezogen. Zur Evaluation der pathophysiologischen Rolle dieses Enzyms an der Leishmaniose wurden *L. major* Deletionsmutanten hergestellt. Der resultierende Klon zeigte im Mausmodell drastisch verminderte Virulenz, was die wichtige Position dieses Genes für die Entwicklung des Pathogens im Wirt unterstreicht.

1 Introduction

1.1 *Leishmania parasites*

Leishmania are protozoan parasites of the family Trypanosomatidae and are the causative organism of the disease *Leishmaniasis*. There are at least 30 different species of *Leishmania* and about 10 infect humans. Depending on the species, this disease consists of a broad range of symptoms. Ulcerative skin lesions occur in cutaneous *Leishmaniasis* and are caused by the species *L. major*, *L. mexicana*, *L. tropica* and *L. aethiopica*. Whereas the cutaneous *Leishmaniasis* is usually self-healing, the mucocutaneous *Leishmaniasis* is more severe and is caused by the species *L. braziliensis braziliensis* (Descoteaux and Turco, 1999). The parasites lead to the destruction of the nose and mouth by producing a mucosal granuloma. However, the most severe form of *Leishmaniasis* is the visceral *Leishmaniasis* (Kala-azar) that leads to death if untreated. In this form, the species *L. donovanii* disseminates and infects the liver, spleen and bone marrow. At present, there are no specific drugs available to treat *Leishmaniasis* and vaccination strategies show only very limited success. Pentavalent antimonials were used to cure visceral *Leishmaniasis* but many parasites are already resistant to this treatment. Second line drugs like pentamidine and amphotericin B are effective to treat all forms of *Leishmaniasis* if administered in high doses, however these drugs are very cost intensive (Croft and Coombs, 2003). New treatment strategies are urgently needed since over 12 million people are infected worldwide. The disease is spread in over 88 countries on all continents except Australia (World Health Organisation).

Leishmania are intracellular pathogens colonizing phagocytes in the human host. In their life cycle the parasites depend on an intermediate host, the sand fly. Thus the propagation of *Leishmaniasis* is strongly connected to the occurrence of its vector. The life cycle and infection mechanism of the parasite are shown in Figure 1. Female sand flies of the genus *Phlebotomus* and *Lutzomyia* transmit the highly infectious metacyclic promastigote *Leishmania* into the mammalian host. Before entering macrophages and other phagocytes like dendritic- or Langerhans cells by a receptor-mediated process, the parasites must resist the non-specific host defence mechanisms like complement lyses. After uptake in the cells, the parasites are located in a phagosomal compartment that is fused with endocytic organelles to form the parasitophorous vacuole. Inside this vacuole *Leishmania* transform into small, non-motile amastigotes with a short flagellum. They proliferate within the macrophages despite the exposure to hydrolytic enzymes and acidic pH (Alexander *et al.*, 1992) until the macrophages rupture and release the parasites into the environment. Freed parasites infect surrounding macrophages. Upon a blood meal of a sand fly, the amastigote containing macrophages or released amas-

tigotes are ingested. Inside the fly the parasites transform into motile, flagellated promastigotes and attache to the midgut of the vector to avoid excretion. During metacyclogenesis, these procyclic forms develop into the non-dividing infective metacyclic promastigotes (Sacks, 1989). The metacyclic promastigotes detach from the midgut wall and migrate to the foregut and oesophagus. They are suspended in the sand fly's salvia that supports the establishment of the parasite infection in the host most likely by inhibiting oxidative metabolic processes and antigen presentation (Lerner *et al.*, 1991, Theodos *et al.*, 1991). During another blood meal *Leishmania* are transmitted into the mammalian host.
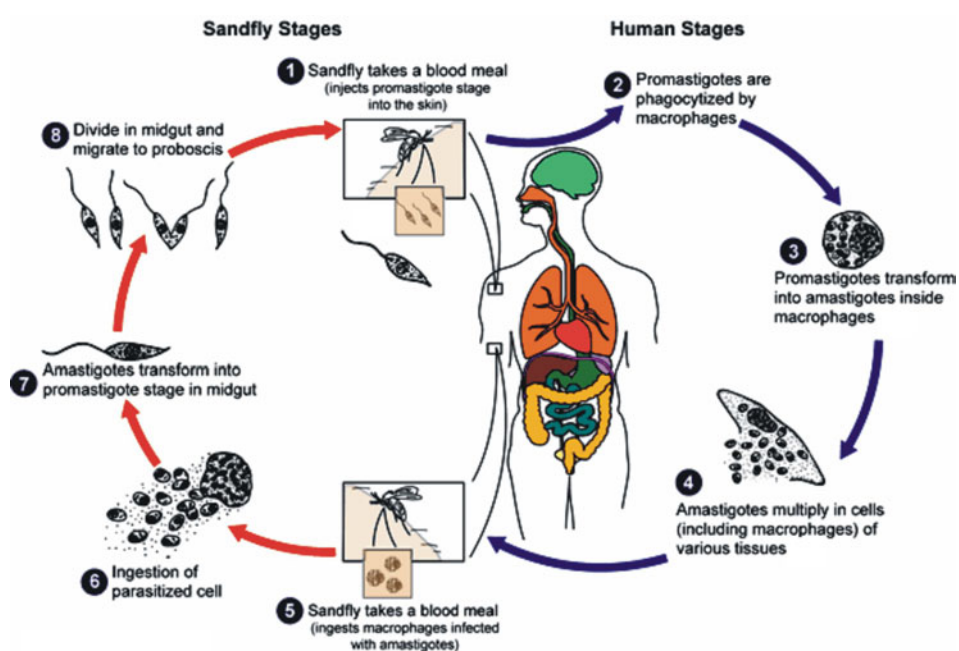
**Figure 1 Life cycle of *Leishmania* *Leishmania* undergo two distinct developmental stages. In the mammalian host they reside within the macrophages as non-motile amastigotes whereas in the sand fly vector the amastigotes transform into the flagellated promastigote form (modified from www.dpd.cdc.gov).

In the two distinct developmental stages, this pathogen survives and proliferates in highly hostile environments. This is thought to be facilitated by surface components of the parasite especially by the glycoconjugates that form a dense cell surface glycocalyx (McConville *et al.*, 2002, Turco *et al.*, 2001). For a comprehensive understanding of the role of the glycoconjugates in the pathogenesis of *Leishmania*, the structure, biosynthesis and function of these molecules is intensively investigated.

1.2 The glycoconjugates of Leishmania

1.2.1 Structure and biosynthesis of *Leishmania* glycoconjugates

The major glycoconjugates on *Leishmania* parasites are the lipophosphoglycan (LPG), the glycosylphosphatidylinsitol (GPI)-anchored proteins, free glycolipids (GIPLs) and the proteophosphoglycans (PPGs). The synthesis of these molecules takes place on both sites of the ER as well as in the lumen of the Golgi apparatus (McConville *et al.*, 2002). Essential for the biosynthesis of glycoconjugates is the metabolic activation of the respective building blocks, the monosaccharides. This is achieved by the formation of nucleotide-sugars, e.g. UDP-galactose, UDP-glucose or GDP-mannose in the cytosol. On the cytoplasmic leaflet of the ER, the nucleotide sugars are transferred by specific transferases either directly on the target structure (see LPG biosynthesis) or on dolichol-phosphate (dolichol-P). The dolichol-P-sugar is flipped through the membrane to serve as sugar donor for transferases in the lumen of the ER. In addition, nucleotide sugar transporters transport the activated nucleotide sugars from the cytosol into the ER or Golgi apparatus where they are used by specific transferases.

As in other eukaryotes, the N-glycan precursors are assembled in the ER on dolichol-P and then transferred *en bloc* to the newly synthesized proteins. However, the parasites do not synthesize the common $Glc_2Man_9GlcNAc_2$ dolichol-PP-linked precursor but a $Man_{6-7}GlcNAc_2$ structure (Glc, glucose; Man, mannose; GlcNAc, *N*-acetylglucosamine). Since no Golgi modification occurs, the proteins bear these biantennary high mannose-type glycans which can be modified with a glucose in α1,3-linkage (Parodi *et al.*, 1993).

LPG is the most abundant glycoconjugate of all promastigote *Leishmania* with a highly conserved backbone structure. It is comprised of a 1-O-alkyl-2-lyso-phosphatidyl-(myo)inositol (PI)-anchore, a glycan core, a repeating galactose-mannose-phosphate (Gal-Man-P) unit with 15 to 30 repeats and a cap structure (Turco *et al.*, 1992, McConville *et al.*, 1993, Figure 2). LPG as well as the type-2 GIPLs (see below) contain two conformers of galactose: the galactopyranose that is common also in higher eukaryotes and the unusual galactofuranose that is not present in humans (see 1.3).

Depending on the species, side chains are attached to the residues of the repeating units. In *L. major*, the C3 hydroxyl group of galactose is glucosylated or galactosylated with one to four galactose residues and often terminated with arabinose. The repeating units of *L. mexicana* are modified with glucose whereas in some *L. donovanii* strains no side chain modifications occur. Differences also occur in the nature of the cap structure, e.g. in *L. major* the cap is comprised of the disaccharide Man(α1,2)Man(α1) and in *L. donovanii* of the trisaccharide Gal(ß1,4)[Man(α1,2) Man(α1)].
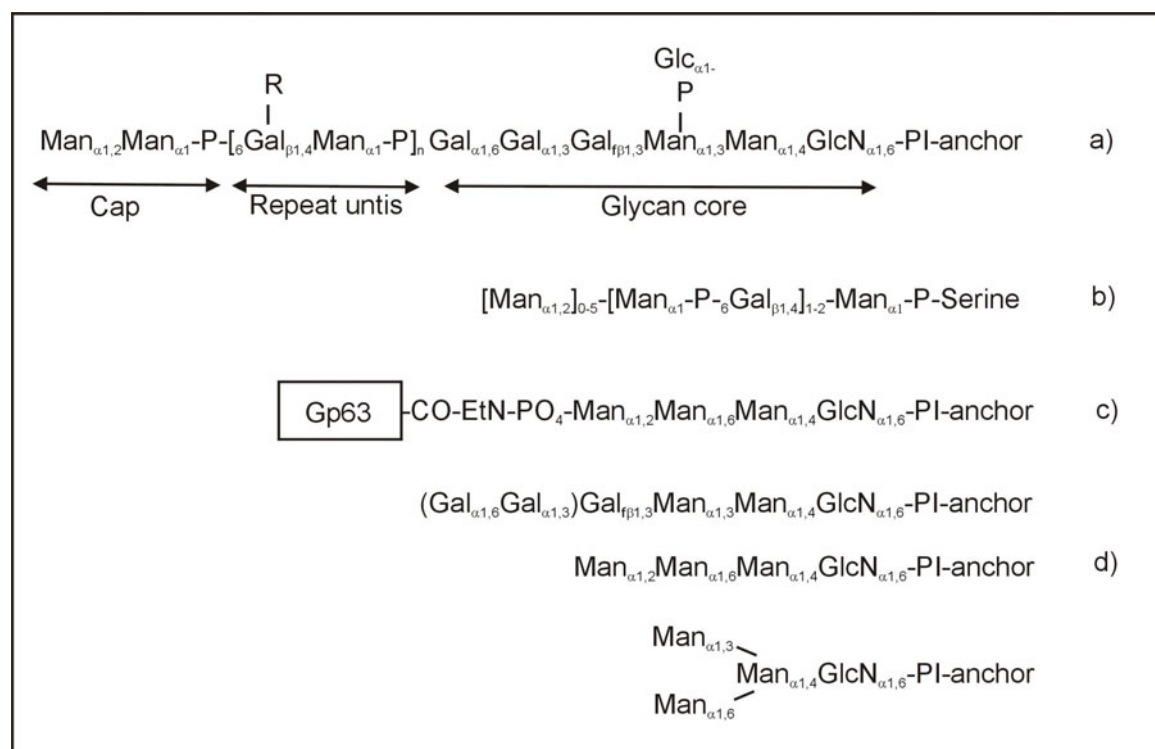
Figure 2 Structure of *Leishmania* surface glycoconjugates: a) *L. major* LPG (R indicates the side chain modifications as mentioned in the text), b) Proteophosphoglycan structures of the secreted acid phosphatase of *L.mexicana* c) the GPI-linked glycoprotein gp63 and d) the three classes of GIPLs, Gal, galactopyranose; Gal_f, galactofuranose; Man, mannose; P, phosphate, PI, phosphatidylinositol, R, side chain modification; Glc, glucose; GlcN, glucosamine; EtN, ethanolamine; n, number of repeating units: 15-30.

The GPI-anchor precursors of LPG are assembled on both sides of the ER by the sequential addition of monosaccharides to a PI-anchor (Ralton *et al.*, 1998). The formation of GlcN(glucosamine) -PI and the addition of the second mannose in α1,3-linkage is thought to occur on the cytoplasmic leaflet of the ER whereas the first mannose is transferred in the lumen of the ER using dolichol-P-mannose as donor substrate (Ilgoutz *et al.*, 1999). All further steps including the addition of galactose, glucose, glucose-1 phosphate, arabinose, mannose and mannose-1 phosphate occur in the Golgi apparatus using the corresponding nucleotide-sugars as donor substrates (Hong *et al.*, 2000, Figure 3).
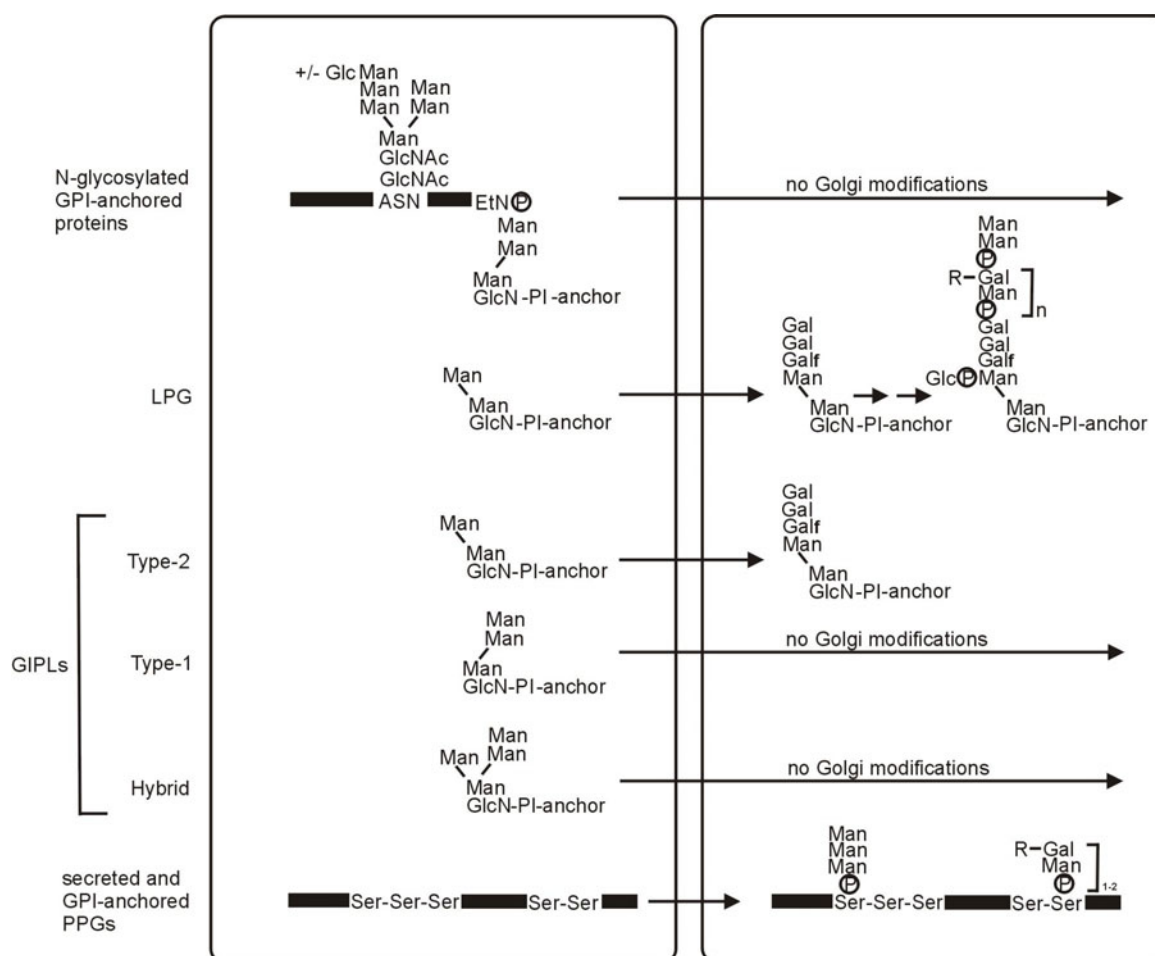
Figure 3 Glycosylation pathway of LPG, PPGs, GIPLs and N-glycosylated GPI-anchored glycoproteins. The N-glycosylated glycoproteins, the type1 and hybrid GIPLs are synthesised in the ER, the PPGs are synthesised in the Golgi while the synthesis of LPG and of type2 GIPLs involves both compartments (modified from McConville *et al.*, 2002).Man, mannose; Gal, galactopyranose; Galf, galactofuranose; P, phosphate, PI, phosphatidylinositol, R, side chain modification; Glc, glucose; GlcN, glucosamine; GlcNAc, N-acetylglucosamine; EtN, ethanolamine; Ser, serine; n, number of repeating units:15-30.

The most abundant type of protein glycosylation is the phosphoglycosylation of a number of cell surface and secreted proteins (Ilg, 2000 (a), Figure 2). This heterogeneous family of proteophosphoglycans (PPGs) has phosphoglycan chains similar to those found in the repeating units of LPG (Jaffe *et al.*, 1990, Bates *et al.*, 1990). The glycan content can rise up to 96% of the mass of the whole molecule (Ilg *et al.,* 1996). As for LPG, the phosphoglycosylation takes place in the Golgi apparatus and is initiated by the transfer of a Manα1−phosphate to serine and threonine residues in serine- and threonine-rich sequences (Moss *et al.*, 1999, Figure 3). It can be elongated with mannose residues or in addition with one or two Gal(ß1,4)Manα1−phosphate repeating units as in the case of the secreted acid phosphatase of *L. mexicana* (Ilg *et al.*, 1994). The length and composition of the phosphoglycan chains vary considerably in different PPGs. In addition, the expression of the PPGs is stage specific and the PPG profile differs from species to species (Ilg

et al., 1994 and 1996). For example, in *L. mexicana* three classes of PPGs are described (Ilg *et al.*, 1999 and 2000 (a)). In the promastigote stage, two forms of the secreted acid phosphatase and a filamentous PPG, which form a gel-like matrix in the midgut of the sand fly, exist whereas in amastigotes only the non-filamentous PPG is secreted. In contrast, *L. major* promastigotes do not express a secreted acid phosphatase and secrete fewer PPGs than *L. mexicana* although some strains contain GPI-anchored PPGs (Ilg *et al.*, 1999).

Beside the GPI anchored PPGs, there are other GPI-linked proteins in *Leishmania*, e.g. the glycoprotein GP63 (Figure 2). GP63 is a metalloproteinase and the major cell surface glycoprotein of promastigotes in all *Leishmania* strains. GP63 is comprised of a C-terminal GPI-linker and three N-linked glycans that are transferred in the ER and not further modified in the Golgi apparatus (McGwire *et al.*, 1996, Ralton *et al.*, 2002; Figure 3). The GPI-anchor synthesis includes the addition of GlcNAc to the PI-anchor with a subsequent de-N-acetylation to form a GlcNα1,6-PI-anchor and the addition of three mannose residues from dolichol-P-mannose and ethanolamine-phosphate in the lumen of the ER. In contrast to LPG, the second mannose residue is added in the lumen of the ER in a α1,6-linkage rather than in a α1,3-linkage (McConville, 2002).

The GIPLs are low molecular weight glycolipids that are synthesized in all developmental stages of the parasite. Three classes of GIPLs can be distinguished that are expressed at different levels in different species and depending on the developmental stage (McConville *et al.*, 1993, Figure 2). The type-1 GIPLs contain the same glycan structure as the protein anchors (Manα1,6Manα1,4GlcNα1,6-PI) whereas the type-2 GIPLs are analogous to the LPG-glycan anchor including one galactofuranose (Gal$_f$) and up to two galactopyranose residues ((Galα1,6Galα1,3)Gal$_f\alpha$1,3Manα1,3Manα1,4GlcNα1,6-PI). The hybrid GIPLs contain features of both the protein and the LPG anchor (Manα1,6(Manα1,3)Manα1,4GlcNα1,6-PI) (Guha-Niyogi *et al.*, 2001). The type-1 and hybrid GIPLs are assembled in the ER whereas the galactose residues of the type-2 GIPLs are added in the Golgi apparatus like for LPG (Figure 3). However, the GIPLs are clearly metabolic end products and contain lipid moieties and side chain modifications distinct from those added to proteins (McConville *et al.*, 1991 and 1993).

1.2.2 Implication of the *L. major* surface glycoconjugates on the survival and proliferation in the vector and host

The cell surface expression of the glycoconjugates in *Leishmania* is highly dynamic and dependent on the developmental stage of the parasite. The promastigotes are coated with a 20-40 nm thick glycocalyx that is mainly comprised of LPG, GPI-anchored proteins, PPGs and GIPLs (Pimenta *et al.*, 1991, McConville *et al.*, 2002). These glycoconjugates are suggested to play important roles on the survival of the parasite within the sand fly and during the initial steps of macrophage infection (Naderer *et al.*, 2004). However, the amastigotes down regulate the expression of LPG and GPI-anchored proteins and are coated with a layer of GIPLs and host derived glycosphingolipids. The almost complete absence of immunogenic proteins and carbohydrates provides an effective mechanism to survive in the parasitophorous vacuole of the macrophages.

Potential roles of LPG, GPI-anchored proteins, GIPLs, and of PPGs on *Leishmania* infectivity are discussed in the following.

1.2.2.1   The role of LPG

LPG has been described to play an important role in the survival of the parasite in the sand fly and in the initial phase of macrophage infection in some *Leishmania* species (e.g. *L. major*) (Guha-Niyogi *et al.*, 2001).

LPG facilitates the ability of *Leishmania* promastigotes to attach and detach from the midgut of the sand fly. It also protects the parasite against digestive enzymes (McConville *et al.*, 1992). In the natural vector of *L. major*, *Phlebotomine papatasi*, a ß-galactose binding lectin recognizes the terminal ß-galactose of the LPG side chain whereas in *L. donovanii* the terminal galactose and mannose residue of the cap structure are required for binding and thus avoid excretion with the digested blood meal (Pimenta *et al.*, 1992, Sacks *et al.*, 1995). The species-specific differences in the modification of the side chains of the repeating unit and the cap structure may account for the insect host specificity of the *Leishmania* species (Pimenta *et al.*, 1994). During metacyclogenesis of the procyclic promastigotes into the infective metacyclic promastigotes, LPG undergoes some structural changes, which promote the detachment from the midgut. The number of the repeating units doubles from 15 to 30 (Sack *et al.* 1995) and in *L. major* doubling of the repeating units is accompanied by the reduction of galactose containing side chains and addition of a terminal arabinose (McConville, 1992, Pimenta, 1992). These alterations are believed to mask the sugars that are involved in the midgut attachment in metacyclic promastigotes and allow the migration to the mouth part of the sand fly.

In addition, the elongation of LPG has been implicated in the prevention of complement lyses of the pathogens in the blood stream of the mammalian host. Metacyclic but not procyclic promastigotes shed the C5b-C9 complex from the parasite surface without insertion into the plasma membrane (Puentes *et al.*, 1990). However, deposition of C3b and C3bi on the cell surface of *Leishmania* by LPG and gp63 allows the entry into the macrophages via receptors-mediated endocytosis (Mosser *et al.*, 1993).

Inside the macrophage, LPG is believed to modulate signal transduction pathways, e.g. by inhibiting the protein kinase C and to delay the fusion of the endosomal compartments with the phagosome (Turco *et al.*, 1992, Desjardins *et al.*, 1997). By the latter event the time window for the differentiation of the promastigote to the amastigote form, which resists the exposure to hydrolytic conditions and acidic pH, may be extended (Naderer *et al.*, 2004). However, a direct influence of the delayed fusion on parasite survival could not be confirmed in experiments carried out with *L. mexicana*. Moreover, a *L. major* mutant lacking LPG showed conversion to the amastigote stage in *in vitro* experiments. The specific lack of LPG in this mutant was achieved by the deletion of the galactofuranosyltransferase (LPG1) gene. The product of this gene is a glycosyltransferase that adds the galactofuranose residue to the LPG precursor (Späth *et al.*, 2000). Interestingly, in *in vitro* studies the *L. major* LPG1 mutant was still able to attach and invade the macrophages but proliferation within the cells was reduced (Späth *et al.*, 2003). In addition, the mutant showed a delayed lesion formation in mice infection tests confirming an important role of LPG in establishing the infection (Späth *et al.*, 2000). However, these data also indicate that invasiveness involves factors beyond the LPG. Potential candidates that may compensate for the LPG functions are other glycoconjugates that remain in the mutant parasite.

In contrast to *L. major*, no structural rearrangements of LPG occur during meta-cyclogenesis of *L. mexicana* promastigotes though the LPG expression is down regulated in the metacyclic promastigotes (Ralton *et al.*, 2003). Consistent with this finding is that *L. mexicana* LPG does not seem to be required for the infection of macrophages (Ilg, 2000 (b)). This indicates that despite the overall similarity of the glycoconjugates, variations in the composition of the glycoconjugates in the different *Leishmania* species may result in variant infection mechanisms.

1.2.2.2   The role of PPG

As mentioned above, filamentous PPGs are secreted by all *Leishmania* promastigotes and form gel-like matrices embedding the parasites (Ilg *et al.*, 1996). It has been suggested that this matrix supports the correct positioning of the parasite in the anterior part of the sand fly's midgut. Evidence that PPGs also protect the parasite from lyses by the

complement system and/or proteases that are present in the midgut, is based on a *L. donovanii* mutant lacking the GDP-mannose transporter gene (LPG2, Descoteaux *et al.*, 1995). Due to this deletion, the synthesis of the mannose containing LPG and PPGs in the Golgi apparatus is inhibited. The LPG2 mutant was rapidly killed in the sand fly midgut whereas the mutant lacking only LPG (LPG1 mutant, Sacks *et al.*, 2000) survived the initial period of the infection. In addition, the deletion of the GDP-mannose transporter in *L. major* showed an almost complete loss of virulence in macrophage- and mice infection assays (Späth *et al.*, 2003). Though the *L.major* LPG1 mutant showed reduced infectivity, the more severe phenotype of the LGP2 mutant suggests that PPGs play a crucial function in establishing the infection in the mammalian host.

PPGs are believed to protect the amastigotes from complement lysis and participate in the formation of the parasitophorous vacuole (Späth *et al.*, 2003). In addition, PPGs may contribute to the attachment and invasion of the parasite into macrophages and may modulate signal transduction pathways in the early stages of the infection (Guha-Niyogi *et al.*, 2001).

However, as in the case of the LPG1 mutant, deletion of the GDP-mannose transporter in *L. mexicana* did not result in the loss of virulence, indicating that neither LPG nor PPGs are essential for the infection mechanism of this strain (Ilg *et al.*, 2001). These findings illustrate that different *Leishmania* species have developed different mechanisms to infect the mammalian host.

1.2.2.3 The role of GP63

GP63 is synthesized as a GPI-linked protein with about 500 000 copies per cell in pro-mastigotes. In the amastigote stage, the membrane bound form is down-regulated whereas the expression of secreted forms is up-regulated (Medina-Acosta *et al.*, 1989). This protease is thought to degrade host macromolecules and to prevent the parasite against complement lyses. It may also facilitate the uptake of the parasite into the host cells via complement components by macrophage receptors (Alexander and Russel, 1992). The generation of GP63 deletion mutants is difficult since GP63 is encoded in a multi-gene family. Mutants partly depleted in GP63 have been obtained, but raised contradicting results. Further investigations are necessary to understand the role of this glycoprotein.

1.2.2.4 The role of GIPLs

In the *Leishmania* amastigotes the levels of both LPG and GP63 are significantly down-regulated and thus the GIPLs are the major glycoconjugates in this developmental stage

(Naderer *et al.*, 2004). Despite their potential importance in the amastigote stage, little is known about the function of these compounds. It has been suggested that the GIPLs protect the amastigote outside and inside the macrophage, e.g. by modulating signalling events (McNeely *et al.* 1989, Proudfoot *et al.* 1995, Tachado *et al.* 1997).

An *L. major* mutant lacking GIPLs and LPG was generated by the targeted gene deletion of the alkyldihydroxyacetonephosphate synthase (ADS1, Zufferey *et al.*, 2003). This enzyme catalyses the first step in the ether phospholipid synthesis, which is a shared structural motif of all GPI-anchored glycoconjugates. Unexpectedly, this deletion did not influence the synthesis of GPI-anchored proteins, like GP63.

Though this mutant showed to be less virulent than the wild type parasites, overall the phenotype resembled that of the *L. major* LPG1 mutant, suggesting that either the GIPLs are not important for infectivity in *L. major* or that other factors compensate for this defect. The latter hypothesis is supported by the finding that the mutants express a novel, unidentified lipid moiety (Zufferey *et al.*, 2003).

In summary, the glycoconjugates presented here seem to influence the infection mechanism in a complex way, but it is difficulty to assign distinct roles to a particular glycoconjugates. Experiments carried out with gene targeted parasites clearly indicate that a certain level of redundancy exist in these systems.

The identification of a more central structure in the *Leishmania* glycosylation pathways and its use as a target to interfere in a broad manner with glycoconjugate biosynthesis is therefore an important goal for the design of new efficient drugs to combat *Leishmaniasis*.

1.3 The role of galactose containing conjugates in L. major

The glycoconjugates of *Leishmania* contain high levels of galactose. In Trypanosomatidae*,* galactose is found as galactopyranose as well as in the unusual conformation galactofuranose (Gal_f). The conversion of UDP-galactopyranose to UDP-galactofuranose is catalysed by the UDP-galactopyranose mutase (Figure 4).

UDP-Gal*p*
(92-95%)
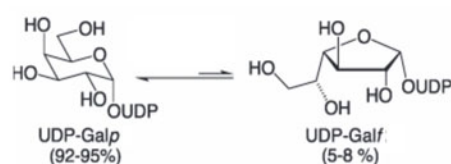
UDP-Gal*f*
(5-8 %)

Figure 4 Conversion of UDP-galactopyranose to UDP-galactofuranose is catalysed by the UDP-galactopyranose mutase.

Galactofuranose is widely found in pathogens such as *Trypanosoma, Aspergillus* or *Mycobacteria* but is absent in the human host. In *Mycobacteria*, it has been shown that Gal$_f$ is essential for growth and viability, but in *Leishmania*, its function is still unclear (Pan *et al.*, 2001). As described above, the gene deletion of a galactofuranosyltransferase (LPG1) in *L. major* resulted in a reduction of virulence in both macrophage and mouse infection models. However, this mutant continued to produce Gal$_f$ containing type-2 GIPLs, which is the primarily synthesized class of GIPLs in *L. major* (Zhang *et al.*, 2004). The GIPLs are the major glycoconjugates of the amastigote cell surface suggesting that these play critical roles in amastigote survival and virulence (Naderer *et al.*, 2004). Though the ADS1 mutant, which lacks LPG and GIPLs, shows the same phenotype than the LPG1 mutant, a potential role of the GIPLs in infectivity cannot be excluded due to compensatory effects (see above). In addition, the cloning and gene deletion of three LPG1 homologous did not reveal mutants devoid of Gal$_f$ containing GIPLs (Zhang *et al.*, 2004) and indicated the existence of further galactosyltransferases. The LPG1 and LPG2 gene deletion mutants of *L. major* and *L. donovanii* suggest that LPG and PPG are important compounds for the survival of the parasite in the midgut of the sand fly and in the initial steps of macrophage infection. However, viable parasites of the *L. major* LPG2 gene deletion mutant were isolated from the site of injection in mice months after infection although the mutant had lost the ability to infect macrophages and form lesions in mice infection models.

Thus, the investigation of unique and singular factors that affect the biosynthesis of LPG, PPGs and type-2 GIPLs instead of targeting numerous genes of protein families, like the galactosyltransferases, is a promising task. Potential candidates are enzymes involved in the biosynthesis of UDP-galactose, e.g. the UDP-glucose pyrophosphorylase or in the transport of the activated sugar, the UDP-galactose transporter (see below).

1.4 Enzymes involved in the galactose metabolism

1.4.1 UDP-glucose pyrophosphorylase

The UDP-glucose pyrophosphorylase (UGP) catalyses the reversible reaction of glucose-1 phosphate and UTP to UDP-glucose and pyrophosphate (Figure 5). The enzyme represents a key position in carbohydrate synthesis and metabolism.
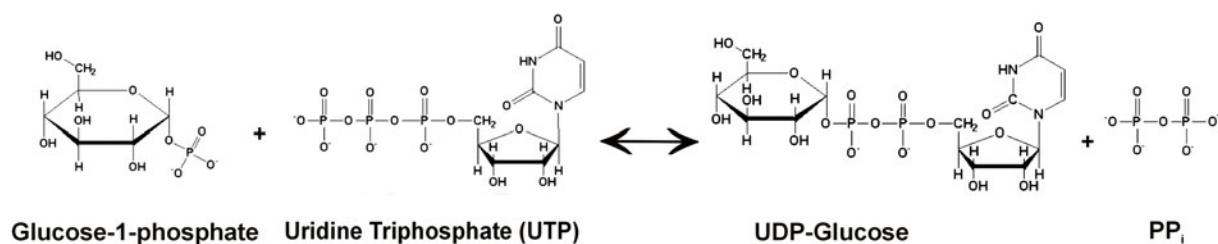
Figure 5 Reaction catalyzed by the UDP-glucose pyrophosphorylase.

In mammals, UDP-glucose is the direct precursor for glycogen and UDP-glucuronic acid and is involved in glycosylation reactions. Furthermore, UDP-glucose is required for the formation of UDP-galactose and the entry of galactose into glycolysis in organisms that utilize the Leloir pathway. In a reaction catalysed by the galactose-1 phosphate uridyl-transferase, UDP-galactose and glucose-1 phosphate are formed from galactose-1 phosphate and UDP-glucose (Figure 6 a). Glucose-1 phosphate can be directly metabolised in glycolysis. UDP-galactose can be recycled to UDP-glucose by the UDP-galactose 4-epimerase or can be used in glycosylation reactions (fig. 6 b).

In addition, UDP-galactose can be directly formed from UDP-glucose since the UDP-galactose 4-epimerase catalyses a reversible reaction.
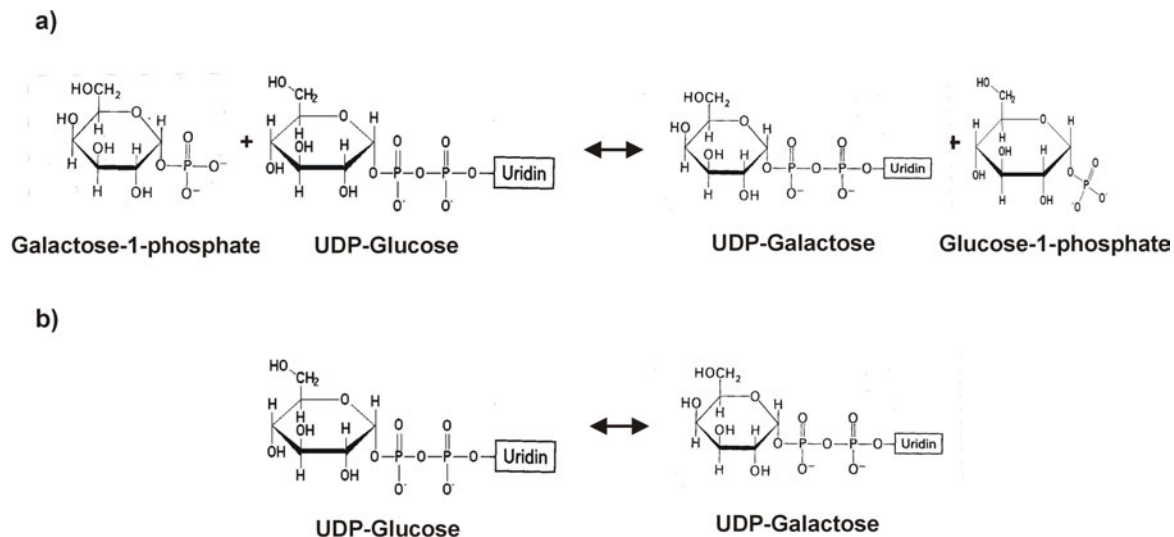
Figure 6 Reactions catalyzed by the galactose-1 phosphate uridyltransferase (a) and the UDP-galactose 4-epimerase (b).

The UGP is ubiquitously expressed in plant and animal tissue as well as in yeast and bacteria. In several gram negative bacteria the UGP is required for the synthesis of the capsular polysaccharide, which is a major virulence factor in these organisms (Geneveaux *et al.*, 1999). In *Klebsiella pneumonia*, deletion of the *galU* gene that encodes the UGP results in the loss of virulence, and in *Streptococcus pneumonia* unencapsulated

bacteria are obtained (Chang *et al.*, 1996, Mollerach *et al.*, 1998). Since, the prokaryotic UGPs show no significant sequence homology to their eukaryotic counterpart, the UGP might be a suitable target for antibacterial drugs (Konishi *et al.*, 1993, Daran *et al.*, 1995, Eimert *et al.*, 1996). In this regard, Kim *et al.* (2004) reported the crystallization and preliminary X-ray study of the UGP from *Helicobactor pylori*. The identification of the active site and catalytic mechanism might help to design specific inhibitors.

Though the sequence homology of the eukaryotic and prokaryotic UGPs is very low, the enzymatic properties seem to be very similar and allow the isolation of UGPs by functional complementation cloning in *E.coli galU* mutants (Peng *et al.*, 1993). Due to a defect in the UGP, the *E.coli galU* mutant has lost its ability to ferment galactose, which can be restored upon the expression of a functional UGP (Sundararajan *et al.,* 1962).

As observed in the family of prokaryotic UGPs, eukaryotic UGPs were found to share a high sequence homology. Enzymes isolated from plants exhibit more than 80 % sequence identity. Between mammalian enzymes the identity was found to range between 92-95 %, whereas the conservation between non-mammalian and mammalian enzymes ranges between 33-57 %. Despite the high homology, residues involved in the catalytic activity are difficult to predict. Site directed affinity labelling and site-directed mutagenesis have revealed the importance of specific lysines in the potato tuber and bovine liver UGP (Katsube *et al.*, 1991, Kazuta *et al.*, 1991 a,b, Konishi *et al.*, 1993). Remarkably, not all the identified essential lysine residues are conserved. On the other hand, Chang *et al.* (1996) analysed a series of conserved amino acids in the human liver UGP, but none could be shown to play a major functional role. Thus, the determination of the three-dimensional structure seems to be the most definitive way to identify residues important for the catalytic activity. Furthermore, the oligomerisation status differs between eukaryotic UGPs. The animal UGPs were reported to occur as octamers (Levine *et al.*, 1969) whereas the plant UGPs were found to be monomers or dimers (Nakano *et al.,* 1989, Sowokinos *et al.*, 1993). Here, oligomeres have been reported to provide a form to sequestrate the active monomer (Martz *et al.*, 2002).

Plant and mammalian UGPs are very specific for their substrates UDP-glucose or glucose-1 phosphate (Turnquist *et al.*, 1974, Kleczkowski, 1994). However, UGPs isolated from human, calf or rabbit liver, from human muscle or yeast were found to exhibit a low affinity also for galactose-1 phosphate (Turnquist *et al.*, 1974, Lai *et al.*, 2000). Thus, despite the high sequence homology, the eukaryotic enzymes seem to differ with respect to their biochemical properties.

1.4.2 The UDP-galactose transporter

The UDP-galactose transporter has been cloned from a number of species (Ishida *et al.*, 1996, Miura *et al.*, 1996, Oelmann *et al.*, 2001, Bakker *et al.*, 2004) and shown to belong to the family of structurally related transmembrane proteins, the so-called nucleotide sugar transporter family. In eukaryotes, nucleotide sugar transporters (NSTs) transport the nucleotide sugars from the cytosol into the lumen of the ER or Golgi apparatus, where the nucleotide sugars are substrates for specific glycosyltransferases.

NSTs are type III membrane proteins with six to ten transmembrane domains (TMDs) as predicted by hydropathy analysis. The study of the transmembrane topology of the murine CMP-sialic acid transporter revealed 10 TMDs with the N-and C-terminus facing the cytosol (Eckhardt *et al.*, 1999). The cytosolic location of the N- and C-terminus was also shown for other nucleotide sugar transporters suggesting an even number of TMDs (Ishida *et al.* 1999, Aoki *et al.,* 1999, Gao *et al.,* 2000). NSTs function as antiporters in an ATP- and ion independent manner (Capasso and Hirschberg, 1984). NSTs exchange the nucleotide sugar with the corresponding nucleoside monophosphate, generated in the organelle lumen by the sequential action of the glycosyltransferases and nucleoside diphosphatases. Over many years, NSTs were regarded as mono-specific transport proteins (Bernisone and Hirschberg, 2000), recent findings however, identified the existence of multi-substrate transporters in human (Muraoka *et al.*, 2001, Segawa *et al.*, 2002), *C. elegans* (Berninsone *et al.*, 2001), *Drosophila* (Goto *et al.*, 2002, Selva *et al.*, 2002) and *Leishmania* (Hong *et al.*, 2000). Still, the substrate specificity with respect to the base of the nucleotide sugar is high and so far, no transporter is known which cross-transports nucleotide sugars containing different bases.

The first genes encoding nucleotide sugar transporters were identified by complementation cloning in cell lines that had a defect in the corresponding nucleotide sugar transporter. Examples are the yeast UDP-*N*-acetylglucosamine transporter (Abeijon *et al.*, 1996), the murine and hamster CMP-sialic acid transporter (Eckhardt *et al.*, 1996 and 1997), and the human UDP-galactose transporter (Miura *et al.*, 1996, Ishida *et al.*, 1996). Later, nucleotide sugar transporters were cloned based on the primary sequence and architectural conservation of these proteins (Oelmann *et al.*, 2001). Today, virtually all putative NSTs have been identified in the existing databases. Their transport specificity cannot be predicted, since primary sequence identities can be high within a species - even for functionally different NSTs - and low for transporters recognising identical substrates but originating from different species (Bakker *et al.*, 2004). Since the functionality of these proteins is highly conserved, the complementation approaches described

above provide an ideal basis for the identification and characterisation of NSTs, also in heterologeous systems (Berninsone and Hirschberg, 2001; Bakker *et al.*, 2004).

1.5 Glycosylation deficient CHO cells

Glycosylation deficient cells were generated to study the pathways of glycoprotein and glycolipid biosynthesis in mammalian cells and to investigate structure-function-relationships of carbohydrates expressed on the cell surface. Most glycosylation deficient cell lines originate from Chinese Hamster Ovary (CHO) cells. CHO cells are functionally haploid, meaning that one allele is inactivated by methylation (Holliday *et al.*,1990). The presence of only one functional allele explains the frequent occurrence of defects in these cells. A large number of CHO cell mutants were obtained by selection with plant lectins (Stanley and Siminovitch, 1977). Lectins are carbohydrate-binding proteins and many exert a cytotoxic effect. Thus, the selection with lectins results in lectin resistant mutants (Lec[R]) that express altered carbohydrate structures on their surface (Stanley, 1984). However, selection with lectins does not guarantee that mutants exhibiting identical phenotypes also exhibit identical genotypes, since the observed phenotype can be due to alterations in a number of enzymes involved in a specific biosynthetic pathway. One example is the selection with the sialic acid binding lectin wheat germ agglutinin (WGA). In mammals, complex N-glycan structures are terminated with sialic acid (Figure 7). Defects in the sialylation machinery lead to an asialo-phenotype with surface glyco-conjugates terminating in penultimate galactose. Asialo-cells are resistant to WGA but develop a high sensitivity against lectins recognising galactose. Many CHO cells with asialo-phenotype have been selected. Based on the underlying gene defect these cell lines could be classified into different complementation groups (Stanley, 1984). For example, CHO cells of the complementation group Lec32 exhibit a defect in the CMP-*N*-acetylneuraminic acid synthetase (CMP-sialic acid synthetase), a nuclear resident enzyme responsible for the activation of sialic acid to CMP-sialic acid (Figure 7). The activation of the monosaccharide is essential for the entry in the glycosylation pathway because only the activated sugar can be transported by the CMP-sialic acid transporter into the Golgi apparatus and used by the Golgi localised sialyltransferases to be incorporated into glycoconjugates (Figure 7, Münster *et al.*, 1998).
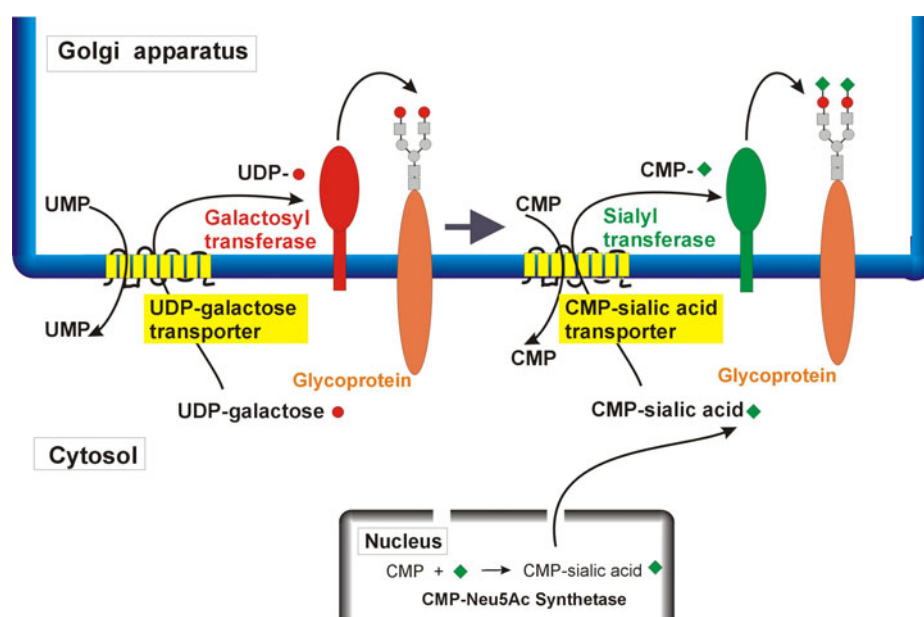
Fig.7 Scheme of the galactosylation and sialylation in the Golgi apparatus.

However, CHO cells of the complementation group Lec2 express the asialo-phenotype because of a defect in the gene encoding the CMP-sialic acid transporter.

Another example is the CHO cell line of the complementation group Lec8. Due to the lack of a functional UDP-galactose transporter these cells exhibit an agalacto-asialo-phenotype (Deutscher *et al.*, 1996). The missing UDP-galactose transport from the cytosol into the Golgi apparatus confers increased stability towards the cytotoxic and galactose binding Ricinus communis agglutinin.

Up to now, over 40 Lec-variants were identified. The glycosylation mutants provide a valuable tool to identify enzymes of the biosynthesis pathway by complementation cloning. Using this technique our laboratory could isolate a number of enzymes involved in the biosynthesis of glycoconjugates like the murine and hamster CMP-sialic acid transporter (Eckhardt *et al.*,1996 and 1997), the murine CMP-*N*-acetylneuraminic acid synthetase (Münster *et al.*, 1998) and as mentioned above, two UDP-galactose trans-porter from *Arabidopsis thaliana* (Bakker *et al.*, 2004).

1.6 Aim of this study

A common theme in drug developmental strategies is the identification of target struc-tures that are unique for the pathogen and thus enable highly selective therapeutic approaches. The identification of such specific targets provides a particular challenge in eukaryotic pathogens that share many biosynthetic pathways with the host. However, for many years it is known that a large degree of variation is found in components that form

the glycocalyx in host and pathogen and the growing knowledge on the underlying biosynthetic pathways has developed new target structures for the therapeutic attack.

The surface compounds LPG, PPG and GIPLs of *L. major* are important structures in establishing the infectivity in the sand fly vector and the mammalian host. A major component of these glycoconjugates is galactose, which in the pathogen is present in two conformers, galactopyranose and galactofuranose. In the animal kingdom galactofuranose is unkown, while the sugar is believed to be essential for the integrity and virulence of various pathogens. In *Mycobacteria* the interference with galactofuranose formation has been demonstrated to be lethal. This finding has stimulated studies aimed at defining the importance of the sugar also in other pathogens.

In the light of this situation, the aim of this study was to identify factors involved in the biosynthesis of galactose containing glycoconjugates in *L. major*. Based on our knowledge in the field of complementation cloning, it was my goal to identify UDP-galactose transporters from *L. major* and to resolve the question, whether the activated forms of the two galactose conformers (UDP-galactofuranose and UDP-galactopyranose) are transported by different proteins. Surprisingly, this strategy of complementation cloning led to the identification of the UDP-glucose pyrophosphorylase from *L. major*, an enzyme even upstream of the UDP-galactose transporter, that represents a key structure in the galactosylation pathway. The identified protein was further analysed with respect to (i) enzymatic characteristics, (ii) structural and kinetic characteristics, and (iii) physiological relevance. As will be demonstrated in this study, the UDP-glucose pyrophosphorylase provides a highly interesting target for therapeutic approaches, since inactivation of the gene in *L. major* significantly reduced the virulence of the pathogen.

2 Material and Methods

2.1 Materials

2.1.1   Eukaryotic cell lines

CHO K1 (C6)   : Chinese hamster ovary cell line, subclone of the fibroblast line
                                CHO K1 (ATCC CRL 9618) produced by Dr. M. Eckhardt

CHOP8   : Chinese hamster ovary cell line Lec 8 defective in the UDP-
                                galactose transporter gene and stable transformed with the
                                polyoma virus large T-antigen (Cummings *et al*., 1993)

CHO Lec8   : Chinese hamster ovary cell line Lec8 (ATCC CRL 1737)

L. major 5 ASKH   : *Leishmania major* promastigotes cell line, kindly provided by
                                Prof. Joachim Clos (BNI Hamburg)

Additional CHO Lec8 cell lines (Lec 3.2.8 and Lec 4.7.8) were kindly provided by
Pamela Stanley (Albert Einstein College of Medicine, NY, USA).

2.1.2 Bacterial strains

E.coli XL-1 blue   : Genotype: *recA1 endA1 gyr96 thi-1 hsdR17 supE44 relA1 lac*
(Stratagene)   [F' *proAB lacI^{q}Z$\triangle$M15 Tn 10* (Tet^r)]

E.coli XL-1 blue   : Genotype : $\triangle$(*mcrA*)*183*
MRF' (Stratagene) $\triangle$(*mcrCB-hsdSMR-mrr) 173 endA1 supE44 thi-1 recA1 gyr96*
                                relA1 lac [F' *proAB lacI^{q}Z$\triangle$M15 Tn 10* (Tet^r)]

E.coli BL21(DE3)   : Genotype: F$^-$ *ompT hsd*S$_B$ (r$_B^-$ m$_B^-$) *gal dcm* (DE3) (Novagen)

E.coli DEV6   : Genotype: *galU65, relA1, spoT1, thi-1, lacZ(Am)*, provided by
                                Elseviers *et al*., (1980) through the *E.coli* Genetic Stock Center,
                                New Haven, USA

2.1.3 Plasmids

pcDNA3   : Eukaryotic expression vector (Invitrogen)

pcDNA3FL   : Eukaryotic expression vector based on pcDNA3 bearing a Flag epitope (N-MBYKDDDDK-C) between the restriction sites *Kpn*I/*Bam*HI (synthesised by Anja Münster)

pOTB7-hUGP1   : cDNA clone of human muscle UGP1 obtained from the RZPD (Deutsches Ressourcenzentrum für Genomforschung GmbH, Berlin) library no.: 958, clone IMAGp958H18235Q2

pCMV-hUGP2   : cDNA clone of human muscle UGP2 obtained from the RZPD (Deutsches Ressourcenzentrum für Genomforschung GmbH, Berlin) library No. 998, clone IMAGp998K047340Q3

pETBos-GlcAT   : Eukaryotic expression plasmid encoding the rat glucuronyltrans-ferase (supplied by Terayama *et a.,* 1997)

peGFP   : Eukaryotic expression plasmid encoding an enhanced green fluorescent protein (Clontech)

pUC18   : Cloning vector and prokaryotic expression vector (Stratagene)

pCR4-Topo   : Cloning vector allowing the insertion of DNA fragments by TA cloning (Invitrogen)

pCMV-Script   : Eukaryotic expression vector (Stratagene)

pET 22 b   : Prokaryotic expression vector for the expression of C-terminal 6xHis tagged proteins under the control of the T7/lac promoter (Novagen).

pET22b-Strep   : Prokaryotic expression vector based on pET22b (Novagen) including an N-terminal StrepII-sequence (WSHPQFEK) instead of the pelB-sequence. The StrepII-adaptor was inserted between

the restriction sites *Nhe*I und *Bam*H I (synthesised by Dr. Martina Mühlenhoff, MH-Hannover).

pYes2/NTA : Yeast expression vector (Invitrogen)

pCR2.1hyg : Cloning vector bearing the hygromycin phosphotransferase gene that is inserted between the restrictions sites *Bsp*HI and *Nhe*I (supplied by Dr. Martin Wiese (BNI, Hamburg)).

pCR2.1phleo : Cloning vector bearing the phleomycin binding protein gene that is inserted between the restrictions sites *Nco*I and AvrII (supplied by Martin Wiese (BNI, Hamburg)).

pCR2.1neo : Cloning vector bearing the neomycin phosphotransferase gene that is inserted between the restrictions sites *Bsp*HI and *Nhe*I (supplied by Martin Wiese (BNI, Hamburg)).

p*Ath*-UGT2 : Eukaryotic expression vector for the expression of the UDP-galactose transporter 2 from *Arabidopsis thaliana* (supplied by Dr. Hans Bakker, MH-Hannover)

pACM1 : Eukaryotic expression vector based on pCMV-Script for expression of a C-terminal truncated *L. major* UGP. The clone was isolated from pool #17 of the *L. major* cDNA library.

pcDNA3-*L. major*UGP : Eukaryotic expression vector based on pcDNA3 for expression of untagged *L. major* UGP. UGP was amplified from pool 19 of the cDNA library using the primer pair ACM4/ACM6 and inserted between the restriction sites *Bam*HI/*Not*I of pcDNA3.

pcDNA3FL-
*L. major*UGP : Eukaryotic expression vector based on pcDNA3FL for expression of N-terminal Flag tagged *L. major* UGP. UGP was amplified from pool 19 of the cDNA library using the primer pair ACM5/ACM6 and inserted between the restriction sites *Bam*HI/*Not*I of pcDNA3FL.

pcDNA3-hUGP1 : Eukaryotic expression vector based on pcDNA3 for expression of untagged human UGP. UGP was amplified from plasmid pOTB7-hUGP1 using the primer pair ACM12/ACM9 and inserted between the restriction sites *Bam*HI/*Not*I of pcDNA3

pcDNA3-hUGP2 : Eukaryotic expression vector based on pcDNA3 for expression of untagged human UGP. UGP was amplified from plasmid pCMV-hUGP2 using the primer pair ACM11/ACM9 and inserted between the restriction sites *Bam*HI/*Not*I of pcDNA3

pcDNAFL-hUGP1 : Eukaryotic expression vector based on pcDNA3FL for expression of N-terminal Flag-tagged human UGP. UGP was amplified from plasmid pOTB7-hUGP1 using the primer pair ACM10/ACM9 and inserted between the restriction sites *Bam*HI/*Not*I of pcDNA3FL

pcDNA3FL-hUGP2 : Eukaryotic expression vector based on pcDNA3FL for expression of N-terminal Flag-tagged human UGP. UGP was amplified from plasmid pCMV-hUGP2 using the primer pair ACM8/ACM9 and inserted between the restriction sites *Bam*HI/*Not*I of pcDNA3FL

pET-UGP-His : Prokaryotic expression vector based on pET-22b for expression of C-terminally His_6- tagged *L. major* UGP. UGP was amplified from plasmid pcDNA3-*L.major*UGP using the primer pair ACM112/ACM69 and inserted between the restriction sites *Nde*I/*Not*I of pET22b.

pET22-UGP/
thrombin-His : Prokaryotic expression vector based on pET-22b for expression of C-terminally His_6- tagged *L. major* UGP. A thrombin cleavage site was introduced with the primer ACM113. UGP was amplified from plasmid pcDNA3-*L.major*UGP using the primer pair ACM112/ACM113 and inserted between the restriction sites *Nde*I/*Not*I of pET22b.

pET-UGP-Δ38   : Prokaryotic expression vector based on pET-22b-Strep for expression of N-terminally by 38 amino acid truncated and StrepII- tagged and C-terminally His$_6$- tagged *L. major* UGP. UGP was amplified from plasmid pcDNA3FL-*L. major* UGP using the primer pair ACM92/ACM69 and inserted between the *Bam*HI/*Not*I restriction sites of pET-22b-Strep.

pET-UGP-Δ69   : Prokaryotic expression vector based on pET-22b-Strep for expression of N-terminally by 69 amino acid truncated and StrepII- tagged and C-terminally His$_6$- tagged *L. major* UGP. UGP was amplified from plasmid pcDNA3FL-*L. major* UGP using the primer pair ACM93/ACM69 and inserted between the *Bam*HI/*Not*I restriction sites of pET-22b-Strep.

pET-UGP-Δ440-494   : Prokaryotic expression vector based on pET-22b-Strep for expression of C-terminally by 54 amino acid truncated and C-terminally His$_6$- tagged and N-terminally StrepII- tagged *L. major* UGP. UGP was amplified from plasmid pcDNA3FL-*L. major* UGP using the primer pair ACM105/ACM5 and inserted between the *Bam*HI/*Not*I restriction sites of pET-22b-Strep.

pET-UGP-Δ390-494   : Prokaryotic expression vector based on pET-22b-Strep for expression of C-terminally by 104 amino acid truncated and C-terminally His$_6$- tagged and N-terminally StrepII- tagged *L. major* UGP. UGP was amplified from plasmid pcDNA3FL-*L. major* UGP using the primer pair ACM106/ACM5 and inserted between the *Bam*HI/*Not*I restriction sites of pET-22b-Strep.

pcDNA3-5'FRs   : Construct used for subcloning of the *L. major* UGP 5' flanking region (FR) for the further generation of a gene deletion cassette. The FR was amplified from genomic DNA using the primer pair ACM54/ACM55 and inserted between the restrictions sites XbaI/*Bam*HI of pcDNA3.

pcDNA3-3'FRs   : Construct used for subcloning of the *L. major* UGP 3' flanking region (FR) for the further generation of a gene deletion cassette. The FR was amplified from genomic DNA using the primer pair

ACM56/ACM57 and inserted between the restrictions sites KpnI/*Bam*HI of pcDNA3.

pcDNA3-3'5'FRs : Construct bearing the *L. major* UGP 5' and 3' FRs in pcDNA3. The 5'FR from plasmid pcDNA3-5'FRs was excised with XbaI/*Bam*HI and inserted into the corresponding sites of pcDNA3-3'FRs.

pUC18-5'3'FRs : Construct to obtain an *Eco*RI site for subcloning of the *L. major* UGP FRs into pYes2/NTA Δ*Bsp*HI/Δ*Nhe*I. The 5' and 3' FRs were excised from pcDNA3-3'5'FRs by a XbaI/ KpnI digest and inserted between the corresponding restriction sites of pUC18.

pYes2/NTAΔ*Bsp*HI : Cloning vector without *Bsp*HI site based on the yeast expression vector pYes2/NTA . The vector pcDNA3 was digested with *Nco*I and the obtained 900 bp fragment ligated into the *Bsp*HI site of pYes2/NTA.

pYes2/NTA
Δ*Bsp*HI/Δ*Nhe*I : Cloning vector without *Bsp*HI and *Nhe*I site based on the yeast expression vector pYes2/NTA. pYes2/NTAΔ*Bsp*HI was digested with *Nhe*I and *Avr*II and religated.

p3'5'FRs : Construct bearing the *L. major* UGP 5' and 3' FRs in pYes2/NTAΔ*Bsp*HI/Δ*Nhe*I. After a XbaI/EcoRI restriction digest of pUC18-5'3'FRs the flanking regions were ligated into the corresponding sites of pYes2/NTA Δ*Nhe*I/Δ*Bsp*HI.

p3'5'FRs-hyg : Construct bearing the hygromycin resistance marker flanked by the *L. major* UGP 5' and 3' FRs. The hygromycin resistant marker was excised with *Bsp*HI/*Nhe*I from pCR2.1hyg and ligated in the corresponding sites of p3'5'FRs.

p3'5'FRs-neo : Construct bearing the neomycin resistance marker flanked by the *L. major* UGP 5' and 3' FRs. The neomycin resistant marker was excised with *Bsp*HI/*Nhe*I from pCR2.1neo and ligated in the corresponding sites of p3'5'FRs.

p3'5'FRs-phleo   : Construct bearing the phleomycin resistance marker flanked by

the *L. major* UGP 5' and 3' FRs. The phleomycin resistant marker

was excised with *Nco*I/*Avr*II from pCR2.1phleo and ligated in the

*Bsp*HI/*Nhe*I sites of p3'5'FRs.

p5'UTR   : Construct bearing 5' flanking region 1095 to 16 nucleotides

upstream of the region used in pcDNA3-5'FRs. The fragments

was amplified from *L. major* genomic DNA with the primer pair

ACM107/ACM108 and inserted into pCR4-Topo.

2.1.4 Oligonucleotides

All oligonucleotides were purchased from MWG.

Sequencing primers for *L. major* UGP (5' ⇒ 3')

ACM1   GGGTGATGCTGAATTAGATG

ACM2   ACCGGCATGGGGCTGTG

Sequencing primers for *L. major* UGP flanking regions (5' ⇒ 3')

ACM61   ACTGGCGAATGGTCAGAAAAG
ACM58   AAGCGTGGTCATCTCGATTAG

Primers for homologous recombination control (5' ⇒ 3')

ACM94   CACGCTCATGTACGAGTT
ACM96   CTGGGAAGACGTTGGCGATGC
ACM99   GACGTCGCGGTGAGTTCAGG
ACM100   GTCCGAGGGCAAAGGAATAG
ACM101   GAACGGCACTGGTCAACTTGG
ACM102   GTGGCCGAGGAGCAGGACTG

Sequencing primers for plasmids (5' ⇒ 3')

T7   TAATACGACTCACTATA
Sp6   GCATTTAGGTGACACTATAGAATAG

T7term   GCTAGTTATTTGCTCAGCGG

pRSet-RPnew   GGGTTATGCTAGTTATTGC

PCR amplification primers (5' ➡ 3')

ACM4   CGCGGGATCCGAAGCAATGGAAAACGAAAACGACATGAA   *Bam*HI

ACM5   CGCGGGATCCGAAAACGACATGAAGTCCCTCAGC   *Not*I

ACM6   CGTGGCGGCCGCTTAGGCACCATCGGGGATCACAAAC   *Not*I

ACM8   CGCGGGATCCTCTCAAGATGGTGCTTC   *Bam*HI

ACM9   ATATGCGGCCGCTCAGTGGTCCAAGATGC   *Not*I

ACM10   CGCGGGATCCTCGAGATTTGTACAAGATC   *Bam*HI

ACM11   ATATGGATCCGCCACCATGTCTCAAGATGGTGC   *Bam*HI

ACM12   ATATGGATCCGCCACCATGTCGAGATTTGTACAAG   *Bam*HI

ACM54   CTGATCTAGAAACGAAGACGAGCTACAGCGCATG   *Xba*I

ACM55   TAAAGGATCCCCATGGCTTCACCTCCGTGACAGC   *Bam*HI/*Not*I

ACM56   GAAAGGATCCGCTAGCTAGGGGTCACAAGCTGCTGA   *Bam*HI/*Nhe*I

ACM57   ATACGGTACCCCGCCGTCATCTGTCGATTGCACAC   *Kpn*I

ACM69   CTTAGCGGCCGCATCTTGTTGGTCGACTGCTGCG   *Not*I

ACM92   AGTAGGATCCGTCAGTAAAGGCGAGACAGGGTC   *Bam*HI

ACM93   AGTAGGATCCGCTGTCCTGCAGAGTACCGTTG   *Bam*HI

ACM105   CTTAGCGGCCGCATTTCCACCAGCGATGGCACGC   *Not*I

ACM106   CTTAGCGGCCGCATGGAGCGCAGAGCGAGCAGATC   *Not*I

ACM107   CTGGTGTGCAGAAGGAAGACG   TA cloning

ACM108   GCATCGCCAACGTCTTCCCAG   TA cloning

ACM112   CTGACTCCATATGGAAAAGCACATGAAGTCCCTC   *Nde*I

ACM113   ATATGCGGCCGCAGAACCACGCGGAACCAGCTTGTTGGTCGACTGCTGCG *Not*I

2.1.5   Chromatography columns

StrepTactin affinity matrix   IBA

HisTrap HP Ni^{2+} column (5ml)   Amersham Biosciences

HiPrep 26/10 Desalting   Amersham Biosciences

Superdex 200 HR 10/30   Amersham Biosciences

2.1.6 Antibodies

2.1.6.1 Primary antibodies

mAb anti-penta His :monoclonal antibody (mouse IgG) directed against the His_6-epitope (HHHHHH) (Qiagen)

mAb 735 :monoclonal antibody (mouse IgG 2a) directed against poly-$\alpha2,8$-*N*-acetylneuraminic acid with a minimum chain length of eight residues (Frosch *et al.*, 1985)

mAb L2-412 : monoclonal antibody directed against glucuronic acid ß1,3-linked to galactose

anti-Flag M5 : monoclonal antibody (mouse IgG1) directed against the Flag-epitope (MDYKDDDDK) (Sigma)

anti-Flag : chicken polyclonal antibody directed against the Flag-epitope (MDYKDDDDK) (Sigma)

WIC79.3 mAb : monoclonal antibody (mouse IgG1) directed against galactose substituted repeating unit of LPG (Gal-Man-PO_4) (ascites fluid supplied by Martin Wiese)

LT6 : monoclonal antibody (mouse IgG1) directed against unsubstituted repeating unit of LPG (Gal-Man-PO_4) (Ilg et al, 1993, hybridoma culture supernatant supplied by Martin Wiese)

Anti-calnexin : polyclonal rabbit serum (supplied by Prof. A.Hellinius, ETH Zürich, Schweiz)

Anti-mannosidaseII : polyclonal rabbit serum (supplied by Prof. K.Moreman; University of Georgia, USA)

2.1.6.2 Secondary antibodies, sera and conjugates

Anti-rabbit-IgG Alexa488-conjugate	Molecular Probes
Anti-mouse-IgG Cy3 conjugate	Sigma
Anti-mouse-IgG FITC conjugate	Dianova
Anti-Digoxigenin Fab AP conjugate	Roche
Anti-mouse-Ig AP conjugate	Dianova
Anti-mouse-Ig HRP conjugate	Dianova
Anti-chicken-IgG AP conjugate	Dianova
Anti-rabbit-Ig HRP conjugate	Dianova
Streptavidin AP	Dianova
DAPI	Sigma

2.1.7 Molecular weight markers

'1 kb DNA ladder'	Invitrogen
'SDS-PAGE molecular weight standards high range'	BioRad
'Prestained Precision Protein Standards'	BioRad

2.1.8 Enzymes

Alkaline calf intestine phosphatase	New England Biolabs
cloned Pfu-DNA-Polymerase	Stratagene
Glucose-6 phosphate dehydrogenase	Roche
Lysozyme	Serva
Phosphoglucomutase	Roche
Restriction enzymes	New England Biolabs
T4-DNA-Ligase	New England Biolabs
Taq-DNA-Polymerase	Sigma
UDP-galactose-4 epimerase	Roche
UDP-glucose dehydrogenase	Roche

Enzymes used for the generation of the *L,major* cDNA library were part of the 'pCMV-ScriptXR cDNA library construction kit' from Stratagene.

2.1.9 Culture media and additives

Adenin	Sigma
Alpha MEM	GibcoBRL
Ampicillin, sodium salt	Serva
Anti-Flag M5 sepharose beads	Sigma
Biotinthyramid	Molecular probes
Carbenicillin, disodium salt	Fluka
Complete and incomplete Freund's adjuvant	Becton Dickinson
European Mistletoe	Sigma
Fetal calf serum	Invitrogen
Hemin	Fluka

Hygromycin B	Sigma
IPTG (Isopropyl-beta-D-thiogalactopyranoside)	Merck
Kanamycin	Sigma
LB-agar	Becton Dickinson
LB-medium	Becton Dickinson
M199 powder	GibcoBRL
MacConkey agar (base)	Becton Dickinson
Neomycin	Sigma
Noble agar	Becton Dickinson
OptiMEM	Invitrogen
paraformaldehyde	Sigma
Penicillin/Streptomycin	Sigma
Phleomycin	Sigma
Poly (L)-lysine	Sigma
Ricinus communis agglutinin	Sigma
Roti^{TM}Phenol	Roth
Trypsin/EDTA (0,5%Trypsin, 0,2% EDTA)	GibcoBRL
Wheat germ agglutinin	Sigma
α-D galactose	Sigma
α-D glucose	Sigma

2.1.10 Kits and further materials

Cell culture bottles and dishes	Sarstedt
Cellulose acetate filter (0,22µm, 0,8 µm)	Sartorius
Electroporation cuvettes	BioRad
Filterpaper	Whatman
Hyperfilm MP	Amersham Biosciences
Microtiterplates 96-well polystyrol (U-bottom)	Greiner
Nitrocellulose membrane (0,45 µm)	Schleicher & Schuell
Nylon membrane (Hybond-N+)	Amersham Biosciences
Oligotex mRNA Mini Kit	Qiagen
pCMV-ScriptXR cDNA library construction kit	Stratagene
PCR-tubes (0,2 ml)	Biozym

Plastic disposable pipettes (5 ml, 10 ml, 25 ml)	Sarstedt
Polypropylentubes (14 ml, 50 ml)	Greiner
Protein Standard kit for gelfiltration	Roche
QIAGEN Plasmid Mini und Midi Kit	Qiagen
QIAquick Gel Extraction Kit	Qiagen
Qiaquick PCR purification kit	Qiagen
Reaction tubes (0.5 ml, 1.5 ml)	Sarstedt
Reaction tubes safelock (1.5 ml, 2 ml)	Eppendorf
RNeasy Midi Kit	Qiagen
Sterile filters Millex GP (0,22 µM)	Milipore
Syringes (2 ml)	Braun

2.1.11 Standard buffer and media

20xSSC	3 M NaCl
	0.3 M Sodiumcitrate pH 7.0
2xLaemmli	200 mM Tris-HCl pH 6.8
	30% (v/v) glycerol
	3% (w/v) SDS
	0.1% (w/v) bromephenol Blue
	5% (v/v) 2-mercaptoethanol
5xGEBS	20% glycerol
	50 mM EDTA
	0.05% bromephenol Blue
	0.5% sarcosyl
5xLaemmli	600 mM Tris-HCl pH 6.8
	40% (v/v) glycerol
	10% (w/v) SDS
	0.4% (w/v) bromephenol Blue
	5% (v/v) 2-mercaptoethanol
AP-buffer	100 mM Tris-HCl pH 9.5
	100 mM NaCl
	5 mM $MgCl_2$
BCIP	25 mg/ml BCIP in 100% DMF

ECL-reagent   125 mM Luminol

                                               45 mM p-Cumarsäure

                                               1M Tris/HCl pH 8.5

                                               15% H_2O_2

NBT   50 mg/ml NBT in 70% (v/v) DMF

PBS   10 mM sodium phosphate pH 7.4

                                               150 mM NaCl

PBS/EDTA   10 mM sodium phosphate, pH 7.4

                                               150 mM NaCl

                                               2 mM EDTA

SOB (SOC)   2% bacto tryptone

                                               0.5% yeast extract

                                               10 mM NaCl

                                               2.5 mM KCl

                                               10 mM MgCl2

                                               10 mM MgSO4

                                               (2% glucose)

TAE   40 mM Tris-Acetat

                                               2 mM EDTA

                                               pH 8.5

TBE   100 mM Tris-HCl, pH 8.0

                                               100 mM Borate

                                               2.5 mM EDTA

TE   10 mM Tris-HCl, pH 8.0

                                               1 mM EDTA

2.1.12 Chemicals

ABTS	Roche
Acetic acid (100 %)	Merck
Aceton	Baker
Acrylamide 40% 4 K-Mix (37.5:1)	Serva
AEC	Sigma
Agarose	Serva
Ammonium chloride	Merck

Ammonium persulphate (APS)	Serva
Aprotinin	Bayer
BCA *Protein Assay Reagent*	Pierce
BCIP (5-Brom-4-chlor-3-indolyl-phosphat)	Fluka
Bestatin	Sigma
Beta-Mercaptoethanol	Sigma
Biotintyramid	Molecular probes
Borate, sodium salt	Merck
Bromphenol Blue, sodium salt	Applichem
BSA (Fraktion V)	Applichem
BSA protein standard	Pierce
Chloroform	Baker
Citric acid	Merck
CSPD	Roche
Desthiobiotin	Sigma
Dimethylformamide (DMF)	Fluka
Dimethylsulfoxide (DMSO)	Merck
Dipotassium hydrogenphosphate	Merck
Disodium hydrogenphosphate	Merck
Disodium hydrogenphosphate	Merck
Dithiothreitol (DTT)	Sigma
dNTPs (100 mM each)	Pharmacia
Dry milk	Applichem
EDTA, Disodium salt (Titriplex III)	Merck
Ethanol, abs.	Baker
Ethidium Bromide	USB Corporation
Fast Red	Sigma
Formaldehyde	Sigma
Galactose-1 phosphate	Sigma
Glucose-1 phosphate	Sigma
Glutardialdehyd	Roche
Glycerine (99%)	KMF
Glycine	Sigma
Gucose-1,6 biphosphate	Roche
Hydrochloric acid (38%)	Baker
Hydrogenperoxid	Fluka
Imidazole	Fluka

IPTG (Isopropyl-beta-D-thiogalactopyranoside)	Merck
Isopropanol (2-Propanol)	Merck
Korsolex plus	Roche
LipofectAMINE transfection reagent	Invitrogen
Magnesium chloride hexahydrate	Merck
Magnesium sulphate	Baker
Manganese chloride	Merck
Methanol	Baker
Moviol	Baker
NAD^+	Roche
$NADP^+$	Roche
Naphtol	Sigma
NBT (Nitrotetrazolium bluechloride)	Fluka
Pepstatin	Roche
Phenylmethylsulfonyl fluorid (PMSF)	Sigma
Ponceau S, sodium salt	Sigma
Potassium dihydrogenphosphate	Merck
Pyrophosphate	Sigma
Roti-Blue Coomassie-stain (5x)	Roth
Saponin	Sigma
Sodium acetate	Merck
Sodium azide	Merck
Sodium chloride	Merck
Sodium dihydrogenphosphate	Merck
Sodium dodecylsulphate (SDS)	Merck
Sodium hydroxide	Merck
Sodium periodate	Sigma
TEMED (N,N,N',N'-Tetramethyl-ethylendiamin)	Serva
TRIS (Tris(hydroxymethyl)-aminomethan)	Merck
UDP-glucose	Sigma
UTP	Roche

All chemicals not explicitly listed above were purchased in p.a. quality from either Merck or Sigma.

2.1.13 Laboratory Equipment

Blotting chamber Fast-Blot B44	Biometra
Easy Enhanced Analysis System	Herolab
(E.A.S.Y RH-3, Videokamera 429K)	
Elektrophoresis chamber for agarose-gels	peqlab
Elektrophoresis chamber for SDS-PAGE	BioMetra
ELISA-Reader: DigiScan	Asys Hitech
FPLC-system ÄKTA	Amersham Biosciences
Heatingblock TB1	BioMetra
HeraSafe Hood	Heraeus
Incubators	Heraeus
Peristaltikpump P-1	Amersham Biosciences
Scales CP 224S (µg) / CP 3202 (g)	Sartorius
Sonifier 450	Branson
Spectrophotometer Ultrospec 2100 pro	Amersham Biosciences
Speedvac RVC 2-18	Christ
Standard Power Pack P25	Biometra
Thermocycler T1 and T Gradient	Biometra
Thermomixer compact	Eppendorf
Centrifuges : - Biofuge fresco	Heraeus
- Biofuge pico	Heraeus
- Multifuge 3 S-R	Heraeus
- Centrifuge 5415C	Eppendorf
- Coulter Avanti J-30I	Beckman
Rotors: - JA 25.50	Beckman
- JLA 10.500	Beckman
- JS-24.15	Beckman
Stratalinker	Stratagene
Electroporator	BioRad

2.2 Cell biological techniques (CHO cells)

2.2.1   Cultivation of CHO cells

CHO cells were cultured in a humidified incubator at 37°C and 5% CO_2. The cells were grown in α-MEM (GibcoBRL) supplemented with 5% fetal calf serum (FCS). Every 3-4 days, confluent cell layers were detached from the cell culture flask with Trypsin/EDTA (GibcoBRL) and transferred to a new devise at a concentration of $5x10^5$ cells/75 cm^2. Cells were counted in a Neubauer chamber.

For long term storage in liquid nitrogen, cells were pelleted by centrifugation (5 min, 2000xg, RT) and resuspended in culture medium containing 10 % FCS and 10 % DMSO at a concentration of $1x10^7$ cells/ml. Aliquots of 1 ml were filled in cryo vials, stored overnight at -80°C and then transferred to liquid nitrogen.

To recover frozen cell pellets, the cells were thawed at room temperature (RT) and transferred into 10 ml α-MEM supplemented with 5% FCS. After centrifugation (5 min, 2000xg, RT) the cell pellet was resuspended in culture medium (5 % FCS) and transferred to a culture flask.

2.2.2   Transient transfection of CHO cells

For the transient transfection of CHO cells, the cells were seeded in 6-well plates (9.6 cm^2) at a concentration of $3x10^5$ cells/well and incubated over night. For each well, a transfection mixture was prepared by combining 1 µg DNA in 100 µl OptiMEM with 6 µl LipofectAmine in 100 µl OptiMEM. Upon cotransfection with cDNA encoding the rat glucuronyltransferase (pEFBos-GlcAT), 0.5 DNA and 0.5 µg pEFBosGlcAT was used. After an incubation of 15-30 min at RT, the mixture was filled up to 1 ml with OptiMEM. Prior to the addition of the transfection mixture, the cell layer was washed once with 1 ml OptiMEM. After 6 hours, 1 ml culture medium was added and the cells analysed after 48 hours.

2.2.3   Immunocytochemistry

For immunocytochemistry, transiently transfected CHO cells (2.2.2), were washed once with 2 ml TBS and were fixed with 1 ml 1.5% glutarealdehyde for 10 min. The cell layer was washed two time with TBS and blocked in 2% milk powder/TBS. Cells cotransfected

with pETBosGlcAT, were stained with rat monoclonal antibody (mAb) L2-412 (1:4000) in the same solution, followed by an alkaline phosphatase conjugated α–rat secondary antibody (1:4000). Polysialic acid was detected with the murine mAb 735 (5 µg/ml) and an alkaline phosphatase-conjugated α–mouse secondary antibody (1:4000). The cells were washed 3-4 times with 2 ml TBST (0.05% Tween) after each antibody incubation. For colour development, the substrate Fast-Red (Sigma) was dissolved in 0.1 M Tris/HCl pH 8.5 and 0.2 mg/ml Naphtol (Sigma) at a concentration of 1 mg/ml and incubated with the cells. The reaction was stopped by the addition of 1 ml water. Plates were analysed under a normal light microscope and red cells per plate were scored. The plates could be stored in 50% glycerol at 4°C for two years.

Signal amplification was achieved by using a HRP-coupled secondary antibody followed by the incubation with a biotintyramid solution (Molecular Probes) in TBS for 10 min at RT, consisting of 0.1 M imidazole pH 7.6; 0.001% H_2O_2 and 1,7 mM biotintyramid. The cells were washed two times in TBST and incubated with Streptavidin AP (1:500).

For colour development using the substrate AEC (3-amino-9ethyl-carbasol, Sigma), the cells were incubated with a HRP-coupled secondary antibody and the AEC staining solution of 50 mM NaAc, 0.016% H_2O_2 and 1 mg/ml AEC . Lilac cells were monitored under a normal light microscope.

2.2.4 Immunofluorescence

Transiently transfected CHO cells (2.2.2) were grown on glass cover slides placed in 6 well plates. The cells were washed two times with PBS and fixed in 4% paraformalde-hyde (PFA) for 20 min at RT. After three washing steps in PBS, additional binding sites were blocked with 0,1% BSA/PBS for 30 min at RT. To permeabilize the cells, 0.2 % saponin was added to the blocking solution. After permeabilization, samples were incubated with the primary antibodies diluted in 0.1% BSA in PBS for 1 hour at RT (mouse α–Flag M5 mAb 1:1000, rabbit α–mannosidase II antiserum 1:2000, rabbit α–calnexin antiserum 1:2000). The cells were washed three times in 0.1% BSA in PBS and bound antibodies were detected with the corresponding secondary antibodies diluted in 0.1% BSA/PBS: α–mouse IgG Cy3 (1:500) and α–rabbit IgG Alexa488 (1:500). After 1 hour at RT, the reactions were stopped by three washing steps in 0.1% BSA/PBS and a final wash in PBS. Slides were mounted in moviol and analyzed under a Zeiss fluorescence microscope.

2.2.5 FACS analysis of CHO cells

The cells were detached from the cell culture flask with PBS/2 mM EDTA and counted in a Neubauer chamber. $1x10^6$ cells per sample were transferred into a 1.5 ml eppendorf tube and centrifuged for 1 min at 1500xg. The pellets were resuspended in 1 ml 0.1% BSA in PBS and again centrifuged at 1500xg for 1 min. The cells were incubated with 50 μl of primary antibody (5 μg/ml: mAb 735: 1:1200) for 15 min at 4 °C. After one washing step with 350 μl 0,1% BSA/PBS, the cell pellets were resuspended in 50 μl of a secondary antibody dilution (α–rat FITC 1:50 in 0.1% BSA/PBS). After 15 min at 4°C, the samples were washed twice with 350 μl 0.1% BSA/PBS and resuspended in 1 ml 0.1%BSA/PBS. In the FACS analysis, 10 000 cells per sample were counted using a Becton Dickinson FACSCalibur.

2.2.6 Selection of galactose negative CHO Lec8 cells

2.2.6.1 Selection via panning

Panning describes a technique to separate cells bearing a certain antigen on the cell surface from cells devoid of this antigen. The cells are incubated with a corresponding immobilized antibody. Positive cells bind to the antibody and can be removed from the cell population. To remove, polysialic acid (PSA) positive cells from a CHO Lec8 cell population, panning plates with immobilized mAb 735 were prepared. Therefore, 10 cm Petri dishes were incubated with 10 ml of a mAb 735 dilution (10 μg/ml) in 50 mM Tris/HCl pH 9.5 for 6h at RT. The antibody dilution was removed and used to coat a second set of Petri dishes at RT over night. The dishes were washed three times with PBS and blocked with 10 ml 1% BSA in PBS at 4°C over night. After two washing steps, the plates were stored at -20°C.

Petri dishes coated with mAb 735 were thawed by the addition of 10 ml culture media (see 2.2.1). The CHO cell layers were treated with PBS/2 mM EDTA to detach the cells from the cell culture flask. $1x10^7$ cells were incubated on the coated Petri dish for 1 hour at 4°C. PSA positive cells adhere to the Petri dish whereas PSA negative cells remain in the supernatant. To obtain a PSA negative cell line, the cells in the supernatant were removed and cultivated.

2.2.6.2 Selection by lectin treatment

To obtain galactose and sialic acid negative CHO Lec8 cells, a dilutions series of the lectins European Mistletoe, Wheat Germ Agglutinin (WGA) and Ricinus communis

agglutinin (RIC) was added to the cell culture medium. As a control, CHO wild type cells, that express galactose and sialic acid containing glycoconjugates on the cell surface, were treated in the same way. Thus, CHO Lec8 cells and CHO wild type cells were seeded on 6 well plates at a concentration of $3x10^5$ cells per well. After 10 hours, the lectins European Mistletoe, WGA and RIC were added to the cell culture media in three separate experiments. The lectin Eurpoean Mistletoe was used in the concentrations of 3 ng/ml, 10 ng/ml, 30 ng/ml, 100 ng/ml 300 ng/ml and 1 µg/ml and WGA in the concentrations of 1 µg/ml, 5 µg/ml, 10 µg/ml, 15 µg/ml and 20 µg/ml. The following RIC concentrations were applied: 300 ng/ml, 1 µg/ml, 3 µg/ml, 10 µg/ml and 30 µg/ml. The galactose and sialic acid positive CHO wild type cells, died more rapidly with increasing lectin concentrations than the CHO Lec8 cells. The success of the selection was monitored by immunocytochemistry using the mAb 735 and the biotintyramid signal amplification step.

2.3 Cell biological techniques (Leishmania major)

2.3.1 Cultivation of Leishmania major (L. major)

Promastigote *Leishmania major* were grown in M199 media supplemented with 10% FCS, 40 mM Hepes pH 7.5, 0.1 mM adenine, 0.0005% hemin, 0.0002 % biotin and 50 U/ml penicillin/streptomycin (M199 culture media). The cultures were maintained in a humidified incubator at 26°C by serial passage of 10 ml cultures at dilutions of 1:100 every 2-3 days. The saturation densities of *L. major* 5ASKH ranged from 4-5 x10^7 cells/ml. If necessary, 5 µg/ml phleomycin, 50 µg/ml neomycin and 50µg/ml hygromycin were added to the culture medium.

For long time storage, 1x10^7 cells were pelleted, resuspended in 500 µl M199 culture media supplemented with 10% DMSO and transferred into cryo tubes. Cells were slowly frozen in the gas phase of the liquid nitrogen tank over night. The next day the tubes were transferred into liquid nitrogen.

To recover frozen *L. major*, the cryo tube was removed from liquid nitrogen and thawed in a water bath at 37°C. The cell suspension was directly added to 10 ml M199 culture medium.

2.3.2 Homolgous gene replacment in L. major promastigotes

Homologlous gene replacement in *L. major* was achieved by the introduction of the gene replacement cassette using electroporation and subsequent selection on selective M199

agar. Protocols were kindly provided by Prof. Jon LeBowitz (Purdue University, West Lafayette, USA) and combined with an improved transfection protocol according to Robinson *et al.*, (2003).Cells suitable for transfections were harvested in the late logarithmic phase, which ranges from 5×10^6 cells/ml to 1×10^7 cells/ml for *L. major* 5ASKH. 1×10^8 cells per sample were pelleted for 10 min at 1300xg and washed once in electroporation buffer (21 mM Hepes, pH 7.5, 137 mM NaCl, 5 mM KCl, 0.7 mM NaHPO$_4$, 6 mM glucose). After a second centrifugation step, the pellet was resuspended in 500 µl electroporation buffer and mixed with 2 µg linearized DNA bearing a resistant marker cassette in a 4 mm cuvette. The cells were electroporated by two pulses using 25µF and 1.5 kV and incubated on ice for 10 min. The sample was transferred into 10 ml M199 culture medium in a cell culture flask. After 24 hours, the whole culture was centrifuged, resuspended in 100 µl culture media and spread on M199 agar (2x M199 culture media combined with an equal volume of 2% noble agar) containing the appropriate antibiotics. The plates were wrapped with parafilm and placed upright in a 26°C incubator. Colonies appeared after 2 weeks and were expanded in liquid culture. The number of colonies is dependend on the transformation efficiency which approaches 10^{-4} at saturating DNA concentrations for *L. major* (Kapler *et al*, 1990, Coburn *et al*, 1991), the plating efficiency and the DNA construct.

2.3.3 FACS analysis of *L. major*

For the FACS analysis, 1×10^6 log phase parasites per sample were centrifuged at 1300xg for 10 min. The cells were washed two times in FACS buffer (PBS, 3% FCS, 0.05% NaN$_3$) and incubated in 100 µl of the primary antibody diluted in FACS buffer for 30 min at 4°C (WIC 79.3 mAb 1:2000). After one washing step, 100 µl of secondary antibody was added to the cells (goat α–mouse FITC, 1:500 in FACs buffer) and incubated for 30 min at 4°C. The cells were washed three times in FACs buffer and finally resuspended in 100 µl FACs buffer containing 4% PFA. Per sample, 50 000 cells were counted with a Becton Dickinson FACSCalibur system.

2.3.4 Immunofluorescence

For immunoflourescence labelling, the parasites were immobilized on 10- well glass coverslips coated with poly(L)-lysine (0.1 mg/ml in PBS). 2×10^4 cells per well were washed once with PBS and fixed in the well by the addition of 4% PFA. After 15 min at RT, the samples were washed twice with PBS and incubated with 50 mM NH$_4$Cl for another 15 min at RT. Additional binding sites were blocked with 2% BSA in PBS for 15

min at RT. The same buffer was used for the incubation with the primary antibody (WIC 79.3 mAb 1:2000 (ascites fluid), LT6 1:2 (hybdridoma culture supernatant)). After 1 hour at RT, the cells were washed 4 times with PBS and incubated with a mixture of secondary antibody and DAPI in 2% BSA/PBS for 30 min at RT (goat α−mouse Cy3 1:500, DAPI 1:100). After five washing steps, the slides were mounted in moviol and analysed with a 40 x magnification of a Zeiss fluorescence microscope.

2.3.5   Mice infection assay

For mice infection assays, 10^7 cells were centrifuged at 1300xg for 10 min, resuspended in 1 ml PBS and again pelleted. The pellet was resuspended in 100 µl PBS and immediately injected into the left hind footpad of a Balb/c mouse (Charles River). Infection was monitored once a week by measuring the infected and the non-infected footpad with a Vernier calliper. The median size difference (+/- MAD) of the infected and uninfected footpad was plotted against the weeks post infection.

2.4   Biochemical techniques

2.4.1   Protein estimation

Protein concentrations were estimated using the 'BCA Protein Assay Reagent' (Pierce) according to the manufacturers instructions. Briefly, reagents A and B were mixed 50:1 immediately before use. 200 µl of the mixture were added to 10 µl sample and incubated at 55°C for 30 min in 96-well microtiter plates. As reference, a dilution series of 25-200 µg/ml BSA was included. The absorbance of all samples was measured at 540 nm using the ELISA-Reader 'DigiScan' (Asys Hitech) and protein concentrations were calculated from the BSA standard curve.

2.4.2   Polyacrylamide gelelectrophoresis (SDS-PAGE)

SDS-PAGE was performed according to Laemmli (Laemmli, 1970). Protein samples were seperated on SDS-polyacrylamide gels composed of a 5 % stacking gel (125 mM Tris/HCl pH 6.8, 0.1 % SDS, 5 % polyacrylamide) and a 10 % separating gel (375 mM Tris/HCl pH 8.8, 0.1 % SDS, 7-14 % polyacrylamide) or 8% ProSieve® 50 (gel solution, Cambrex) gradient gel. Gels were prepared by mixing buffer, SDS and the acrylamide stock solution (37.5 % acrylamide, 1 % bisacrylamide or ProSieve) and polymerisation was initiated by adding 0.1 % TEMED and 1 % ammonium persulphate. Samples were mixed with 2x or 5x Laemmli-buffer and heated to 95 °C for 5 min. Electrophoresis was

performed in SDS-electrophoresis buffer (50 mM Tris, 350 mM glycine, 0.1 % SDS) at 15 mA (stacking gel) and 20 mA (separating gel) per gel.

2.4.3   Coomassie staining of polyacrylamide gels

For Coomassie staining of protein gels, the colloidal staining solution Roti®-Blue (Roth) was used.   Directly after electrophoresis (2.4.2), the gels were incubated in 20 ml 1xRoti®-Blue in 20 % methanol overnight. The gels were destained in drying buffer (20 % ethanol, 10 % glycerol) and dried after 3-4 hours.

2.4.4   Silver staining of polyacrylamide gels

For silver staining the gels were incubated overnight in fixing solution (30 % ethanol, 10 % acetic acid, 1.85 % formaldehyde). After two washing steps (20 min, 50 % ethanol) the gels were incubated for exactly 1 min in thiosulphate solution (20 mg/100 ml), washed three times for 20 sec in deionised water and incubated for 20 min in staining solution (0.2 % (w/w) $AgNO_3$, 2.8 % formaldehyde). After two washing steps in deionised water for 20 sec, the gels were incubated in freshly prepared developer solution (6 % (w/w) $NaCO_3$, 2 % (v/v) thiosulphate solution, 1.85 % formaldehyde) until protein bands were lighting up. The reaction was stopped by transferring the gels to stop solution (30 % ethanol, 10 % acetic acid) and gels were dried after 1 h incubation in drying-buffer (20 % ethanol, 10 % glycerol).

2.4.5   Western Blotting

Proteins separated by SDS PAGE were transferred to nitrocellulose membranes using a *semidry* blotting chamber (Biometra) at 2 mA/cm^2 for 1 h.   Gel and membrane were placed between two layers of *Whatman* filter paper soaked in blotting buffer (48 mM Tris, 39 mM glycine). To check the transfer efficiency and to label the bands of the unstained molecular weight standard, the membrane was reversibly stained in Ponceau S-solution (0.2 % (w/v) Ponceau S in 3 % TCA) and destained in deionised water and PBS.

2.4.6   Immunostaining of Western Blots

The nitrocellulose membranes (2.4.5) were blocked overnight in blocking buffer consisting of 2% milk powder/ PBS or 2% BSA/PBS for AP- or HRP detection, respectively. After three washing steps for 5 min in PBS, the membranes were incubated for 1 h with the primary antibodies in the corresponding blocking solution (anti-penta His mAb

1µg/ml, chicken anti-Flag serum 1:500; WIC 79.3 mAb 1:2000 (ascites fluid)). The blots were washed three times for 5 min with PBS and incubated either with a HRP- or AP-coupled secondary antibody in blocking buffer for 1 hour at RT.

2.4.6.1   Detection of AP coupled secondary antibody

After secondary antibody incubation (α−mouse Ig coupled to AP: 1:4000, α−chicken IgG coupled to AP 1:4000), the membranes were rinsed three times with PBS and once with AP buffer (100 mM Tris-HCl pH 9.5, 100 mM NaCl, 5 mM MgCl$_2$). The visualization of the proteins was achieved by incubation with the substrate BCIP/NBT (0.3 mg/ml NBT, 0.15 mg/ml BCIP in AP-buffer). The reaction was stopped by the addition of water.

2.4.6.2   Detection of HRP coupled secondary antibody

For the detection of HRP-coupled secondary antibody (α−mouse Ig coupled to HRP: 1:50 000 in 2% BSA/PBS) the ECL system was used. The membranes were washed 4 times for 10 min in TBST (0,1 % Tween). The ECL detection solution was prepared by mixing a Luminol solution (250 mM Luminol, 90 mM p-Cumarsäure, 1 M Tris/HCl, pH 8.5) with a hydrogenperoxid solution (1 M Tris/HCl, pH 8.5, 30% H$_2$O$_2$) in a 1:1 ratio. After 15 min of incubation, the ECL solution was soaked off the membrane. The blot was wrapped in a plastic sheet and the signals exposed for 1-10 min to a film (Hyperfilm MP).

2.4.7   Solubilisation of CHO cells

The cells were washed once with PBS. The lysis buffer (50 mM Hepes pH 8.0, 250 mM NaCl, 1 mM EDTA, 0.5% IGEPAL, 10% glycerol, 28 µg/ml Aprotinin, 1 mM PMSF) was directly added onto the cell layer. The buffer and the cells were incubated for 3 min and transferred to an eppendorf tube. After incubation for 30 min at 4°C, the cell debris was removed by centrifugation at 13000xg for 30 min at 4°C. An aliquot of the cell lysate was mixed with 5x Laemmli buffer and separated by SDS PAGE (2.4.2) and the rest used for immunoprecipitation experiments (2.4.8).

2.4.8   Immunoprecipitations

For immunoprecipitations, at least 5x10^6 cells per sample were lysed in 1 ml lysis buffer as described in 2.4.7. and the cell lysates incubated with 15 µl of a 50% slurry α-Flag M2 agarose beads (Sigma). After 2 hours at 4°C under permanent rotation, the samples were centrifuged at 5000xg for 30 seconds. The supernatant was removed and the

beads washed four times with 1 ml lysis buffer (50 mM Hepes pH 8.0, 250 mM NaCl, 1 mM EDTA, 0.5% IGEPAL, 10% glycerol). The samples were resuspended in 30 µl 2x Laemmli buffer, boiled at 95°C for 5 min and separated on a SDS PAGE (2.4.2).

2.4.9 Preparation of *L. major* lysates

2.4.9.1   Preparation of lysates for LPG analysis

For the LPG analysis, 1×10^8 parasites were centrifuged at 1300 xg for 10 min and washed two times with cold PBS. The cell pellets were resuspended in 100 µl lysis buffer (50 mM Tris/HCl pH 8,0, 0,1% Triton X-100, 1 mM PMSF, 2 µg/ml Leupeptin, 5 µg/ml Pepstatin) and sonified in a beaker resonator 4 times for 30 seconds (Branson, 100% Duty cycle, output control 5, 4°C). The success of the lysis was monitored under a normal light microscope. Cell debris was removed by centrifugation at 13000xg for 10 min at 4°C. 2x Laemmli buffer was added to an aliquot of the cell lysates and 12,5 µg protein per sample were loaded on a 8% ProSieve gel (2.4.2).

2.4.9.2   Preparation of lysates for *in vitro* activity assays

The parasites were pelleted at 1300xg for 10 min and washed to times in cold PBS. The pellet was resuspended in *in vitro* activity assay buffer (50 mM Tris/HCl pH 7.8, 10 mM MgCl$_2$, 1 mM PMSF, 2 µg/ml Leupeptin, 5 µg/ml Pepstatin) at a concentration of 1×10^9 parasites per ml. The cells were sonified in a beaker resonator 4 times for 30 seconds (Branson, 100% Duty cycle, output control 5, 4°C). Cell debris was removed by centrifugation at 13000 xg for 10 min at 4°C. The supernatant was immediately tested in an *in vitro* activity assay (2.4.13.1).

2.4.10 Expression of recombinant protein in *E.coli*

For the recombinant expression in *E.coli*, the pET vector system (Novagen) was used. The corresponding expression plasmid was transformed into *E.coli* BL21 (DE3) and grown on an selective LB agar plate (supplemented with ampicillin). A fresh colony was transferred directly into 20 -2000 ml LB medium supplemented with 200 µg/ml carbenicillin. The culture was incubated at 15°C under vigorous shaking (160-200 rpm) and expression induced at an optical density of OD$_{600nm}$ =0.6 with 1 mM IPTG. After 20-24 hours, the culture was harvested by centrifugation (6000xg, 15 min, 4°C) and washed once with PBS. The pellet was stored at -20°C.

2.4.10.1 Preparation of soluble and insoluble *E.coli* fractions

For analytical preparations, bacterial pellets from 1 ml expression culture were resuspended in 100 µl TE per 1 OD. 100 µg/ml lysozyme were added to the suspension and incubated for 15 min at 37°C. After sonification in a beaker resonator (Branson, 100 % duty cycle, output control 5) for 2 min at 4 °C the soluble (supernatant) and insoluble fractions (pellet) were separated by centrifugation (15 min, 13000xg, 4 °C). The soluble fraction was mixed 1:1 with 2x Laemmli buffer whereas the insoluble fraction was resuspended in 1/5 the original volume TE of 2x Laemmli buffer. The samples were separated on a SDS PAGE (2.4.2) and analysed by Coommassie staining (2.4.3) and Western Blot (2.4.5).

For large scale protein purifications, a 0,5-2L expression culture was prepared (2.4.10), centrifuged at 6000xg for 15 min (4°C) and resuspended in 10 ml buffer A culture per litre culture (50 mM Tris/HCl pH 8.0, 300 mM NaCl, 40 µg/ml bestatin, 1 mM PMSF, 4 µg/ml pepstatin). The bacteria were lysed by sonification with a microtip (Branson sonifier, 50% duty cycle, output control 5) 8 times for 30 sec with a break of 30 seconds between the repeats. The suspension was centrifuged at 20000xg for 15 min (4°C). The supernatant was filtered through a 0.22 µm Millex-GP filter and applied on the appropriate column.

2.4.11 Purification of UDP-glucose pyrophosphorylase from *L. major*

2.4.11.1 Ni^{2+}-chelating chromatography

Recombinant *L. major* UGP carrying a C-terminal His$_6$-tag was expressed in *E.coli* BL21 (DE3) and lysates of a 2 litre culture prepared as described in 2.4.10.1. A 5 ml His-TrapHP Ni^{2+} column (Amersham Biosciences) was equilibrated with 5 column volumes (CV) buffer A (50 mM Tris/HCl pH 8.0, 300 mM NaCl) using a peristaltic pump. The lysate was passed over the column for 3 times at a flow rate of 1 ml/min and an aliquot of the flow through boiled with 2x Laemmli buffer for subsequent SDS PAGE analysis ((2.4.2). The column was washed with 10 CV buffer A and connected to an FPLC (Äkta FPLC, Amersham Biosciences). The following wash and elution steps were performed with filtered (0,8 µm cellulose acetate filter) and degassed buffers. After a further wash with 1 CV buffer A, unbound protein was eluted with 40 mM imidazole. 1 ml fractions were collected throughout the purification. The *L. major* UGP was eluted with 300 mM imidazole using a step gradient. The peak fractions containing the protein were pooled and subjected to a desalting step.

To clean the column, the gradient was increased to 500 mM imidazole to remove all protein. The column was washed with 10 CV buffer A and 10 CV water. For storage at 4°C, the column was equilibrated with 20% ethanol.

2.4.11.2 StrepII-affinity chromatography

A E.coli BL21 (DE3) lysate from 0,5 L culture containing a N-terminal StrepII tagged *L. major* UGP was prepared as described in 2.4.10.1. A 1 ml StrepTactin affinity column (IBA) was equilibrated with buffer A (50 mM Tris/HCl pH 8.0, 300 mM NaCl) using a peristaltic pump. The lysate was applied 5 times at a flow rate of 1 ml/min. Unbound protein was removed by washing with 10 CV buffer A and the column connected to an FPLC (Äkta FPLC, Amersham Biosciences). The following wash and elution steps were performed with filtered (0.8 µm cellulose acetate filter) and degassed buffers. Bound protein was eluted with buffer A containing 2.5 mM desthiobiotin. Protein fractions were pooled and analysed on SDS PAGE followed by Coomassie blue staining and Western blotting (2.4.5, 2.4.3). The StrepTactin column was regenerated in two subsequent steps with buffer R (50 mM Tris/HCl pH 8.0, 300 mM NaCl, 1 mM hydroxyl-azophenyl-benzoic acid) and buffer A. The column was washed with 3 CV water and stored in 20% ethanol.

2.4.11.3 Desalting column

The pooled fraction collected after the Ni^{2+}-chelating chromatography, were subjected to a desalting step using a FPLC (Äkta FPLC, Amersham Biosciences). All buffers were filtered (0,8 µm cellulose acetate filter) and degassed. A HiPrep 26/10 column (Amersham Biosciences) was equilibrated with 2 CV (1 CV=53 ml) of 50 mM Tris/HCl, pH 7.8, 10 mM MgCl2 at a flow rate of 3 ml/min but not exceeding a pressure of 0.28 MPa. The sample was applied and the peak fraction collected. The protein was aliquoted and flash frozen in liquid nitrogen for storage at -80°C.

The column was regenerated with 2 CV water and 1 CV 20% ethanol.

2.4.12 Size exclusion column

The oligomerisation status of the purified His-tagged UGP was analysed on a Superdex 200 HR 10/30 gel filtration column. The column was equilibrated in 2 CV (1 CV=24 ml) 50 mM Tris/HCl, pH 7.8, 10 mM $MgCl_2$. In gel filtration runs including the substrates for the UGP, the buffer was supplemented with 1 mM UTP, 1 mM 2-mercaptoethanol and 1 mM glucose-1 phosphate. All buffers were filtered with a 0.22 µm cellulose acetate filter and degassed. 100 µl of the purified, filtered (0,22µm cellulose acetate filter) UGP at a con-

centration of 4 mg/ml was applied to the column and eluted in 1 ml fractions at a flow rate of 0.5 ml/min. The fractions were analysed by Coomassie stained SDS PAGE, Western Blotting and by an *in vitro* activity assay (2.4.3, 2.4.5, 2.4.13.1)

To calibrate the column, two additional runs were performed using the protein standard kit from Sigma according to manufacturer's instructions. These were the same conditions (buffers, flow rate, etc) as for the UGP gel filtration. In a first run, bovine serum albumin (BSA) at a concentration of 10 mg/ml was applied to the column. In a second separate run a mixture of the two proteins bovine carbonic anhydrase and yeast alcohol dehydrogenase at concentration of 3 mg/ml and 5 mg/ml, respectively was used.

2.4.13 Activity assays of UGP

2.4.13.1 *In vitro* activity assay

The *in vitro* activity of the UGP was measured by coupled enzymatic assays. In the forward reaction, the reaction mixture contained 50 mM Tris/HCl pH 7.8, 10 mM $MgCl_2$, 1 mM 2-mercaptoethanol, 1 mM UTP, 1 mM glucose-1 phosphate, 1 mM NAD^+ and 0.05 units UDP-glucose dehydrogenase (Roche). In the reverse reaction, the following compounds were mixed: 50 mM Tris/HCl pH 7.8, 10 mM $MgCl_2$, 1 mM 2-mercaptoethanol, 50 mM UDP-glucose, 50 mM pyrophosphate, 25 mM $NADP^+$, 1 mM Glucose-1.6 biphosphate, 2.5 units phosphoglucomutase, 2.5 units glucose-6 phosphate dehydrogenase. The reaction was started by the addition of 2 ng purified protein in a total reaction volume of 750 µl or by the addition of 1µl to 25 µl parasite or bacterial lysate. The subsequent reduction of NAD^+ to $NADH+H^+$ was measured at 340 nm in a photospectrometer. The initial linear rates of cofactor reduction were used to calculate the enzyme activity by the conversion of the increase in OD_{340} nm to micromoles of $NAD(P)H+H^+$ production based on its extinction coefficient (ε= 3,4 $cm^2/\mu Mol$). The protein concentration was determined by BCA test (2.4.1). To determine the K_m values, one substrate was present at a fixed saturating concentration while the other substrate concentration was varied. The initial rates were plotted against the substrate concentration and the Microsoft Exel Solver was used to approximate the data to the Michael Menten equitation ($V=V_{max}([S]/([S]+Km)$). In addition, Lineweaver Burk plots were used to show the linear dependence and to calculate the K_m and V_{max} values.

In reactions using galactose-1 phosphate as substrate the following compounds were mixed: 50 mM Tris/HCl pH 7.8, 10 mM $MgCl_2$, 1 mM 2-mercaptoethanol, 1 mM UTP, 2 mM galactose-1 phosphate, 1 mM NAD^+, 0.05 units UDP-glucose dehyrogenase, 0.05

units UDP-galactose 4-epimerase. The reaction was started and monitored as described above.

2.4.13.2 *In vivo* activity assay

The *in vivo* activity of UGPs was tested by the complementation of the *E.coli* strain DEV6 *galU* lacking a functional UGP. A defect in the UGP renders the bacterium unable to grow on galactose containing MacConkey agar (base). Complementation restores the wild type phenotype and is indicated by a colour change of the colonies from white to red by the pH indicator phenol red and the size of colonies. However, this method does not allow a quantification of the *in vivo* activity.

UGP constructs cloned into a pET vector were transformed into competent *E.coli* DEV6 (2.5.10) and spread on LB/agar plates containing 100 µg/ml ampicillin. The plates were incubated overnight at 37°C. MacConkey (base) agar plates supplemented with 100 µg/ml ampicillin, 1 mM IPTG and either 2% galactose or 2% glucose as carbohydrate source were prepared. A few colonies from each LB/agar plates were streaked on one glucose- and one galactose-containing MacConkey agar plate. The addition of glucose to the MacConkey agar plates served as a control that the transformed plasmid did not exhibit a lethal phenotype on this kind of plates. The dishes were incubated at 37°C overnight. Big red colonies indicated a complementation of the UGP defect by the transformed construct.

2.4.14 Production of polyclonal *L. major* UGP antisera

2.4.14.1 Immunisation of rabbits

The production of a polyclonal serum was achieved by the immunization of 5 female New Zeeland rabbits (Charles River). The immunisation mixture was applied subcutaneously. For the priming, 500 µg purified full length *L. major* UGP recombinantly expressed in *E.coli* (2.4.11.1, 2.4.11.3) was mixed with 500 µl complete Freund's adjuvant. To obtain an emulsion, two syringes connected through a three-way valve were used. Equal volumes of the antigen and the adjuvant were filled in separate syringes, connected and mixed by first pressing the aqueous antigen solution into the oil of the adjuvant. The emulsion was subcutaneously applied at ten different points on the back of the rabbit.

After 3, 9 and 15 weeks, boosts were given containing 500 µg antigen and 500 µl incomplete Freund's adjuvant. The emulsion was prepared as for the priming and the emulsion was subcutaneously applied at 5 different points on the back of the rabbit. 10 ml blood was taken before the first immunisation and 10 days after each boost. The blood was

incubated at RT for 4 hours followed by an incubation over night at 4°C to allow agglutination. The serum was obtained by centrifugation of the clocked blood at 3600xg for 15 min at 10°C. The antibody titer of the serum was tested in an ELISA and the serum stored at -20°C.

2.4.14.2 Coating of *L. major* UGP on ELISA plates

96-well microtiter plates (U-from, Greiner) were coated with 100 ng per well recombinantly expressed and purified *L. major* UGP (5µg/ml) at RT for 1 hour. The plates were washed twice with PBS and blocked with 150 µl 1% BSA/PBS over night. After two washing steps, residual buffer was removed and the plates either used directly or stored at -20°C.

2.4.14.3 Determination of antibody titer in rabbit sera

A serial dilution of the antisera from 1:200 to 1:12800 in 1% BSA/PBS were prepared. The coated ELISA plates (2.4.14.2) were incubated with 20 µl/well rabbit antisera dilution. The preimmunsera were diluted 1:200 and 1:400 and incubated on the same microtiter plate. Two wells were treated with 20 µl anti-penta His mAb (Qiagen, 1:500) and another two wells with PBS as positive and negative control, respectively. Additional controls included the incubation without antisera as secondary antibody control and the treatment of an uncoated well with all used antibodies and buffers. After 1 hour at RT, the plates were washed 3 times and incubated with 10 µl/well secondary antibody dilution (α−rabbit HRP 1:2000, α−mouse HRP 1:2000) in 1% BSA/PBS for 1 hour at RT. The plates were washed three times with PBS and incubated with 40 µl ABTS (2,2''-Azino-di[3-ethylbenzthiazolinsulfonate] for 30 min. The ABTS was dissolved in ABTS buffer according to manufacturers instruction (Roche). The samples were analysed at 405 nm using the ELISA-Reader 'DigiScan' (Asys Hitech).

2.5 Molecular biological techniques

2.5.1 Precipitation of nucleic acids

DNA was precipitated from aqueous solutions by the addition of 1/3 volume 7.5 M ammoniumacetate (pH 5) or 0.1 volume of 3 M sodium acetate (pH 5.2) and 2.5 volumes ethanol (100%) for 1-2 hours at -80°C or over night at -20°C. After centrifugation (13000xg, 30 min, RT), the supernatant was decanted and the pellet washed with 500 µl

70% ethanol. The sample was centrifuged for additional 10 min and the supernatant completely removed. The pellet was dried and dissolved in water or TE.

2.5.2   Phenol Chloroform extraction

In order to remove proteins from DNA containing samples, the samples were extracted with phenol/chloroform and precipitated (2.5.1).

Thus, an equal volume of Roti^{TM}Phenol was added to the DNA sample, mixed and centrifuged at 13000xg, RT for 5 min. The upper aqueous solution was removed and combined with an equal volume of chloroform. The sample was again centrifuged (13000xg, 5 min, RT) and the DNA of the aqueous solution precipitated (2.5.1).

2.5.3   Hot phenol extraction

To improve the quality of _L. major_ mRNA, a hot phenol extraction was applied.

Equal volumes of Roti^{TM}Phenol and extraction buffer (100 mM LiCl, 100 mM Tris/HCl pH 8.0, 10 mM EDTA, 1% SDS, 3% PVV) were heated to 80°C until one phase was obtained. 1/10 volume of mRNA solution was added and mixed. The solution was combined with ¼ volume chloroform and centrifuged for 5 min at 13000xg. The upper phase was precipitated by the addition of 1/10 volume sodium acetate (pH 5.2) and 2 volumes ethanol (100%). After 30 min at -20°C, the sample was centrifuged (13000xg, 10 min, 4°C) and the dried pellet dissolved in 2 times the original volume water. The mRNA was further purified by the addition of 3 M LiCl and precipitated over night at 4°C. After centrifugation the pellet was washed with 5 volumes 80% ethanol. The dried pellet was resuspended in water. The quality of the mRNA was analysed by a RNA agarose gel electrophoresis (2.5.16).

2.5.4   Determination of DNA and RNA concentrations

DNA and RNA concentrations were determined photometrically and calculated from the absorbance measured at 260 nm: c(DNA) = absorbance(260 nm) x 50 µg/ml and c(RNA) = absorbance(260nm)x40 µg/ml.

Very low DNA concentrations were estimated on ethidium bromide plates by comparing the signal intensity with serial dilutions of a DNA sample with known concentration. 100 ml of 0.8% agaorse in TAE buffer was molten and cooled down to 50°C. The solution was supplemented with 1 µg/ml ethidium bromide and poured in 5 Petri dishes. After the plates hardened, they were kept at 4°C. The standard was prepared by seven serial dilutions in 100 mM EDTA in a range of 10 ng/µl to 200 ng/µl and stored at -20°C.

1μl of standard and sample dilutions was carefully spotted on the agar and incubated for 15 min at RT. The DNA was detected at 302 nm using the 'Easy Enhanced Analysis System' (Herolab).

2.5.5 Agarose gel electrophoresis of DNA

DNA samples were diluted in 5xGEBS and separated on horizontal agarose gels (0.6 to 1.5 % agarose in TBE buffer). To extract DNA fragments from agarose gels, ethidium bromide containing agarose gels in TAE buffer were used. Electrophoresis was performed at 5 V/cm in TBE buffer. The DNA was detected after staining in ethidium bromide (50 μg/ml) at 302 nm. For documentation the 'Easy Enhanced Analysis System' (Herolab) was used.

2.5.6 General cloning techniques

2.5.6.1 Restriction enzyme digest and dephosphorylation of DNA

Restriction enzymes and reaction buffers were used according to the manufacturers instructions (New England Biolabs). For preparative digests, 2 μg of DNA were incubated with 5 U of enzyme in a total volume of 50 μl with the added volume of enzyme less than 10%. The reaction was incubated over night at 37°C.   For analytical digests, 1 μg of plasmid DNA was incubated for 2 hours at 37°C with 5 U of enzyme.

The 5′-phosphate groups of vector DNA that was linearized with one restriction enzyme, were removed to avoid self-ligation of the vector fragments. Per μg of vector DNA 1 U of calf intestine alkaline phosphatase (NEB) was directly added to the restriction enzyme mix.

2.5.6.2 Isolation of DNA fragments from agarose gels

To isolate DNA fragments after restriction enzyme digest, DNA was separated on an agarose gel and the desired fragments were excised from the gel. For further DNA purification the 'Qiaquick PCR Purification Kit' (Qiagen) was used according to the manufacturers instructions. The gel slice was completely dissolved in 300 μl buffer QG per 100 mg gel at 50°C and applied to a Qiaquick column. The column was centrifuged (1 min, 13000xg) and the flow through discarded. After one washing step with 500 μl buffer PE, bound DNA was eluted in 50 μl EBC (10 mM Tris-Cl pH 8.5).

2.5.6.3 Ligation of DNA

30 ng of digested (and if necessary dephosphorylated) vector DNA and a 3 molar excess of the respective insert were incubated with 1 Weiss-U of T4-DNA-Ligase (NEB) in 20 µl ligation buffer (50 mM Tris-HCl pH 7.8, 10 mM MgCl$_2$, 1 mM ATP, 10 mM DTT, 25 µg/ml BSA). The ligation mix was incubated overnight at 16°C and transformed into competent *E.coli* cells.

The sequencing of constructs generated by PCR amplification steps was done by the companies MWG and GATC.

2.5.7   Analytical plasmid preparation

For analytical plasmid preparations, the 'Qiaprep spin Miniprep Kit' was used according to the manufacturers instructions. 3 ml LB medium containing the appropriate antibiotic were inoculated with a single bacterial colony from a selective agar plate and incubated for 12-16 h at 37°C and 250 rpm. 2 ml of the culture were pelleted by centrifugation (1 min, 13000xg, RT) and resuspended in 250 µl buffer P1 (50 mM Tris/HCl pH 8.0, 10 mM EDTA, 100 µg/ml RnaseA). 250 µl of buffer P2 (1 % SDS, 0.2 M NaOH) and 350 µl of chilled buffer P3 (3.0 M potassium acetate, pH 5.5) were added, each buffer addition followed by a cautions mixing step. The samples were centrifuged (10 min, 13000xg, RT) and the supernatant applied on a Qiaprep spin column. The column was washed with 750 µl buffer PE and the DNA eluted with 50 µl TE buffer.

2.5.8   Preparative plasmid preparation

For plasmid isolation in preparative scale the 'Qiagen plasmid Kit Midi' was used according to the manufacturers instructions.
A 100 ml LB medium containing the appropriate antibiotic was inoculated with a single bacterial colony from a selective agar plate for 12-16 h at 37°C and 200 rpm. The culture was centrifuged (15 min, 6000xg, 4°C) and the bacterial pellet resuspended in 4 ml buffer P1 (50 mM Tris/HCl pH 8.0, 10 mM EDTA, 100 µg/ml RnaseA). After the addition of 4 ml buffer P2 (1 % SDS, 0.2 M NaOH) and cautious mixing the bacterial lysis was allowed to proceed for 5 min at room temperature. Then 4 ml of chilled buffer P3 (3.0 M potassium acetate, pH 5.5) were added, the sample was again cautiously mixed, incubated on ice for 15 min and centrifuged (30 min, 20000xg, 4°C). The supernatant was poured over a filter and applied to a QIAGEN-Tip 100 column equilibrated in buffer QBT (750 mM NaCl, 50 mM MOPS pH 7.0, 15% isopropanol, 0.15% (v/v) TritonX-100). After two washing

steps with 10 ml buffer QC (1 M NaCl, 50 mM MOPS pH 7.0, 15% isopropanol) the bound plasmid DNA was eluted in 5 ml buffer QF (1.25 M NaCl, 50 mM Tris-HCl pH 8.5, 15% isopropanol) and 3.5 ml isopropanol were added to the eluent. After centrifugation (30 min, 20000xg, 4°C), the pelleted DNA was washed in 2 ml ethanol (70 %) and recentrifuged (15 min, 20000xg, 4°C). The dried DNA pellet was dissolved in 100 µl TE buffer and stored at -20°C. The DNA concentration was determined as described in 2.5.4

2.5.9   Transformation of competent *E.coli*

2.5.9.1   Transformation of chemically competent *E.coli*

100 µl of competent *E.coli* were thawed on ice and 10 ng of plasmid DNA or 20 µl of ligation mix (2.5.6.3) were added. The mix was left on ice for 30 min, subjected to a 45 sec heat shock at 42°C and incubated on ice for 2 min. 1 ml of LB-medium was added, the cell suspension was incubated at 37°C for 1 hour and plated on selective LB-agar plates containing the appropriate antibiotics.

2.5.9.2   Transfomration of electrocompetent *E.coli*

Electrocompetent XL1-Blue MRF' were purchased from Strategene and electroporated according to the manufacturers instructions. 40 µl competent *E.coli* were thawed on ice and mixed with 5 µl of a ligation reaction. The mixture was transferred into a 0.1 cm cuvette and placed into a Bio-Rad electroporator. The sample was pulsed once with 1.7kV, 200 ohms and 25 µF. Immediately, 960 µl of sterile SOC medium was added and the cell suspension transferred to a 15 ml culture tube. After 1 hour incubation at 37°C (200 rpm), the transformation was spread on selective LB-agar plates containing the appropriate antibiotic.

2.5.10 **Preparation of chemically competent *E.coli***

Chemically competent cells were prepared according to a protocol published by Molthoff *et al.,* (1990). *E.coli* were grown on LB agar plates containing the appropriate antibiotic. One colony was inoculated in 2 ml SOB and incubated over night at 37°C. 200 ml SOB medium were inoculated with 1 ml of the starter culture and incubated for 1-2 days (200 rpm) at 18°C until an OD_{600nm} of 0.6 was reached. The culture was centrifuged at 2000xg for 10 min at 4°C. The supernatant was removed and the pellet resuspended in 1/3 of the original volume cooled TB (250 mM KCl, 10 mM Hepes, free acid, 15 mM $CaCl_2$, 55 mM $MgCl_2$). The solution was centrifuged as before and the pellet resuspended in 1/12 of the

original volume TB. DMSO was added to a final concentration of 7% and the cells divided into 100 µl batches. The batches were immediately flash frozen in liquid nitrogen and stored at -80°C.

2.5.11 Preparation of *E.coli* DMSO stocks

For long time storage, 930 µl of an *E.coli* over night culture was mixed with 70 µl DMSO (final 7%) and frozen at -80°C.

2.5.12 Polymerase chain reaction (PCR)

2.5.12.1 Amplification of fragments for cloning

To amplify DNA-fragments by PCR reaction, 10 ng of plasmid DNA or genomic DNA, sense and antisense primer (25 pmol each), 2,5 U *Pfu*-polymerase (Stratagene), dNTP´s (20 µM each) and 5% DMSO were mixed in a total volume of 50 µl 1xPCR buffer (Stratagene). The PCR-mix was initially denatured at 95°C for 2 min in a thermocycler followed by 8 consecutive cycles of: 45 sec denaturing at 95°C, 45 sec annealing of the oligonucleotide primers (5°C below their calculated melting point) and elongation at 72°C for 120 sec per kb of synthesis product. Another 17 cycles followed with increasing the elongation time in each round for 10 sec. PCR reaction were either performed using the 'GeneAmp System 2400' (Perkin Elmer) or the 'T1-Thermocycler' (Biometra). The samples were subjected to a PCR clean up reaction using the 'Qiaquick PCR purification kit'. The PCR reaction was mixed with 5 volumes of buffer PB and applied on a Qiaquick column. After centrifugation for 1 min at 13000xg, the column was washed with 750 µl buffer PE and bound DNA fragments eluted in 50 µl TE. The DNA concentration of the eluent was determined on ethidium bromide agarose plates (2.5.4) and directly used for restriction digests (2.5.6.1).

2.5.12.2 Analysis of *L. major* ugp gene deletion mutants by polymerase chain reaction

To analyse the correct insertion of the resistant marker cassettes into the *Leishmania* genome, the obtained clones were subjected to a 5' and 3' PCR reaction. In the 5' PCR reaction, a sense oligonucleotide primer (ACM96) was designed that bound 5' to the 5' flanking region used for homologous recombination. The antisense primer (ACM99: Hyg, ACM101: Phleo) was directed against the 5' end of the resistance marker to yield an PCR product of about 1.5 kb. In the 3' PCR reaction, the antisense primer (ACM 94) annealed to a sequence 3' of the 3' flanking region used for homologous recombination,

whereas the sense primer was directed against the 3' end of the resistant marker (ACM 100: Hyg, ACM102: Phleo). As for the 5' end the PCR product encompassed 1500 nucleotides. In a 20 µl reaction, 10 ng genomic DNA, 4 pmol of sense and antisense primer, dNTP's (20 µM each), 0.5 U *Taq* polymerase and 5% DMSO were mixed in 1x PCR buffer (Sigma). After 7 min of a initial denaturation step at 95°C, the PCR-mix was incubated in a Thermocycler for 30 of the following cycles: 45 sec denaturation at 95°C, 45 sec annealing at 60°C, 1 min elongation at 72°C. In a final step, a 10 min elongation at 72°C was applied. The samples were loaded on a 1% agarose gel and the DNA visualized with ethidium bromide (2.5.5). Clones positive for both reactions were subjected to Southern Blot analysis (2.5.14).

2.5.12.3 Preparation of digoxigenin (DIG) labelled DNA probes

For the synthesis of DIG-labelled DNA probes, a dNTP mix containing 2 mM dATP/dGTP/dCTP, 1.3 mM dTTP and 0.7 mM DIG-11-dUTP was prepared. To amplify the probes, 10 ng of plasmid DNA (pCR2.1hyg, pCR2.1phleo, p5'UTR, pcDNA3-*L. major*UGP), 4 pmol of sense and anitsense primer (Hyg probe: ACM85/ACM86; Phleo probe: ACM87/ACM88; UGP probe: ACM52/ACM53, 5'UTR probe ACM 54/ACM62), 5 µl of dNTP mix and 1.25 U *Taq* polymerase in a total volume of 50 µl in 1x Taq PCR buffer were mixed. After 3 min of an initial denaturation step at 95°C, the PCR-mix was incubated in a Thermocycler for 30 of the following cycles: 10 sec denaturation at 95°C, 30 sec annealing at 58°C, 1 min elongation at 72°C. In a final step, a 7 min elongation at 72°C was applied. Except for the UGP probe that was gel purified (2.5.6.2) after synthesis, the PCR products were directly used in Southern Blot analysis.

2.5.13 Isolation of genomic DNA from *Leishmania*

To isolate genomic DNA from *Leishmania*, $1x10^8$ cells were centrifuged (1300xg, 10 min 4°C) and resuspended in 400 µl TELT (50 mM Tris/HCl, pH 8.0, 62.5 mM EDTA, 2.5 M LiCl, 4% Triton X-100). After an incubation for 5 min at RT, 400 µl Roti^TM^Phenol was added and mixed for 5 min at 4°C. To separate the phases, the solution was centrifuged for 10 min at 14000xg and 4°C. The upper phase was combined with 400 µl chloroform/isoamylalcohol (24:1), incubated for 5 min at 4°C and centrifuged as before. The DNA of the aqueous phase was mixed with 1 ml ethanol (100%), incubated on ice for 5 min and centrifuged. The supernatant was removed and the pellet washed with 1 ml 70% ethanol. After centrifugation, the dried pellet was resuspended in 100 µl TE and the DNA stored at 4°C.

2.5.14 Southern Blot analysis

2.5.14.1 Preparation of the blots

For the preparation of the blots, 2.5 µg DNA was digested with 5 U enzyme in a total volume of 25 µl at 37°C over night. The complete digest and 1 ng of PCR product of the corresponding DNA probe were separated on a 0.7% agarose gel containing 5 µg/ml ethidium bromide. The gel was incubated for 15 min in 250 mM HCl to depurinate the DNA and two times for 10 min in denaturing solution (0.5 M NaOH, 1.5 M NaCl).

The DNA fragments were transferred to a nylon membrane by capillary forces in denaturing solution over night. The set up is described in the following:

1 glass plate

1 thick whatmann filter paper soaked in denaturing solution

1 thin whatmann filter paper soaked in denaturing solution

agarose gel up side down

nylon membrane, soaked in denaturing solution

3 thin whatmann filter paper, soaked in denaturing solution

6 layer dry cellulose filters

glass plate

The next day, the membrane was washed for 10 min in 50 mM sodium phosphate buffer pH 7.2 at RT and dried. The DNA was fixed to the membrane by UV crosslinking (Stratalinker, Stratagene). The membrane was hybridised and developed as described in 2.5.14.2 and 2.5.14.3.

2.5.14.2 Hybridisation of Southern Blots

The crosslinked membrane was prehybridised in high SDS (7% SDS, 50% formamid, 5x SSC, 50 mM NaPO4, pH 7.0, 0.1% N-lauroylsarcosine, 2% blocking solution (Roche)) for 1 hour at 42°C. The DIG-labelled probe was combined with an equal volume of TE, denatured for 5 min at 95°C and immediately placed on ice. The probe solution was incubated with the membrane in 10 ml high SDS over night at 42°C. After the hybridisation, the membrane was rinsed once in 1 x SSC (0.1% SDS) and washed two times in 2xSSC (0.1% SDS) for 15 min at RT. After two washing steps with 0.1x SSC (0.1% SDS) for 30 min at 65°C, the bound probe was detected with CSPD (2.5.14.3).

2.5.14.3 Chemiluminescence detection

The membrane was rinsed once in buffer 1 (0.1 M maleic acid, 0.15M NaCl, pH 7.5) and blocked for 30 min with buffer 2 (10x blocking solution (Roche) diluted 1:10 in buffer 1). The bound probe was detected with AP-coupled α–DIG Fab fragment (1:10000 in buffer 2) for 10 min at RT. The membrane was washed three times with buffer 1 containing 0.3% Tween. After equilibration in buffer 3 (100 mM Tris/HCl pH 9.5, 100 mM NaCl), the membrane was incubated with 10-12 drops of CSPD (Disodium 3-(4-methoxyspiro {1.2-dioxetan-3.2'-85'-chloro} –tricyclo [3.1.1.13.7] decan}-4-yl)phenylphosphate, Roche) for 15 min at 37°C. The CSPD was removed and the membrane sealed into plastic foil. Due to the dephosphorylation of the CSPD by the AP activity, light of 477 nm was emitted. The signals were visualized on Hyperfilms MP.

2.5.15 Isolation of total RNA and mRNA

For the purification of total RNA, the 'RNeasy Midi Kit' was used according to manufacturers instructions. 100 mg cells were pelleted and resuspended in 2 ml RLT buffer containing 20 µl 2-mercaptoethanol (14.5 M stock solution) and passed over two Qiashredder columns (Qiagen) to lyse the cells. The lysate was carefully mixed with 1 volume of 70% ethanol. The sample was applied to the RNeasy midi spin column and centrifuged for 5 min at 4000xg. The flow through was discarded and the column washed once with 3.8 ml buffer RW1 and twice with 2.5 ml buffer RPE by centrifugation. Total RNA was eluted in two steps with 150 µl RNase-free water each time.

mRNA was isolated from the purified RNA using the 'Oligotex mRNA Mini Kit' according to manufacturers instructions. The volume of the total RNA was adjusted to 250 µl with RNase free water, mixed with 250 µl buffer OBB (20 mM Tris/HCl pH 7.5, 1M NaCl, 2 mM EDTA, 0.2% SDS,) and 15 µl Oligotex suspension (1 mg polysteren latex particles coupled to $dC_{10}T_{30}$ oligonucleotides in 10 ml of 10 mM Tris/HCl pH 7.5, 500 mM NaCl, 1 mM EDTA, 0.1 % SDS, 0.1% NaN_3). The buffer QBB and the Oligotex suspension were prewarmed to 37°C. To disrupt secondary structures of the RNA, the sample is heated to 70°C for 3 min. The hybridisation of the poly(A)-RNA to the Oligotex beads was mediated for 10 min at RT. The Oligotex-mRNA complex was centrifuged for 2 min at 13000xg and the supernatant was removed. The beads were resuspended in 400 µl buffer OW2 (10 mM Tris/HCl pH 7.5, 150 mM NaCl, 1 mM EDTA) and applied on a spin column. The column was centrifuged for 1 min 13000xg and the flow through discarded. After one washing step with 400 µl buffer OW2, mRNA was eluted by the addition of 40 µl buffer OEB (5 mM Tris/HCl pH 7.5) prewarmed to 70°C. To achieve a maximum yield, the elution step was repeated and the eluats combined.

2.5.16 Agarose gel electrophoresis of RNA

RNA was separated on a 1.2 % agarose gel according to a protocol from Kevil *et al.*, (1997) that avoids the use of formamide. The agarose was dissolved in 1x TBE buffer including 1 µg/ml ethidium bromide. The samples were mixed with 6x loading buffer (0.25% w/v bromphenol blue, 0.25% w/v xylene cyanol, 30% w/v glycerol, 1.2% SDS, 60 mM Sodium phosphate (pH 6.8)), denatured for 5 min at 75°C and immediately loaded on the agarose gel. The gel was electrophoresed at 7-10 V/cm for 90 min and analysed using the 'Easy Enhanced Analysis System' (Herolab).

2.5.17 Generation of a cDNA library

The *L. major* cDNA library was constructed using the 'pCMV-ScriptXR cDNA library construction kit' from Stratagene. In contrast to the manufacturers instructions, the size fractionation was achieved by agarose gel electrophoresis. This change allowed the generation of the cDNA library without the use of radiolabeled nucleotides.

In the reverse transcription of the mRNA, a 50 base oligo(dT) linker primer containing a *Xho*I restriction site and methylated dCTP was used. After second strand synthesis, an *Eco*RI adapter was annealed to the 5' end of the DNA and the cDNA digested with XhoI. Since *Xho*I only cuts in the linker primer but not in the hemimethylated cDNA, the cDNA can be cloned unidirectional into the eukaryotic expression vector pCMV-Script pre-digested with *Eco*RI and *Xho*I.

For the first strand cDNA synthesis, 5 µg of mRNA were mixed with 5 µl first strand buffer, 3 µl of first strand methyl nucleotide mixture, 2 µl of linker primer (1.4 µg/µl),1 µl of RNase Block Ribonuclease Inhibitor (40 U/µl) and 1.5 µl StrataScript reverse transcriptase (50 U/µl) in a total volume of 50 µl. After incubation for 1 hour at 42°C, 20 µl of 10x second strand buffer, 6 µl of second strand dNTP mixture, 2 µl of RNaseH (1.5 U/µl) and 11 µl of DNA polymerase I (9 U/µl) and 116 µl of RNase free water were added and incubated for 2.5 hours at 16°C to allow the second strand synthesis. The cDNA was blunted by the addition of 23 µl blunting dNTP mix and 2 µl of cloned *Pfu* DNA polymerase. After 30 min at 72°C, the reaction was extracted with phenol/chloroform and precipitated over night by the addition of sodium acetate and ethanol (2.5.1). The dried pellet was resuspended in 9 µl of *Eco*RI adapter, 1 µl 10x ligase buffer, 1 µl of 10 mM ATP and 1 µl of T4 DNA ligase (4U/µl). The reaction was incubated for 2 days at 4°C followed by a heat inactivation for 30 min at 70°C. The phosphorylation of the *Eco*RI ends was achieved by adding 1 µl 10x ligase buffer, 2 µl of 10 mM ATP, 6 µl water and 1 µl of T4 polynucleotide kinase (10 U/µl) and incubation for 30 min at 37°C. As for the ligase, the kinase was heat inactivated for 30 min at 70°C. The cDNA was digested with

*Xho*I for 1.5 hours at 37°C by the addition of 28 µl *Xho*I buffer supplement and 3 µl of *Xho*I (40 U/µl).

The reaction was precipitated over night at -20°C by adding 5 µl 10xSTE buffer (1 M NaCl, 200 mM Tris/HCl pH 7.5, 100 mM EDTA) and 125 µl of 100% ethanol. The dried pellet was resuspended in 20 µl 5 mM Tris/HCl pH 8.0/ 2 mM EDTA and separated on a 0.9% TAE agarose gel containing 5 µg/ml ethidium bromide. DNA fragments of 500-5000 bp were isolated using the 'Qiaquick Gel Extraction kit' (2.5.6.2).

150 ng purified cDNA was ligated into 300 ng pre-digested pCMV-Script vector for two days at 4°C. The ligation reaction was precipitated by the addition of ammonium acetate and 100% ethanol (2.5.1). The dried pellet was resuspended in 10 µl water and electroporated into 80 µl XL-1 blue MRF' electrocompetent *E.coli* cells (2.5.9.2). The transformation was spread over 80 LB agar plates supplemented with 50 µg/ml kanamycin. About 20 000 colonies per plate were obtained. The plates were soaked in 10 ml LB medium. 1 ml DMSO stocks (7% DMSO final) of each plate were prepared and stored at -80°C (2.5.11). 2 ml of each culture were used to prepare plasmid DNA (2.5.7). The rest of the culture was kept as 2 ml pellets at -20°C. One plate referred to one cDNA library pool.

2.5.18 Complementation cloning

Complementation cloning is used to isolate a specific gene from a cDNA library. A cell line defective in the desired gene, is transfected with pools of the cDNA library. Pools containing the appropriate plasmid DNA restore the wild type phenotype, which can be detected by specific antibodies in immunocytochemistry. To enrich the plasmid DNA of the *L. major* UDP-galactose transporter the following steps were applied:

The pools of the cDNA library and a plasmid encoding the rat glucuronyltransferase (pEFBos-GlcAT) were transfected in CHO Lec8 cells lacking a functional UDP-galactose transporter (2.2.2). After 48 hours, the reexpression of galactose on the cell surface was detected in immunocytochemistry using the mAb L2-412 (2.2.3). Positive pools were subdivided (sibling selection). Therefore, a small aliquot of the corresponding DMSO stock (2.5.11) was inoculated into 3 ml LB medium and depending on the desired size of the subpools x µl spread on LB agar plates containing 50 µg/ml kanamycin. After over night incubation at 37°C, the colonies were soaked off the plates. The culture was used to prepare plasmid DNA and new DMSO stocks. The plasmid DNA was again transfected and the procedure repeated until the pools size allowed the analysis of single colonies.

3 Results

3.1 Identification of the target gene

3.1.1 Cloning strategy

In order to identify the UDP-galactose transporter of *L. major*, complementation cloning in CHO Lec8 cells, which lack the UDP-galactose transporter (Deutscher *et al.*, 1986) was performed. In CHO WT cells, the UDP-galactose transporter transports the activated sugar, UDP-galactose, from the cytosol into the lumen of the Golgi apparatus. In the Golgi, UDP-galactose functions as a substrate of galactosyltransferases. The galactosy-lated glycans can be further modified by sialyltransferases (see Figure 8). In the case of the neuronal cell adhesion molecule (NCAM), the homopolymer of α2,8-linked sialic acids, the polysialic acid, can be added by polysialyltransferases. CHO Lec8 cells that lack a functional UDP-galactose transporter are unable to generate the acceptor struc-tures for the subsequent sialylation and polysialylation reactions (see Figure 8).
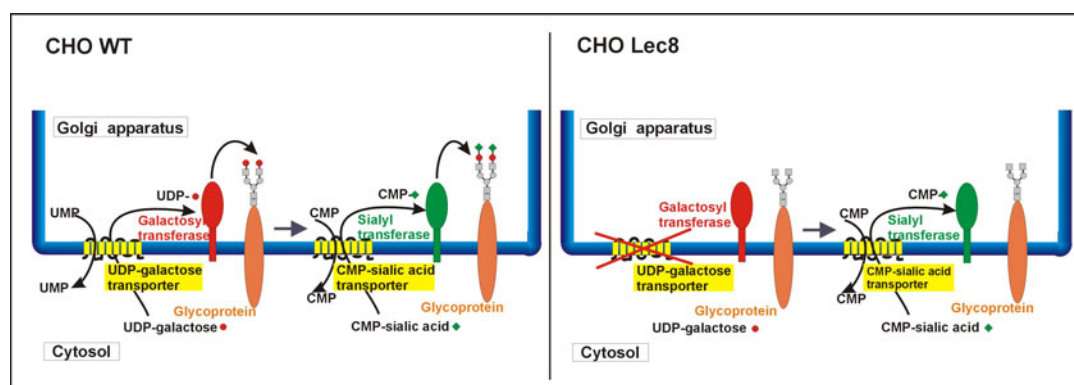
Figure 8. **Comparison of CHO WT and CHO Lec8 cells**. Due to the missing UDP-galactose transporter in CHO Lec8 cells, no galactosylation and sialylation takes place.

Reconstitution of the UDP-galactose transport activity in Lec8 cells restores the wild type situation resulting in the reexpression of galactosylated and (poly-) sialylated glycans. A *L. major* cDNA library was constructed and transfected into CHO Lec8 cells for the isolation of the *L. major* UDP-galactose transporter by complementation cloning. In immunocytochemistry, complementation could be detected either with the monoclonal antibody (mAb) 735, specifically recognising polysialic acid (polySia) or with the mAb L2-412, which recognises glucuronic acid ß1,3-linked to galactose. This epitope is normally not present in CHO cells but can be generated by transfection of a plasmid encoding a rat glucuronyltransferase (pEFBos-GlcAT, Terayama *et al*, 1997) into these cells. Moni-

toring of the complementation process via mAb L2-412 therefore requires co-transfection of the pEFBos-GlcAT plasmid DNA (see Figure 9).
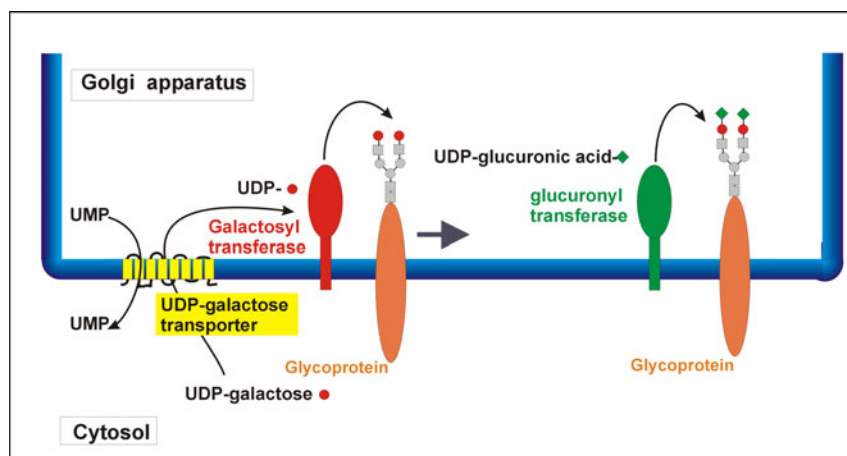
Figure 9 Principle of complementation cloning in CHO Lec8 cells. By coexpression of a functional UDP-galactose transporter and a glucuronyltransferase, the epitop recognized by the mAb L2-412 (glucuronic acid ß1,3-linked to galactose) is formed and can be detected.

A problem in association with this cloning strategy resided in the fact that these highly sensitive monitoring systems demonstrated a basal (even so very low) galactosylation capacity of the CHO Lec8 cells. Further optimisation steps were therefore required to improve the signal-noise ratio in the experimental system.

3.1.1.1   Optimisation of cell culture and antibody staining conditions

CHO Lec8 cells have been selected after chemical mutagensis using the cytotoxity of plant lectins (Stanley *et al*., 1981). Due to the missing terminal glycosylation they show resistance to the sialic acid binding lectin WGA (wheat germ agglutinin) and the galactose binding lectins European mistletoe and Ricinus communis agglutinin. Assuming that the lacking selection pressure during culturing of Lec8 cells may have let to the appearance of revertants, the cells were resubmitted to the lectin selection procedure (2.2.6.2). However, this treatment did not reduce the background galactosylation.

In a second approach, a panning step was carried out with the help of the mAb 735 immobilised on Petri dishes (2.2.6.2). Using this technique, polySia positive cells that bind to the coated Petri dish can be separated from polySia negative cells that remain in the supernatant. However, overlaying of CHO Lec8 cells resulted in 100% binding to the Petri dishes.

Finally, also the subcloning of CHO Lec8 cells did not reveal a cell line with blocked galactosylation. Together these experiments clearly demonstrated that Lec8 cells exhibited a basal galactosylation capacity, which was not sufficient to limit growth of cells in

the presence of cytotoxic lectins but detectable, if highly sensitive surface staining methods were applied.

In order to solve the problem the staining protocol was adjusted to generate an optimal signal to noise ratio, which allowed the clear differentiation between complementation and background galactosylation in immunocytochemistry. As a first step, different staining procedures with the mAb 735 were tested. Because, the signal intensity with an alkaline phosphatase (AP)-coupled secondary antibody was not high enough, a signal amplification step using a biotinylation reaction with biotintyramid was applied (2.2.3). Biotin was detected with AP-conjugated streptavidin and the substrate Fast Red. However, the amplification step also augmented the background staining (data not shown). This was also the case, if the mAb L2-412 was used to monitor complementation (see Figure 10 a). However, the direct detection of the mAb L2-412 with an AP-coupled secondary antibody and development with the substrate Fast Red revealed a good signal to noise ratio (see Figure 10 b and compare Figure 13 b, c lanes 2 and 3). This protocol was used to identify the *L. major* UDP-galactose transporter by complementation cloning.
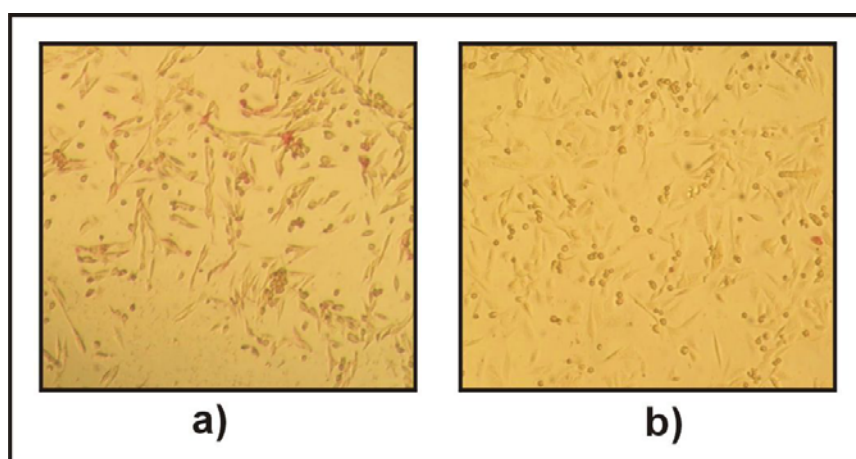
Figure 10 Optimisation of the CHO Lec8 cell staining protocol. The cells were transfected with pEFBos-GlcAT encoding a rat glucuronyltransferase and analysed by immunocytochemistry. In a) the cells were stained with mAb L2-412 and HRP-coupled secondary antibody. The peroxidase activity of the HRP-coupled secondary antibody generates biotin radicals upon incubation with biotintyramid that biotinylate near by structures. Biotin was detected with AP-conjugated streptavidin and the substrate Fast Red. In b) the epitope was detected without the additional amplification step using the mAb L2-412 and AP-conjugate secondary antibody.
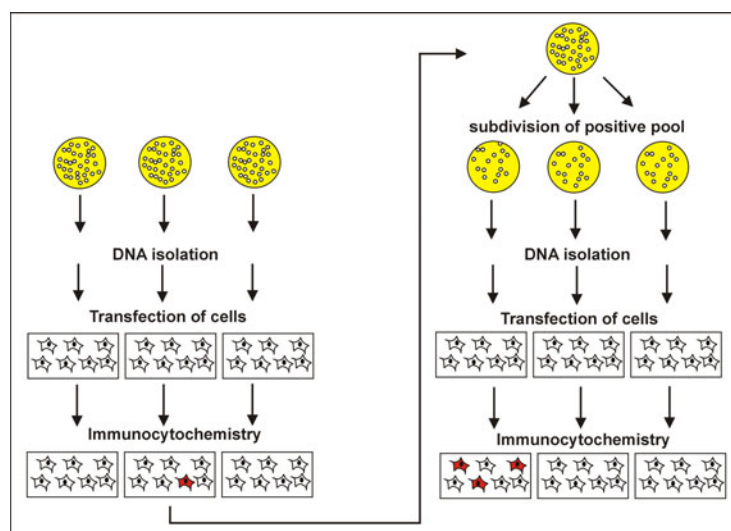
3.1.2 Generation of a *L. major* cDNA library

Procyclic promastigote *Leishmania major* upregulate galactose containing side chain modifications of the virulence factor LPG. In order to generate a cDNA library containing enzymes involved in the galactosylation of phosphoglycans, mRNA from procyclic promastigote *L. major* was isolated (2.5.15). The mRNA was further purified by a hot phenol extraction followed by a LiCl precipitation to improve the reversed transcription into unidirectional cDNA (2.5.3). The cDNA was size fractionated and fragments between 500 bp and 5000 bp were ligated into the pCMV-Script vector, pre-digested with *Eco*RI and *Xho*I. The ligation reaction was transformed into electrocompetent XL-1 blue MRF' *E.coli* cells (2.5.17). 86 pools of 20 000 independent colonies were generated yielding a total number of 1.7 million independent clones. A DMSO stock and a plasmid mini-preparation of each pool was prepared (2.5.7, 2.5.11). The pCMV-Script vector is a mammalian expression vector driven by the human cytomegalovirus (CMV) immediate early promoter and promotes constitutive expression of cloned inserts in the mammalian cell. Since the vector does not contain an ATG initation codon, only cDNA inserts containing start codons are expressed.

3.1.3 Complementation cloning in CHO Lec8 cells

To isolate a cDNA that complements the CHO Lec8 cell defect, plasmid DNA of 22 pools was transfected, with each pool consisting of 20 000 independent colonies. Plasmids encoding the *Arabidopsis thaliana* (*A.th.*) UDP-galactose transporter 2 (p*Ath*-UGT2, Bakker et al 2004, Figure 12 f) and the empty vector pCMV-Script (Figure 12 h) were transfected as positive and negative controls, respectively. Cotransfection of the plasmid pEFBos-GlcAT enabled immunocytochemistry with the mAb L2-412 (see 3.1.1 and 2.2.3). Positive cells stained red after incubation with alkaline AP-coupled secondary antibody and the AP substrate Fast Red.

Compared to the empty vector control, eight positive pools were identified (Figure 12 a). The positive pool # 17 was selected for further sibling selection (Figure 11 and 2.5.18). Therefore, an aliquot of the corresponding *E.coli* stock was subdivided into 27 pools and amplified on LB/agar plates. 15 pools of 1200-1500 (# 17.1 - 17.15) and 12 pools of about a 100-120 independent colonies (# 17.16 – 17.27) were obtained. The colonies were combined and plasmid DNA and *E. coli* stocks were prepared from each culture. The DNA of the smaller pools (# 17.16 - 17.27) was combined to one pool of 1200 colonies.

Figure 11 Principle of sibling selection. The pools of a *L. major* cDNA library were transfected in CHO Lec8 cells and analysed by immunocytochemistry. A positive pool was identified (indicated by red stained cells) and the corresponding *E. coli* stock further subdivided. The cDNA of subpools was again transfected into CHO Lec8 cells. The procedure was repeated until a single clone was obtained.

The pools were transfected in CHO Lec8 cells and analysed by immunocytochemistry as described before. One positive pool was detected. Since this pool was the combined pool # 17.16 – 17.27 (Figure 12b), the DNA of the 12 individual pools was transfected in the consecutive round. Again, one pool was positive (# 17.22, Figure 12 c) and the corresponding *E. coli* stock was further subdivided into 19 pools of 50-60 independent colonies. To conserve the individual colonies, a replica plate of each pool was prepared. After transfection of the plasmid DNA and immunocytochemistry, four pools showed a clear enrichment of a complementing cDNA (17.22.14; 17.22.16, 17.22.23; 17.22.27; Figure 12d). The individual colonies of one pool (17.22.14) were picked and grouped into 9 pools of 7 colonies. Again, a replica LB/agar plate of the single colonies was prepared. The analysis of the pools identified 1 positive pool (17.22.14 E, Figure 12e). The plasmid DNA of the 7 individual clones was transfected and two positive clones were detected by immunocytochemistry (17.22.14 E1; 17.22.14E2, Figure 12f). To confirm the complementing activity, single colonies from each clone were prepared and the DNA again transfected into CHO Lec8 cells. All colonies derived from these two clones were positive and named pACM1. Table 1 gives a summary of the number of screened clones and positive pools in each round.

round	number of pools	number of colonies/pool	number of positive pools
1	22	~20000	8
2	16	1200-1500	1
3	12	100-150	1
4	19	50-60	4
5	9	7	1
6	7	1	2

Table 1 Summary of the sibling selection procedure. The table indicates the numbers of screened pools, of clones per pool, and of identified positive pools per complementation cloning round.
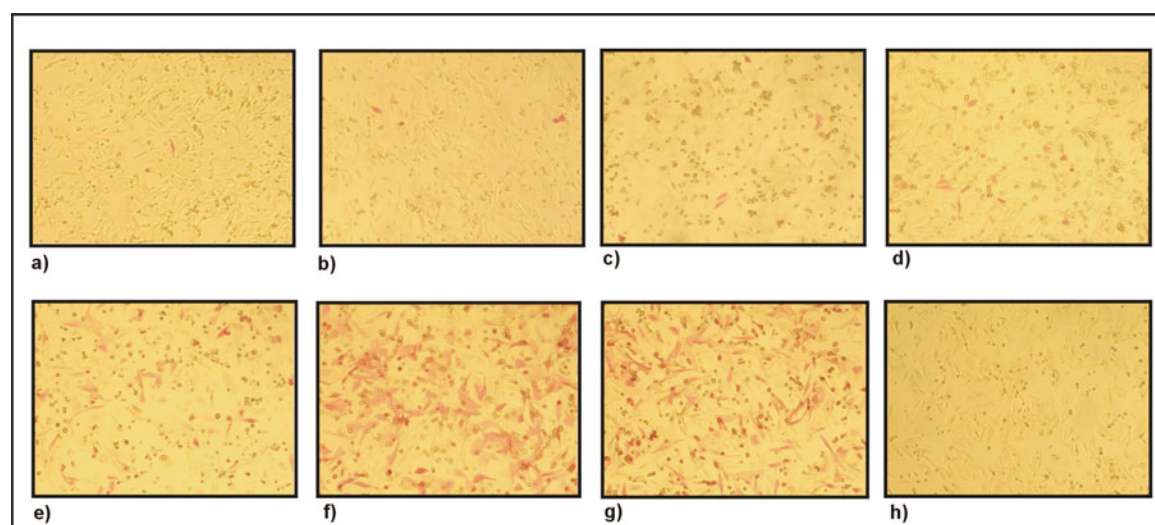
Figure 12 Identification of a *L. major* cDNA clone complementing CHO Lec8 cells. CHO Lec8 cells were transfected with pEFBos-GlcAT encoding a rat glucuronyltransferase and a pool of the *L. major* cDNA library containing a) 20 000, b) 1200-1500 (17.16-27) c) 100-150 (17.22), d) 50-60 (17.22.14) and e) 7 (17.22.14E) independent clones. In immunocytochemistry the cells were analysed with the mAb L2-412 and an AP-coupled secondary antibody. Due to the use of the substrate Fast Red, complemented cells stain red. In f) the complementation by the single clone 17.22.14E2 (pACM1) and in g) the positive control *A. th*. UDP-galactose transporter is shown. The negative control with the empty vector is shown in h).

3.1.4 Confirmation of CHO Lec8 cell complementation by the isolated *L. major* clone

In the immunocytochemistry staining protocol used above, bound mAb L2-412 was detected with an AP-coupled secondary antibody. To exclude any cross reactivity with the alkaline phosphatase resulting in a false positive signal, positive cells were detected with a secondary antibody coupled to horseradish peroxidase (HRP) using AEC (3-amino-9 ethyl-carbasol) as a substrate. This protocol confirmed CHO Lec8 cell comple-mentation by the isolated clone (Figure 13a).

In addition, incubation without secondary antibody resulted in a completely negative background excluding an alkaline phosphatase activity of the *L. major* clone itself (data not shown).

An alternative protocol to identify *Lec8* complementation is the detection of polySia with the mAb 735. This protocol did not require the cotransfection of other transferases but the signal intensity by direct detection was comparably low and a signal amplification step had to be applied (see 3.1.1.1). The result of this experiment confirmed the complementation of Lec8 cells by pACM1 (Figure 13b).
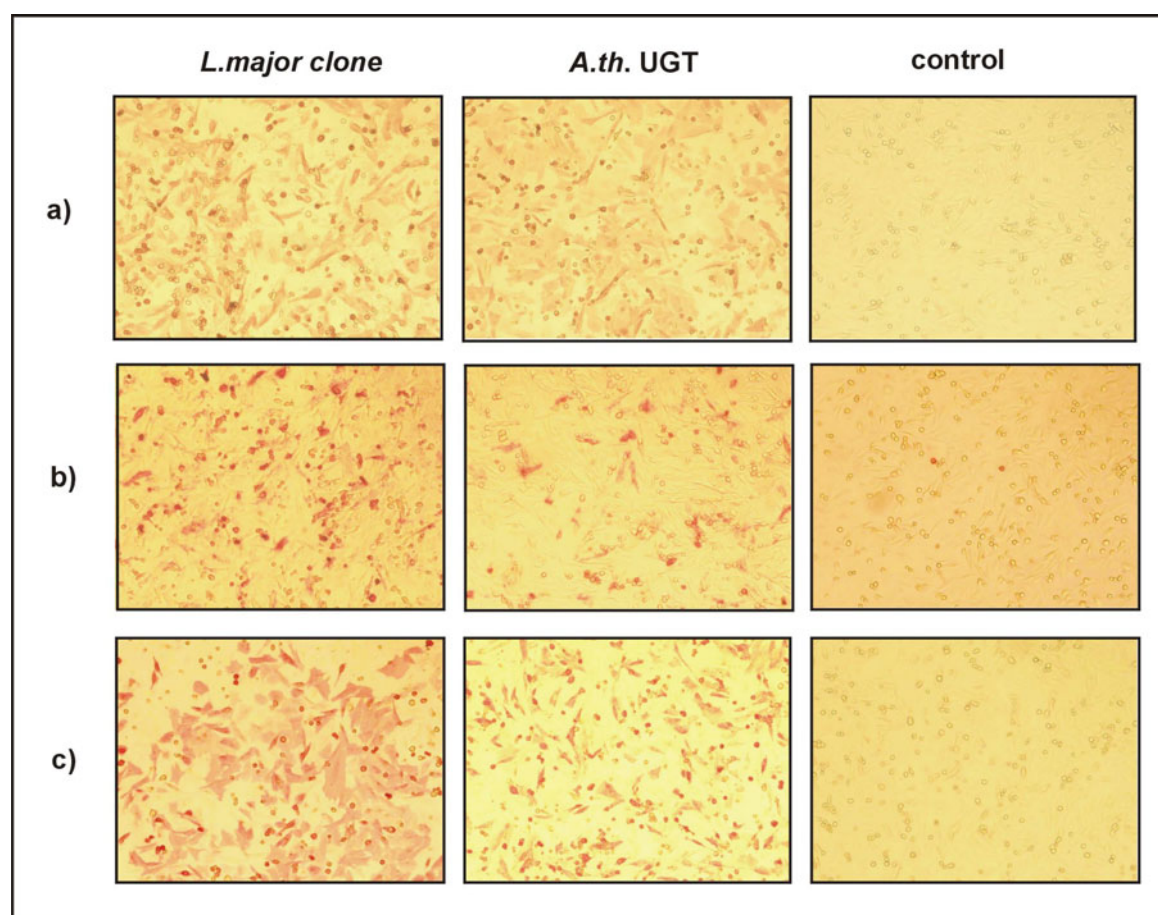
Figure 13 Confirmation of CHO Lec8 cell complementation by the isolated *L. major* clone pACM1. The cells were transfected with clone pACM1 (lane 1), pcDNA3-*A.th*.UGT2 (lane 2), or empty vector control (lane 3). Rat glucuronyltransferase cDNA was cotransfected in a) and c). After 48 hours, cells were stained in a) with the mAb L2-412, α−rat HRP-coupled secondary antibody, and the substrate AEC. In b) the cells were analysed with the mAb735 and α−mouse HRP-secondary antibody. Here, staining was amplified by biotinylation as described in the text. In c) cells were stained using the mAb L2-412 in combination with α−rat AP-coupled secondary antibody and the substrate Fast Red.

To directly compare the results of the different staining methods, cells were transfected with pACM1 and pEFBos-GlcAT and stained with the same protocol as described above for the complementation cloning (Figure 13c). Each time the *A.th.* UDP-galactose trans-

porter 2 and an empty vector were expressed as positive and negative controls, respectively (Figure 13, lanes 2 and 3).

All experiments clearly confirmed the complementing activity of the isolated clone pACM1. As mentioned in 3.1.1.1, the mAb 735 staining procedure resulted in a higher background level (compare Figure 13, lane 3).

3.1.5 Analysis of the isolated cDNA clone

3.1.5.1 Analysis of the nucleotide sequence

The clone pACM1 was sequenced with vector primers. For the complete sequencing of the insert, additional primers were designed from the obtained sequence information.

The analysis of the 1582 bp nucleotide sequence revealed an open reading frame of 1462 bp, or 490 amino acids using the first in frame start codon at position 124. Though a poly-(A) tail was present in the cDNA there was no in frame stop codon, indicating that the isolated clone was not complete. A BLAST search in the database of the *L. major* genome project (The Wellcome Trust Sanger Institute, program Omni Blast) identified a sequence of 733 bp that aligned to the nucleotides 1460-1587 of the isolated cDNA clone (Figure 14). Since *L. major* have no introns, the missing sequence of 46 nucleotides including the first in frame stop codon could be identified.

```
1437  CTGGTGGAATGCAAACGCGTGACGGTGAAGGGGCTGGTTCAGTTCGGTGCTGGCAACGTGCTCACAGGCACGGTCACGAT
   1  CTGGTGGAATGCAAACGCGTGACGGTGAAGGGGCTGGTTCAGTTCGGTGCTGGCAACGTGCTCACAGGCACGGTCACGAT


1517  CGAGAACACGGACAGCGCCTCGGCGTTTGTGATCCCCGATGGTGCCAAAAAAAAAAAAAAAAAAAAAA
  81  CGAGAACACGGACAGCGCCTCGGCGTTTGTGATCCCCGATGGTGCCAAGCTGAACGACACAACGGCGTCACCGCAGCAGT


 161  CGACCAACAAGTAGGGGTCACAAGCTGCTGAGCAAAATGACGATGCACAGATGTAGCGTCGCACTGAGCATGGCCGACAA

 241  AACCGGTCGAGCGGGGCGGGGAAGGGTGCAGCACCGCTGATGCCCGGCGGCAAGTGCACTCATGTCTCTCTCTATATATA
 321  TATATGTCTGTGTATAGGTATATGCTTGTATGTGCAGGTGTCCACTGTTGGCTGCCCCCCCCTCTGAAGAGCCACTAACA
 401  TCACAGCAGCTCCTTCGTCGTGAGGTGAGGCGGCGGCAGCAGTCGGTGCCTGCCTGCACTCCCTCCCCACCTACGATACT
 481  CTACCCCACCCCCTCCACCAACGTCTTTAACGTGTTGCTACGCAGAAACACGCGTGCGTGCGTGTGTGCTATTCCCTGCC
 561  TTATCCCCTTCCCTTCTTCGTCTTCTACCGGCATGTGCTCAACAATCTCGCGCCCCTCCGCGGATGAAGCTAGTACCAAA
 621  GAGGGGCGTCAGCATCGCTGTGGTGTTGGCGATCGCCCCCCCCACGCTGCCCTCTCCCCCATTGCCCCACTTGCACGCAT
 701  CCACGCACACCAC
```

Figure 14 Sequence alignment of the nucleotides 1437-1565 of the isolated cDNA pACM1(upper lanes) and a sequence stretch (LM23_BIN_Contig1792) of the *L. major* genome project database (lower lanes) obtained by chromosome shot gun sequencing (The Wellcome Trust Sanger Institute). The poly-(A) tail is underlined. The first in frame stop codon is underlined .

Using the primers ACM04 and ACM07 the complete open reading frame was amplified by PCR from the *L. major* cDNA library pool #19, a positive pool identified in the first round of complementation cloning. After *Bam*HI/*Not*I digest, the PCR fragment was cloned into the mammalian expression vector pcDNA3 resulting in the construct pcDNA3-*L. major* UGP.

The open reading frame of the resulting sequence consisted of 1485 bp which encodes for a protein of 495 amino acids (Figure 15) with a predicted molecular mass of 54.5 kDa. This sequence complemented the CHO Lec8 cells as well as the initially isolated truncated form. If not stated otherwise, the complete sequence cloned into the vector pcDNA3 (pcDNA3-*L. major*UGP) was used in all subsequent experiments.

Since conserved DNA motifs that usually characterise promoters in other eukaryotes are absent in *Leishmania* (Kapler *et al.*, 1990), the sequence upstream of the isolated cDNA was analysed for a second in frame start codon. As for the 3' region, a sequence of 600 bp was obtained in the database of the *L. major* genome project (The Wellcome Trust Sanger Institute). No second in frame start codon could be detected up to position -460. At this site polydinucleotide repeats were present that mark the intertranscript region of *Leishmania* genes. This data indicated that the isolated clone is complete at the 5'end.

```
-123                                                       CACGAGGCTTTATTGTCATTGATCTACTTAGCAT
 -90  CATCTGCAAAACCCACTCGCACCTCCTGACCGGCACTCTACCCCTAATCCCGCTATCCTCCTCGCTCGTGCTGTCACGGAGGTGAAGCA

   1   M   E   N   D   M   K   S   L   S   A   A   A   Q   A   C   V   K   K   M   R   D   A   K   V   N   E   A   C   I   R
   1  ATGGAAACGACATGAAGTCCCTCAGCGCCGCCGCTCAGGCGTGCGTAAAGAAGATGCGCGACGCCAAGGTGAACGAGGCATGCATTCGC

  31   T   F   I   A   Q   H   V   M   V   S   K   G   E   T   G   S   I   P   D   S   A   I   M   P   V   D   S   L   D   A
  91  ACCTTCATCGCACAGCACGTCATGGTCAGTAAAGGCGAGACAGGGTCCATTCCCGACTCCGCCATCATGCCGGTCGACTCCCTCGATGCC

  61   L   D   S   L   T   I   E   C   D   N   A   V   L   Q   S   T   V   V   L   K   L   N   G   G   L   G   T   G   M   G
 181  CTGGACAGCCTCACCATTGAGTGCGACAACGCTGTCCTGCAGAGTACCGTTGTGCTGAAGCTGAACGGCGGCCTCGGCACCGGCATGGGG

  91   L   C   D   A   K   T   L   L   E   V   K   D   G   K   T   F   L   D   F   T   A   L   Q   V   Q   Y   L   R   Q   H
 271  CTGTGCGACGCCAAGACGCTGCTCGAGGTCAAGGATGGCAAGACGTTTCTTGACTTTACAGCGCTTCAGGTACAGTACCTTCGCCAGCAC

 121   C   S   E   H   L   R   F   M   L   M   D   S   F   N   T   S   A   S   T   K   S   F   L   K   A   R   Y   P   W   L
 361  TGCAGCGAGCACCTGCGCTTTATGTTGATGGACAGCTTCAACACCTCCGCTAGCACCAAGAGCTTTCTGAAGGCGCGCTACCCGTGGCTG

 151   Y   Q   V   F   D   S   E   V   E   L   M   Q   N   Q   V   P   K   I   L   Q   D   T   L   E   P   A   A   W   A   E
 451  TACCAGGTCTTTGACTCAGAGGTGGAGCTGATGCAGAATCAGGTGCCCAAAATACTGCAGGACACGCTCGAGCCGGCGGCCTGGGCCGAG

 181   N   P   A   Y   E   W   A   P   P   G   H   G   D   I   Y   T   A   L   Y   G   S   G   K   L   Q   E   L   V   E   Q
 541  AACCCGGCGTACGAGTGGGCGCCGCCGGGGCACGGTGACATCTACACCGCTCTGTATGGCTCCGGCAAGCTACAGGAACTCGTCGAGCAG

 211   G   Y   R   Y   M   F   V   S   N   G   D   N   L   G   A   T   I   D   K   R   V   L   A   Y   M   E   K   E   K   I
 631  GGCTACCGCTACATGTTCGTCAGCAACGGGGACAACCTCGGCGCCACCATCGACAAGCGCGTGCTGGCGTACATGGAGAAAGAGAAGATC

 241   D   F   L   M   E   V   C   R   R   T   E   S   D   K   K   G   G   H   L   A   R   Q   T   V   Y   V   K   G   K   D
 721  GACTTTCTGATGGAGGTGTGCCGCCGAACGGAGAGCGACAAGAAAGGCGGTCACCTGGCTCGGCAGACGGTGTATGTGAAGGGCAAGGAC

 271   G   Q   P   D   A   E   K   R   V   L   L   L   R   E   S   A   Q   C   P   K   A   D   M   E   S   F   Q   D   I   N
 811  GGTCAACCAGACGCCGAGAAGAGGGTGCTGCTGCTGCGGGAGTCCGCCCAGTGCCCCAAGGCGGACATGGAAAGCTTCCAGGACATCAAC

 301   K   Y   S   F   F   N   T   N   N   L   W   I   R   L   P   V   L   L   E   T   M   Q   E   H   G   G   T   L   P   L
 901  AAGTACTCCTTCTTCAACACGAACAACCTATGGATCAGGCTCCCGGTGCTCCTGGAGACGATGCAGGAGCACGGCGGCACGCTGCCGCTG

 331   P   V   I   R   N   E   K   T   V   D   S   S   N   S   A   S   P   K   V   Y   Q   L   E   T   A   M   G   A   A   I
 991  CCGGTCATCCGAAACGAGAAGACGGTCGATTCATCTAATTCAGCATCACCCAAGGTGTATCAACTGGAAACTGCCATGGGTGCCGCGATC

 361   A   M   F   E   S   A   S   A   I   V   V   P   R   S   R   F   A   P   V   K   T   C   A   D   L   L   A   L   R   S
1081  GCCATGTTCGAAAGCGCATCGGCCATTGTCGTGCCGCGCAGCCGCTTCGCGCCAGTGAAGACGTGCGCCGATCTGCTCGCTCTGCGCTCC

 391   D   A   Y   V   V   T   D   D   F   R   L   V   L   D   D   R   C   H   G   H   P   P   V   V   D   L   D   S   A   H
1171  GACGCCTACGTCGTGACGGACGACTTCCGGCTCGTCCTGGACGATCGCTGCCACGGCCACCCGCCTGTCGTTGACCTCGACAGCGCGCAC

 421   Y   K   M   M   N   G   F   E   K   L   V   Q   H   G   V   P   S   L   V   E   C   K   R   V   T   V   K   G   L   V
1261  TACAAGATGATGAATGGCTTTGAGAAGCTCGTGCAACACGGCGTGCCATCGCTGGTGGAATGCAAACGCGTGACGGTGAAGGGGCTGGTT

 451   Q   F   G   A   G   N   V   L   T   G   T   V   T   I   E   N   T   D   S   A   S   A   F   V   I   P   D   G   A   K
1351  CAGTTCGGTGCTGGCAACGTGCTCACAGGCACGGTCACGATCGAGAACACGGACAGCGCCTCGGCGTTTGTGATCCCCGATGGTGCCAAG

 481   L   N   D   T   T   A   S   P   Q   Q   S   T   N   K   -
1441  CTGAACGACACAACGGCGTCACCGCAGCAGTCGACCAACAAGTAG
```

Figure 15 Open reading frame, amino acid sequence and 5' untranslated region of the isolated cDNA, underlined letters represent the start and stop codon
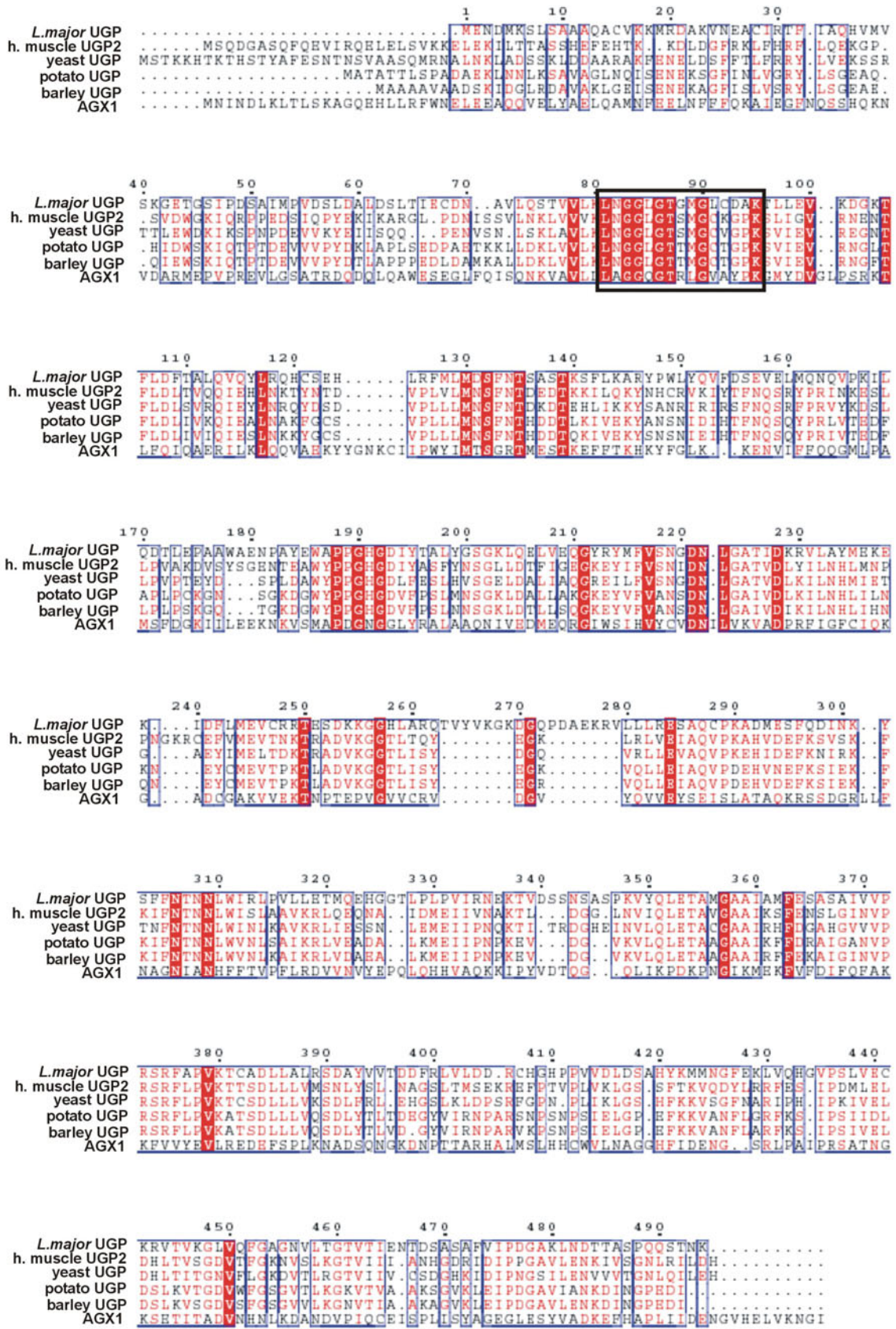
3.1.5.2 Analysis of the amino acid sequence

The cloned sequence was aligned to sequences of UDP-galactose transporters from different species but no homology was found. A blast search using the program BLASTX2.2.3 and the databases GenBank, PDB, Swissprot, PIR and PRF of the National Center for Biotechnology (NCBI) revealed that the cloned sequence showed a very high homology to eukaryotic UDP-glucose pyrophosphorylases (UGPs).

As mentioned in 1.4.1, UGPs catalyse the formation of UDP-glucose and pyrophosphate from UTP and glucose-1 phosphate in a reversible reaction.

A sequence alignment with a human UGP (muscle form 2) (EMBL BC002954), the *S.cerevisiae* UGP (EMBL X69584), and two plant UGPs (potato (EMBL D00667) and barley (EMBL X91347) showed a sequence identity of 40%, 38%, 37% and 39% and a sequence homology of 53%, 57%,55% and 56%, respectively (Figure 16). Several motifs consisting of 15-20 amino acids are strongly conserved in various eukaryotic UGPs but the function of these motifs is not clear yet. Characteristic for all eukaryotic UGPs is a segment of conserved residues encompassing alignment positions 80-95 (KLNGGLGTXMGX$_4$K). A very similar motif (XLXGGXGTXXGX$_4$K) is also conserved in UDP-*N*-actetylglucosamine/galactosamine pyrophosphorylases (UAPs) and is named the pyrophosphorylase consensus motif (see Figure 16, Peneff *et al*., 2001). According to the solved crystal structure of the humane UAP (AGX), this motif is involved in binding the nucleotide moiety of the nucleotide sugar (Peneff *et al*., 2001).

This result was very surprising since it was completely unexpected that a UGP can complement the CHO Lec8 cell phenotype. A potential explanation is that overexpression of this enzyme most likely increases the cellular concentration of UDP-glucose and consequently also of UDP-galactose via the Leloir pathway (1.4.1). As mentioned in 3.1.1, the CHO Lec8 cells exhibit a basal galactosylation capacity though they lack a functional UDP-galactose transporter. Besides other mechanisms, it seems possible that a second nucleotide sugar transporter exists, which exhibits a low transport activity for UDP-galactose as described for some multi-substrate transporters (Martinez-Duncker *et al*., 2003). Thus, an increase in substrate concentration in the cytosol by the UGP might stimulate the UDP-galactose transport into the Golgi and restore the wild type situation in CHO Lec8 cells.

Figure 16 Sequence alignment (see next page). The amino acid sequences of *L. major*, human (EMBL BC002954) and *S.cerevisiae* (EMBL X69584), potato (EMBL D00667) and barley (EMBL X91347) UGPs (program MultAlin version 5.4.1, Corpet *et al*., 1988) are aligned. In addition, the human UAP (AGX1, EMBL X 900524) is shown. Conserved amino acids are highlighted with a red background, amino acids that are conserved in two out of the six sequences are given in red, stretches of conserved residues are boxed with blue lanes. The pyrophosphorylase consensus motif is boxed with a black line.

```
                        1         10        20        30
L.major UGP     ..................MENDMKSLSAAAQACVKKMRDAKVNEACIRTF.IAQHVMV
h. muscle UGP2  ..........MSQDGASQFQEVIRQELELSVKKELEKILTTASSHEFEHTK..KDLDGFRKLPHRH.LQEKGP.
yeast UGP       MSTKKHTKTHSTYAFESNTNSVAASQMRNALNKLADSSKLDDAARAKFENELDSFFTLFRRY.LVEKSSR
potato UGP      ................MATATTLSPADAEKLNNLKSAVAGLNQISENEKSGFINLVGRY.LSGEAQ.
barley UGP      ....................MAAAAVAADSKIDGLRDAVAKLGEISENEKAGFISLVSRY.LSGEAE.
AGX1            ......MNINDLKLTLSKAGQEHLLRFWNELEEAQQVELYAELQAMNFEELNFFFQKAIEGFNQSSHQKN


              40        50        60        70        80        90        100
L.major UGP     SKGETGSIPDSAIMPVDSLDALDSLTIECDN..AVLQSTVVLLNGGLGTGMGLCDAKTLLEV..KDGKT
h. muscle UGP2  .SVDWGKIQRPPEDSIQPYEKIKARGL.PDNISSVLNKLVVVLNGGLGTSVGCKGEKSLIGV..RNENT
yeast UGP       TTLEWDKIKSPNPDEVVKYEIISQQ...PENVSN.LSKLAVLLNGGLGTSVGCVGEKSVIBV..REGNT
potato UGP      .HIDWSKIQTPTDEVVPYIKLAPLSEDPAHTKKLLDKLVVLLNGGLGTTVGCIGEKSVIBV..RNGLT
barley UGP      .QIEWSKIQTPTDEVVPYIDTLAPPPEDLDAMKALLDKLVVLLNGGLGTTVGCTGEKSVIBV..RNGFT
AGX1            VDARMEPVPREVLGSATRDQDQLQAWESEGLFQISQNKVAVLLAGGQGTRLGVAYEKGMYDVGLPSRKT


              110       120       130       140       150       160
L.major UGP     FLDFTALQVQYLRQHCSEH.....LRFMLMDSFNTSASTKSFLKARYPWLYQVFDSEVELMQNQVPKIL
h. muscle UGP2  FLDLTVQQIEHLNKTYNTD.....VPLVLMNSFNTDEDTKKILQKYNHCRVKIYTFNQSRYPRINKESL
yeast UGP       FLDLSVRQIEYLNRQYLSD.....VPLLLMNSFNTDKDTEHLIKKYSANRIRIRSFNQSRFPRVYKDSL
potato UGP      FLDLIVKQIEALNAKFGCS.....VPLLLMNSFNTHDDTLKIVEKYANSNIDIHTFNQSQYPRLVTBDF
barley UGP      FLDLIVIQIESLNKKYGCS.....VPLLLMNSFNTHDDTQKIVEKYSNSNIEIHTFNQSQYPRIVTBDF
AGX1            LFQIQAERILKLQQVAEKYYGNKCIIPWYIMTSGRTMESTKEFFTKHKYFGLK..KENVIFFQQGMLPA


              170       180       190       200       210       220       230
L.major UGP     QDTLEPAAWAENPAYEWAPPGHGDIYTALYGSGKLQELVEQGYRYMFVSNGDN.LGATIDKRVLAYMEKE
h. muscle UGP2  LPVAKDVSYSGENTBAWYPPGHGDIYASFYNSGLLDTFIGEGKEYIFVSNIDN.LGATVDLYILNHLMNP
yeast UGP       LPVPTEYD...SPLLAWYPPGHGDLPESLHVSGELDALIAQGREILFVSNGDN.LGATVDLKILNHMIET
potato UGP      APLPCKGN...SGKIGWYPPGHGDVPPSLMNSGKLDALLAKGKEYVFVANSDN.LGAIVDLKILNHLILN
barley UGP      LPLPSKGQ...TGKDGWYPPGHGDVFPSINNSGKLDTLISQGKEYVFVANSDN.LGAIVDIKILNHLIHN
AGX1            MSFDGKILLEEKNKVSMAPDGNGGLYRALAAQNIVEDMEQRGIWSIHVYCVDNILVKVADPRFIGFCIQK


              240       250       260       270       280       290       300
L.major UGP     KI.....IDFLMEVCRRTESDKKGGHLARQTVYVKGKDGQPDAEKRVLLLRESAQCPKADMESFQDINK..Y
h. muscle UGP2  PNGKRCEFVMEVTNKTRADVKGGTLTQY......EGK.....LRLVEIAQVPKAHVDEPKSVSK..F
yeast UGP       G....AEYIMELTDKTRADVKGGTLISY......DGQ.....VRLLEVAQVPKEHIDEFKNIRK..F
potato UGP      KN....EYCMEVTPKTLADVKGGTLISY......EGK.....VQLLEIAQVPDEHVNEEKSIEK..F
barley UGP      QN....EYCMEVTPKTLADVKGGTLISY......EGR.....VQLLEIAQVPDEHVDEPKSIEK..F
AGX1            G...ADCGAKVVEKTNPTEPVGVVCRV......DGV.....YQVVEYSEISLATAQKRSSDGRLLF


              310       320       330       340       350       360       370
L.major UGP     SFFNTNNLWIRLPVLLETMQEHGGTLPLPVIRNEKTVDSSNSASPKVYQLETAMGAAIAMFESASAIVVP
h. muscle UGP2  KIFNTNNLWISLAAVKRLQBQNA..IDMEIIVNAKTL...DGG.LNVIQLETAVGAAIKSFENSLGINVP
yeast UGP       TNFNTNNLWINLKVKRLIBSSN..LEMEIIPNQKTI.TRDGHEINVLQLETACGAAIRHFIGAHGVVVP
potato UGP      KIFNTNNLWVNLSAIKRLVBADA..LKMEIIPNPKEV...DG..VKVLQLETAAGAAIKFFIRAIGANVP
barley UGP      KIFNTNNLWVNLKAIKRLVDABA..LKMEIIPNPKEV...DG..VKVLQLETAAGAAIRFFEKAIGINVP
AGX1            NAGNIANHFFTVPFLRDVVNVYEPQLQHHVAQKKIPYVDTQG..QLIKPDKPNGIKMEKEVFDIFQFAK


              380       390       400       410       420       430       440
L.major UGP     RSRFAPVKTCADLLALRSDAYVVTDDFRLVLDD.RCHGHPPVWDLDSAHYKMMNGFEKLVQHGVPSLVEC
h. muscle UGP2  RSRFLPVKTTSDLLLVMSNLYSL.NAGSLTMSEKREFPTVPLVKLGS.SFTKVQDYLRRFES.IPDMLEL
yeast UGP       RSRFLPVKTCSDLLLVKSDLHRL.EHGSLKLDPSRFGPN.PLIKLGS.HFKKVSGFNARIPH.IPKIVEL
potato UGP      RSRFLPVKATSDLLLVQSDLYTLTDEGYVIRNPARSNPSNPSIELGP.EFKKVANFLQRFKS.IPSIIDL
barley UGP      RSRFLPVKATSDLLLVQSDLYTLVD.GYVIRNPARVKPSNPSIELGP.EFKKVANFLARFKS.IPSIVEL
AGX1            KFVVYEVLREDEFSPLKNADSQNGKDNPTTARHALMSLHHCWVLNAGGHFIDENG..SRLPAIPRSATNG


              450       460       470       480       490
L.major UGP     KRVTVKGLVQPGAGNVLTGTVTIENTDSASAFVIPDGAKLNDTTASPQQSTNK..........
h. muscle UGP2  DHLTVSGDVTFGKNVSLKGTVIII.ANHGDRIDIPPGAVLENKIVSGNLRILDH.........
yeast UGP       DHLTITGNVFLGKDVTLRGTVIIV.QSDGHKIDIPNGSILENVVVTGNLQILEH.........
potato UGP      DSLKVTGDVWFGSGVTLKGKVTVA.AKSGVKLEIPDGAVIANKDINGPEDI.........
barley UGP      DSLKVSGDVSFGSGVVLKGNVTIA.AKAGVKLEIPDGAVLENKDINGPEDI.........
AGX1            KSETITADVNHNLKDANDVPIQCEISPLISYAGEGLESYVADKEFHAPLIIDENGVHELVKNGI
```

All experiments described so far were carried out in CHOP8 cells, a CHO Lec8 cell line stably transformed with the polyoma virus large T antigen (Cummings *et al.*, 1993). In order to exclude the possibility that the observed complementation effect is only visible on the genetic background of these cells, three additional CHO Lec8 variants were analysed for complementation by the *L. major* UGP.

3.1.6 Complementation of different CHO Lec8 subclones

Analysing the mutations that cause the Lec8 phenotpye, Oelmann *et al.* (2001) showed that the UDP-galactose transport defects result from different mutational events. While a truncation from nucleotide 275 to 374 in the coding region of the UDP-galactose trans-porte gene leads to the introduction of a premature stop codon (protein ends after amino acid 92) in the commercially available Lec8 cells (Lec8), the mutations in Lec3.2.8 and Lec4.8.7A interfere with the expression of the gene. In both cell lines no stable mRNA encoding for a UDP-galactose transporter was detectable.

To characterise the basal glycosylation capacities in these different mutants, the first experiment carried out in this study, was a FACS analysis for polySia surface expression using the mAb 735 and a FITC-labelled secondary antibody (2.2.5). For control, CHO WT cells (positive control) and CHO cells of the complementation group Lec2 (subclone 6B2; negative control) were included in the experiment. Lec2 cells lack a functional CMP-sialic acid transporter and are therefore devoid of sialic acid and polySia. The mutant Lec3.2.8 was not included in the FACS experiment because these cells have a defect in both the CMP-sialic acid and UDP-galactose transporters.
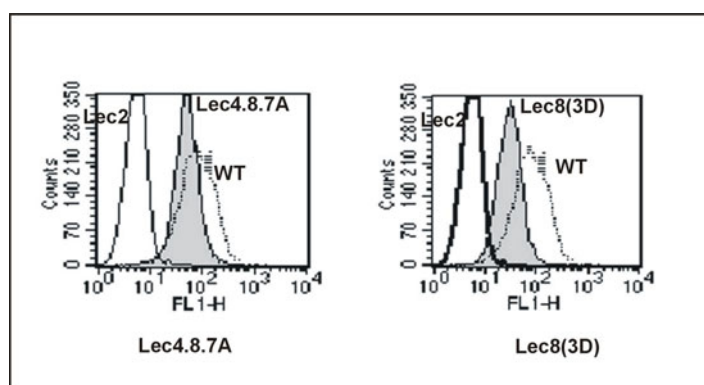
Figure 17 FACS analysis of different CHO cell variants. a) CHO Lec8(3D) and b) CHO Lec 4.8.7A were stained with the mAb 735 that recognizes polySia and FITC-labelled secondary antibody. CHO Lec2 cells and CHO WT cells were taken as negative and positive controls, respectively. In each experiment 10 000 cells were counted.

As can be seen in Figure 17, commercially available CHO Lec8 (subclone 3D, Lec8(3D)) and Lec4.8.7A cells clearly express polySia on their surface. In the case of the cell line Lec4.8.7A the galactose/polySia level is higher than in the other mutant.

In a second experiment the basal galactosylation capacity of Lec8(3D), CHOP8, Lec4.8.7A and Lec3.2.8 was analysed by immunocytochemistry after transfection of cells with pEFBos-GlcAT (Figure 18) and staining with the mAb L2-412. Since no signal was obtained with the direct detection system, an amplification by biotinylation using biotinty-ramid was carried out (see 3.1.1.1 and 2.2.3). As shown in Figure 18, all cell lines showed intensively stained cells. Again, the cell line Lec4.8.7A demonstrated to be most positive, while CHOP8 cells showed the lowest background. Due to a transfection efficiency of about 30% and due to the lower sensitivity of the immunocytochemistry, not all cells were stained as would have been expected from the FACS analysis.
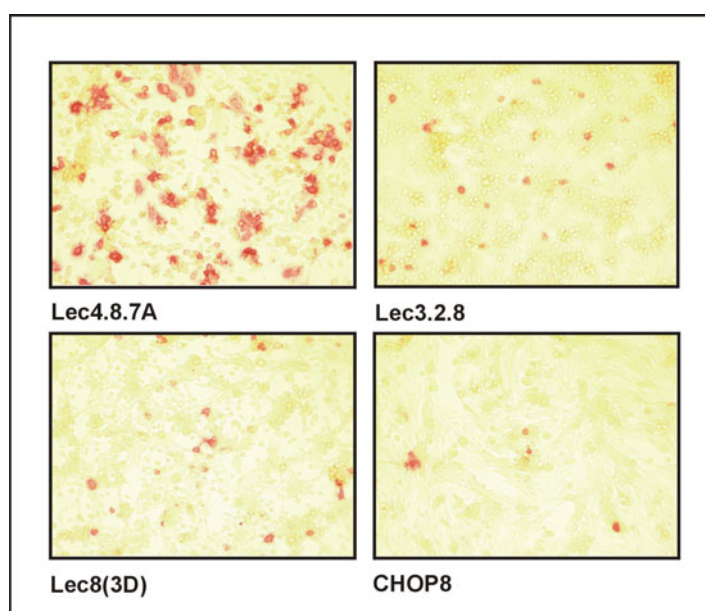
Figure 18 Analysis of galactose expression in CHO Lec8 variants. Background expression of galactosylated surface structures was determined by immunocytochemistry using mAb L2-412 after transfection with pEFBos-GlcAT encoding a rat glucuronyltransferase. After incubation with α–rat secondary antibody coupled to HRP and biotinthyramid, positive cells were detected with streptavidin AP using Fast Red as a substrate.

These results clearly showed that the CHO Lec8 cell tested here are still able to galactosylate and polysialylate glycans though they lack a functional UDP-galactose transporter. The highest background staining was observed in Lec4.7.8A cells though these cells are completely devoid of stable UDP-galactose transporter mRNA.

In the next step, the complementary activity of the *L. major* UGP was analysed. Therefore, Lec8(3D), Lec3.2.8, and Lec4.7.8A cells were co-transfected with pcDNA3-*L. major*UGP plus pEFBos-GlcAT and stained with mAb L2-412. A plasmid encoding the hamster UDP-galactose transporter (pcDNA3-hamUGT) and the empty vector were transfected as positive and negative control, respectively. In excellent agreement with the hypothesis that the basal galactose transport visible in Lec8 mutants is responsible for the complementation by the *L. major* UGP, all tested Lec8 variants were complemented by this clone. Results are shown in Fig 11. Worthwhile to mention at this point is that the cell lines, which exhibit a higher basal galactosylation capacity than CHOP8 cells, showed an increased background even without signal amplification as can be seen in Figure 19 lane 3.
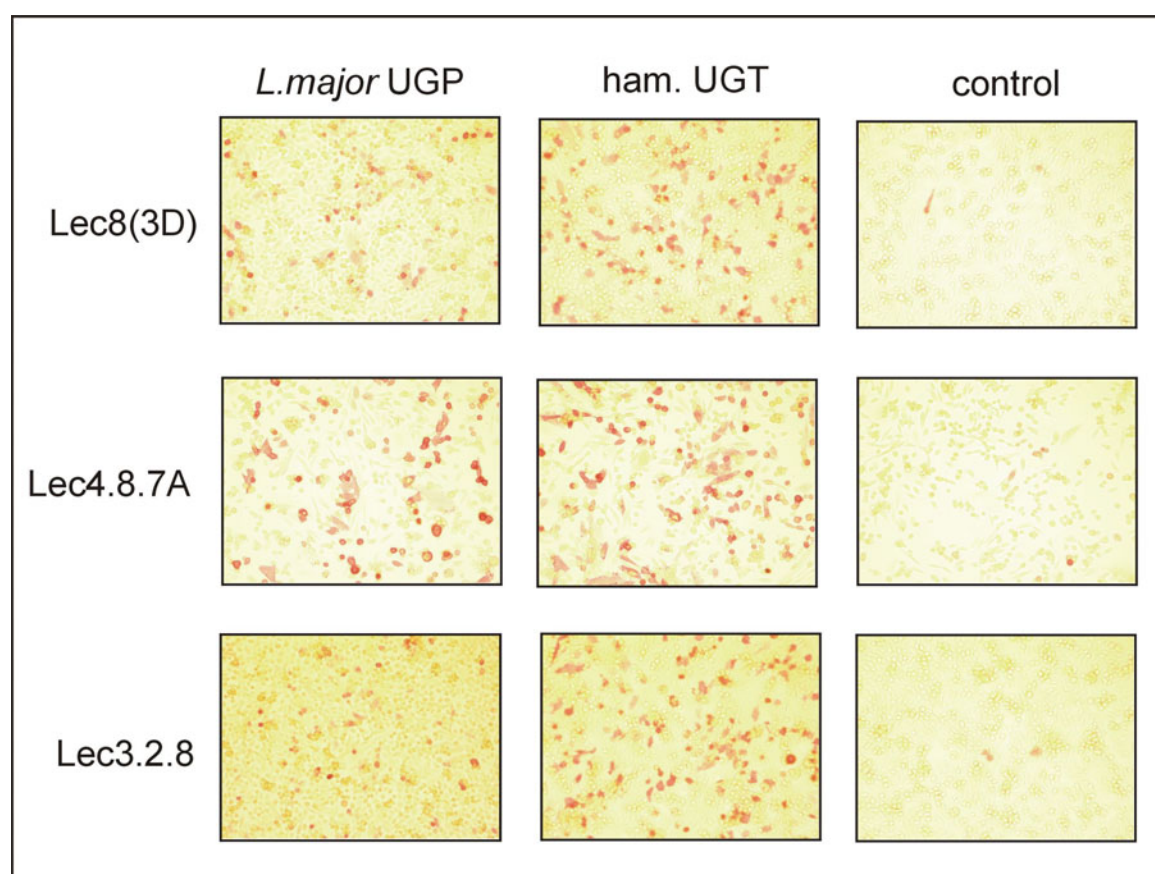
Figure 19 Complementation of different Lec8 variants by *L. major* UGP. Lec8(3D), Lec 3.2.8 and Lec 4.7.8A cells were transfected with pcDNA3-*L. major*UGP (lane 1) and pcDNA3-ham.UGT encoding the hamster UDP-galactose transporter (lane 2) and pcDNA3 (lane 3, control) as positive and negative controls, respectively. The co-expression of the rat glucuronyltransferase allowed the detection with the mAb L2-412 and AP-coupled secondary antibody by immunocytochemistry. Positive cells stained red.

3.1.7 Search for UGP negative pools

Since *L. major* UGP efficiently complemented CHO Lec8 cells, the identification of the *L. major* UDP-galactose transporter depends on the availability of cDNA pools that do not contain UGP. As mentioned before (Table 1), 8 out of 22 cDNA pools tested, complemented Lec8 cells in the initial screen. In order to distinguish Lec8 cell complementation by pools containing the *L. major* UGP or the *L. major* UDP-galactose transporter, all pools of the library were screened for the presence of the UGP cDNA. Based on the isolated cDNA, the primers ACM1/ACM2 were designed to amplify a 750 bp fragment by PCR. From 86 pools of the library 64 allowed the amplification of a specific PCR product. The remaining 22 pools were tested in Lec8 complementation experiments but none was positive. This indicated that the potential UDP-galactose transporter was in the same pool(s) as the UGP and its complementing activity was masked by this enzyme. Therefore, it is difficult to isolate the UDP-galactose transporter by Lec8 complementation from this cDNA library.

In addition, all positive subpools from pool #17 generated during the complementation cloning were tested since it seemed possible that the UDP-galactose transporter cDNA was also present in pool #17. Unfortunately, all pools complementing Lec8 cells also contained the UGP (Figure 20).
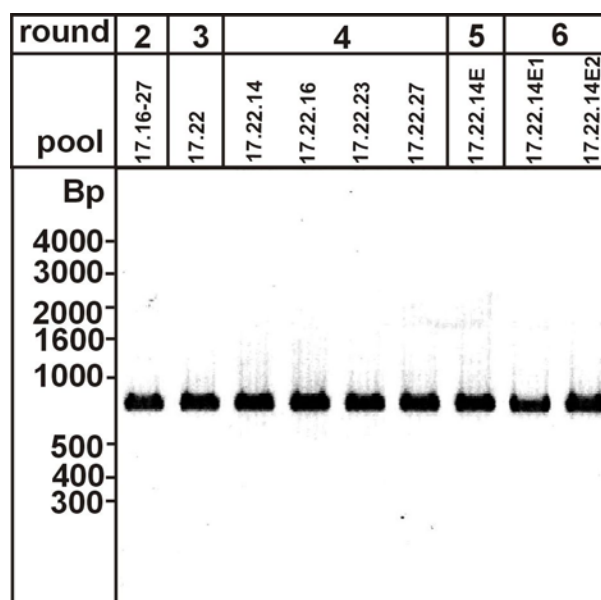
Figure 20 PCR-screening for the presence of the *L. major* UGP in positive subpools identified in the course of complementation cloning. The cDNA of the positive subpools # 17.16-27, 17.22, 17.22.14, 17.22.16, 17.22.23, 17.22.27, 17.22.14E, and 17.22.14E1+2 were screened by PCR as described in the text.

3.1.8 Complementation experiments using human UGPs

In order to investigate if other UGPs can complement the Lec8 phenotype, two human UGPs from muscle were analysed. The sequences of both UGPs are identical except that one enzyme exhibits a longer N-terminus of 11 amino acids due to alternative splicing. The cDNA clones were obtained from the RZPD (Deutsches Ressourcenzentrum für Genomforschung GmbH, Berlin, see 2.1.3). Both enzymes were cloned into the vector pcDNA3. The constructs pcDNA3-*L. major*UGP, pcDNA3-hUGP1 (long form) and pcDNA3-hUGP2 (short form) along with the plasmid pEFBos-GlcAT were transfected into CHOP8 cells. The re-expression of galactose-dependent epitopes was detected with mAb L2-412 and AP-coupled secondary antibody. Interestingly, the two human UGPs could not complement the CHO Lec8 phenotype whereas the expression of the *L. major* UGP resulted in complementation (Figure 21).
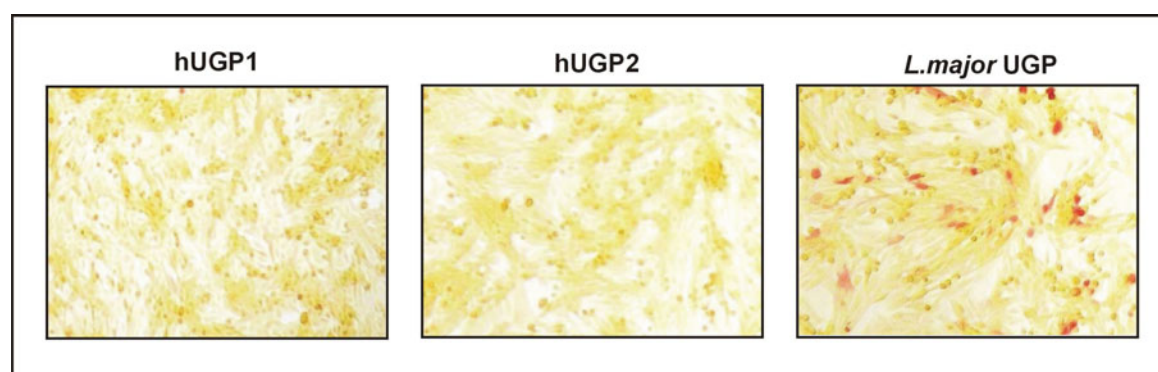
Figure 21 Functional comparison of mammalian and *L. major* UGP. Complementation in CHO Lec8 cells has been used to functionally compare the *L. major* and two human UGPs. The constructs pcDNA3-hUGP1 (lane 1), pcDNA3-hUGP2 (lane 2), and pcDNA3-*Lmajor* UGP (lane 3) were transfected into CHOP8 cells. The rat glucuronyltransferase was co-expresed and positive cells were detected with the mAb L-2-412 and AP-coupled secondary antibody.

Protein expression levels and stability were analysed by Western blotting (2.4.5). Since there is no antibody available, which directly recognises UGPs, a Flag-epitop tag was fused to the N-terminus. The tagged *L. major* UGP, the two human muscle UGPs and a negative control were expressed in CHO Lec8 cells. After 48 hours, the cells were lysed with lysis buffer (2.4.7) and proteins immunoprecipitated with α-Flag M5 agarose beads (2.4.8). Aliquots of the lysates and the immunoprecipitates were separated on SDS-PAGE (2.4.2). In the Western blot analysis, *L. major* UGP was detected in the lysate as well as after immunoprecipitation (Figure 22).
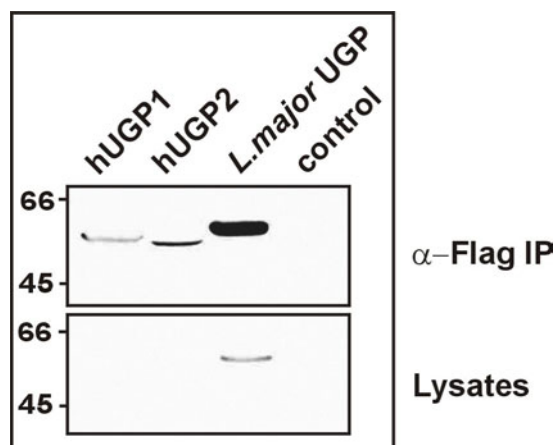
Figure 22 Expression of Flag-tagged UGPs. The constructs pcDNAFL-hUGP1, pcDNA3FL-hUGP2, pcDNA3FL-*L. major*UGP encoding the Flag-tagged humane muscle form 1 and 2 and the *L. major* UGP, respectively, were transiently expressed in CHO Lec8 cells. The empty vector pcDNA3FL was used as a negative control. Total cell lysates as well as proteins immunoprecipitated with the α-Flag antibody were separated on a 10% SDS PAGE and detected in Western blot using chicken α-Flag primary antibody, AP-conjugated α–chicken secondary antibody and BCIP/NBT as substrates.

The two human enzymes were also expressed and could be detected after immunopre-cipitation. Since the expression level was lower compared to the *L. major* UGP, no specific bands were visible in the lysates.

In addition, the Flag-tagged constructs were tested for complementing activity in CHO Lec8 cells, but as describe above, the human UGPs did not complement Lec8 cells (data not shown).

Though the sequence homology is very high, the *L. major* and human UGPs differ in their ability to complement Lec8 cells. One explanation might be that the *L. major* UGP exhib-its other enzymatic properties or protein stability than the human orthologous. To further investigate this assumption, the functional and kinetic characteristics of the *L. major* UGP were analysed as described in the following paragraphs.

3.2 Biochemical characterisation of the L. major *UDP-glucose pyrophosphorylase*

3.2.1 Expression and purification of the *L. major* UGP

For the functional, structural and kinetic characterisation, the *L. major* UGP was recombinantly expressed in *E.coli* BL21(DE3) and affinity purified. Since there was no antibody available that specifically recognised the UGP, a His-tag was fused to the C-terminus and the protein expressed under the control of the T7/lac promoter in the prokaryotic expression vector pET22b (pET-UGP-His).

The construct was transformed into *E.coli* BL21 (DE3) and the expression induced with 1mM IPTG for 24 hours at 15°C (2.4.10). The expression at higher temperatures resulted in the formation of inclusion bodies. The cells were lysed by sonification and the soluble and insoluble fraction analysed in SDS-PAGE (2.4.10.1). After Roti-Blue blue staining and Western blotting using α-pentaHis mAb, a protein of about 55 kDa could be detected at equal amounts in the soluble and insoluble fraction (Figure 23 and 2.4.3/6). The molecular weight corresponded to the calculated MW of *L. major* UGP.
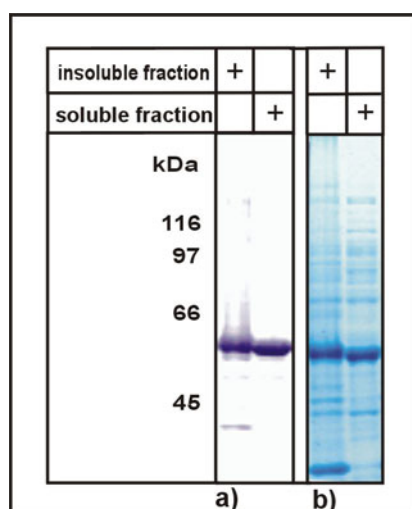
Figure 23 Expression of His-tagged UGP in *E.coli* BL21 (DE3). The construct pET-UGP-His was transformed into *E.coli* BL21(DE3) and the expression induced at an OD_{600nm} of 0.6 with 1 mM IPTG. After incubation at 15°C for 24 hours, soluble and insoluble fractions were prepared by sonification. The lysates were separated on a 10% SDS-PAGE. The proteins were detected by Western blotting using mAb α–pentaHis (a) or Roti-Blue staining (b).

After small-scale purification tests, the soluble fraction of a 2 litre culture was passed over a 5 ml HisTrapHP Ni^{2+}-column (Amersham Pharmacia) to affinity purify the *L. major* UGP (2.4.11). After washing with loading buffer, the unspecific bound protein was eluted with 40 mM imidazole (fractions 1 to 28). The *L. major* UGP was eluted with 300 mM

imidazole using a step gradient (fractions 29 to 50). The fractions 36 to 40 were pooled (Figure 24).
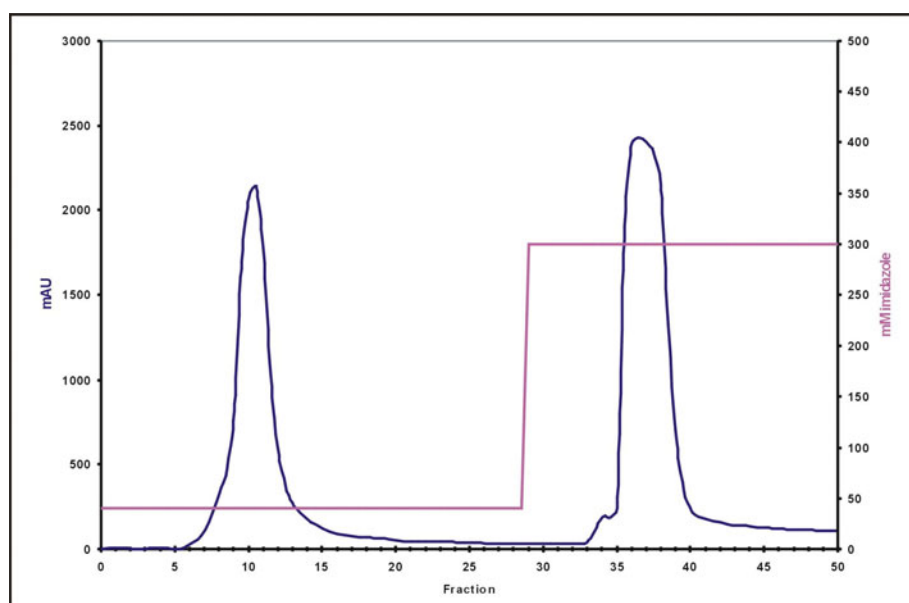
Figure 24 Elution profile of a HisTrapHP Ni^{2+}-column. The soluble fraction of a 2 L *E.coli* BL21 (DE3) culture overexpressing *L. major* UGP was loaded onto the column. The blue line represents the amount of eluted protein (primary y-axis), the red line indicates the imidazole concentration (secondary y-axis). After washing the column with 5 column volumes (CV) of loading buffer, unspecific bound proteins were eluted with 40 mM imidazole (fractions 1 to 28). Using a step gradient, the *L. major* UGP was eluted with 300 mM imidazole (fractions 29 to 50) and the fractions 36 to 40 were combined.

The pooled fractions were desalted with a HiPrep 26/10 column and stored at -80°C in a buffer containing 50 mM Tris/HCl pH 7.8, 10 mM MgCl$_2$ (2.4.11.3). The protein concentration was determined by a BCA test (2.4.1). About 20 mg protein per 1 litre bacterial culture was obtained. Because protein crystallisation was one of the intended goals, the stability of the protein in solution was tested at 4°C or at -20°C. Under both conditions precipitates were observed after a time period of 2-3 months if the protein concentration was over 4 mg/ml.

An aliquot of the purified protein and aliquots of the soluble *E.coli* fraction and the flow through of the Ni^{2+}-column were separated on SDS-PAGE and analysed by silver staining (Figure 25a and 2.4.4). The overexpressed protein bound very efficiently to the Ni^{2+}-column and after elution and desalting a purity of about 95% was achieved. A Western blot analysis using mAb α−pentaHis confirmed that the purified protein of 55 kDa was the *L. major* UGP (Figure 25b). A further purification of the *L. major* UGP was not necessary and the protein was used for all following characterisation studies.
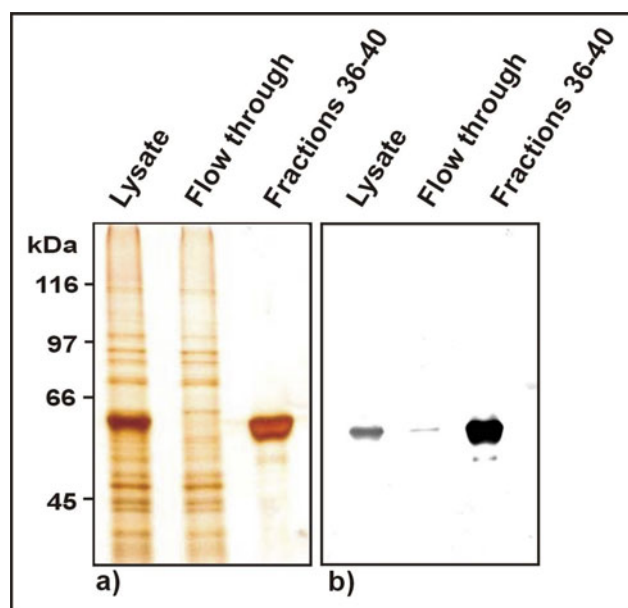
Figure 25 Purification of recombinant His-tagged UGP. Silver stain (a) and Western blot (b) analysis of the purification procedure. Aliquots of the lysate, the flow through of the Ni^{2+}-column and the purified protein were separated on a 10% SDS-PAGE. Proteins were analysed by silver staining and by Western blotting. The Western blot was developed with an mAb α–pentaHis and AP-coupled secondary antibody using BCIP/NBT as substrate.

In addition, constructs bearing an N-terminal StrepII-tag (IBA) were used in expression and purification trials (2.4.11.2). The StrepII-tag is an octapeptide that binds to Strep-Tactin, a modified streptavidin, which allows a mild elution of the protein. While proteins were expressed in the soluble fraction if bacteria were grown at 15°C and turned out to be active if tested *in vitro* (see 3.2.2) and *in vivo* (see 3.2.3), the purification failed because the proteins did not bind to the affinity column.

3.2.2 *In vitro* testing of *L. major* UGP

3.2.2.1 Kinetic analysis of *L. major* UGP

The purified enzyme was analysed in an *in vitro* activity assay (Chang *et al.,* 1993, Duggelby *et al.,* 1996, Francois *et al.,* 1999). In the forward reaction, the activity was measured by using a coupled enzymatic reaction with the enzyme UDP-glucose dehydrogenase (2.4.13.1). The UDP-glucose dehydrogenase catalyses the formation of UDP-glucuronic acid and NADH+H$^+$ from UDP-glucose and NAD$^+$. In the reverse direction, the addition of phosphoglycomutase and glucose-6 phosphate dehydrogenase to the reaction leads to the synthesis of 6-phosphoglucono-δ lacton and NADPH (2.4.13.1). The subsequent reduction of NAD$^+$ to NADH+H$^+$ and NADP$^+$ to NADPH+H$^+$ in the forward and reverse reaction, respectively, was monitored in a spectrophotometer. The initial linear rates of cofactor reduction were used to calculate the enzyme activity by the

conversion of the increase in OD_{340nm} to micromoles of $NAD(P)H+H^+$ production based on its extinction coefficient. The protein concentration was determined in the BCA test (2.4.1).

In both directions, the enzyme displays a Michaelis Menten kinetic. Using a Lineweaver Burk plot the apparent K_m values for all substrates were determined (Figure 26).

The UTP concentration was varied between 0.02 mM to 1 mM. At a saturating glucose-1 phosphate concentration of 2 mM, the K_m value for UTP was 70µM ± 5µM. The determination of the K_m of 192µM ± 4 µM for glucose-1 phosphate was done at a fixed UTP concentration of 1 mM and varying the glucose-1 phosphate concentration from 0.02 mM to 2 mM. The V_{max} of the forward reaction was 3347 ± 54 µmol/min per mg protein.

In the reverse reaction the non-varied substrate was present at a fixed concentration of 2 mM. The apparent K_m values for UDP-glucose and pyrophosphate (PP_i) were 104.8µM ± 4µM and 200µM ± 40µM, respectively. The analysis was performed by varying the UDP-glucose concentration from 0.05 mM to 2 mM and the pyrophosphate concentration from 0.02 mM to 2 mM. V_{max} of the reverse reaction was 2316 ± 27µmol/min per mg protein. The results are summarised in Table 1.
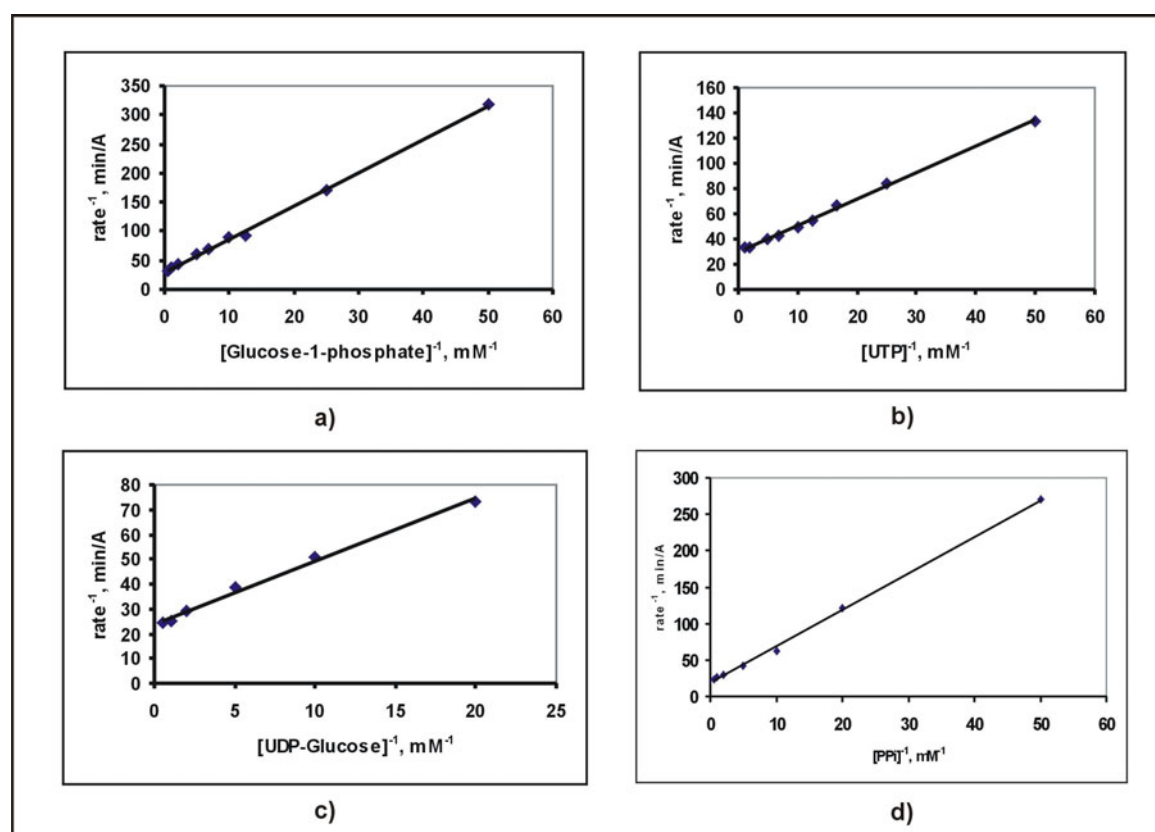
Figure 26 Kinetic characterisation of *L. major* UGP. The K_m values for glucose-1 phosphate (a), UTP (b), UDP-glucose (c) and PP_i (d) were determined at a constant concentration of 1 mM UTP, 2 mM glucose-1 phosphate, 2 mM PP_i and 2 mM UDP-glucose, respectively. The results are shown as double reciprocal blots (Lineweaver Burk).

Reaction	Constant	Value
forward	K_m (UTP)	70µM ± 5µM
	K_m(Glucose-1-phosphate)	192µM ± 4 µM
	V_{max}	3347 ± 54 µmol/min/mg
reverse	K_m (UDP-Glucose)	104.8µM ± 4µM
	K_m (PP$_i$)	200µM ± 40µM
	V_{max}	2316 ± 27 µmol/min/mg

Table 1 Summary of the kinetic constants of *L. major* UGP.

3.2.2.2 *In vitro* activity assay using galactose-1 phophate as substrate

Lai *et al.* (2000) reported that the *S.cerevisiae* UGP catalysed the conversion of galactose-1 phosphate and UTP to UDP-galactose and pyrophosphate *in vitro*. In addition, the overexpression of the UGP from *S.cerevisiae* and from human could rescue a galactose-1 phosphate uridyltransferase deficient yeast strain (Lai *et al.,* 2000). As mentioned in 1.4.1, the galactose-1 phosphate uridyltransferase catalyses the reaction galactose-1 phosphate + UDP-glucose → UDP-galactose + glucose-1 phosphate. A defect in this enzymes leads to the metabolisation of galactose-1 phosphate to e.g. galactitol, which is a toxic substance, if produced in higher concentration. The accumulation of toxic substances is the cause for the classical galactosemia in humans. The observed rescue of the mutant yeast strain by the two UGPs clearly indicated that galactose-1 phosphate is a substrate for UGP. This is in agreement with the report on human, calf and rabbit liver UGP by Turnquist *et al.,* (1974).

Because Lec8 complementation by the *L. major* UGP was explained by the increase in the UDP-galactose concentration, the next test was carried out to identify, if also the *L. major* enzyme can directly use galactose-1 phosphate as substrate. In an *in vitro* activity assay the formation of UDP-galactose from galactose-1 phosphate and UTP was monitored by a coupled reaction with UDP-galactose 4-epimerase and UDP-glucose dehydrogenase. As for the coupled assays described above the reduction of NAD was detected in a spectrophotometer. The activity was 0.87 µmol/min per mg protein and about a factor of 3000 lower than using glucose-1 phosphate as a substrate. Under physiological conditions in the cell this activity can probably be neglected.

3.2.3 *In vivo* activity assay of the *L. major* UGP

In *E.coli,* the deficiency of the UGP renders the bacterium incapable of fermenting galactose (Sundararajan *et al*., 1962). This is most likely due to the lack of UDP-glucose in the galactose-1 phosphate uridyltransferase reaction leading to the accumulation of toxic substances as mentioned above. As a consequence the mutant is not able to grow on agar containing galactose as the only carbohydrate source. Upon transformation with a functional UGP, the phenotype is restored. The complementing activity can be determined by the colour and size of the colonies on MacConkey-galactose agar. Galactose fermentation is indicated by the growth of big, red colonies due to the decrease in pH. Mutants defective in the UGP show poor growth of white colonies on this kind of agar (2.4.13.2).

To prove *in vivo* activity of the isolated *L. major* UGP, the construct pET-UGP-His and, for control, the empty vector pET22b were transformed into the *E.coli galU* mutant strain DEV6 (Elseviers *et al.,*1980, *E.coli* Stock Center, New Haven, USA). The colonies were grown on galactose and IPTG containing MacConkey agar at 37°C for 15 hours. Growth of big red colonies could be observed indicating that a functional active UGP was expressed (Figure 27).
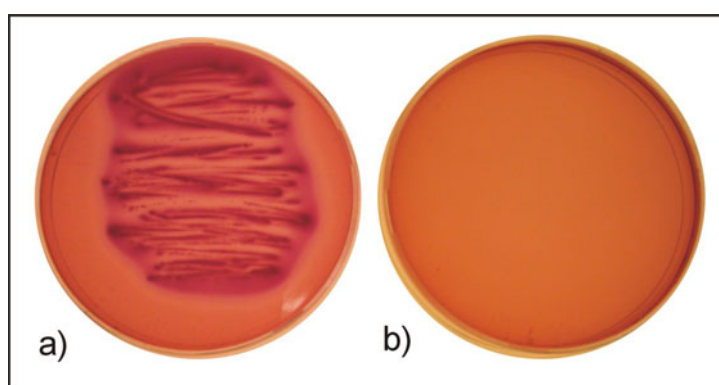
Figure 27 Complementation of the *E.coli galU* mutant DEV6 by the *L. major* UGP. The mutant was transformed with pET-UGP-His (a) and as a control with the empty vector pET22b (b) and grown on 2% galactose and 1 mM IPTG containing MacConkey agar.

This assay was performed to prove the expression of functional proteins from all constructs used in purification trials (see 3.2.1).

3.2.4 Determination of the oligomerisation status of *L. major* UGP

The amino acid sequence of eukaryotic UGPs are highly conserved. Despite this fact, the oligomerisation status differs between UGPs of various species. The animal UGPs were reported to form octamers (Levine *et al.,* 1969), whereas the plant UGPases were found

to be mono- or dimers (Nakano *et al.,* 1989, Sowokinos *et al.,* 1993). In a more recent study carried out in plants, the monomer has been described to be the active enzyme, while oligomers of various sizes seem to exist. Oligomers may be used to sequestrate the protein and thus control the concentration of the active enzyme (Martz *et al*., 2002).

To investigate the oligomerisation status of *L. major* UGP, purified protein was used to perform gelfiltration experiments (Figure 28 and 2.4.12). A superdex 200 HR10/30 column was calibrated with the standards yeast alcohol dehydrogenase, bovine serume albumin and bovine carbonic anhydrase, which exhibit molecular masses of 150 kDa, 66 kDa and 29 kDa and retention volumes of 12.3 ml (pink line), 13.5 ml (blue line) and 16.0 ml (pink line), respectively. The main peak of the *L. major* UGP was detected at a retention volume of 14.2 ml (green line) indicating migration as a monomer. Additional analysis of the fractions by SDS-PAGE and Roti-Blue staining confirmed the presence of the UGP as a monomer (Figure 29). A smaller peak obtained at a retention volume of 12.6 ml was also detected and could indicate dimer formation. Since comparable peaks were also present in the profiles of the standard proteins, *in vitro* activity testing was used to identify the nature of eluted proteins. In Figure 29, the blue line represents the elution profile of the *L. major* UGP after gelfiltration and the pink line indicates the activity of the single fractions. In the forward reaction (see 3.2.2), the main activity could be detected in fractions representing the monomer. Because no second activity peak was observed, the material eluting at the position of a potential dimer, may count for inactive, aggregated protein. In summary, these data clearly demonstrate that the monomer is the active protein.
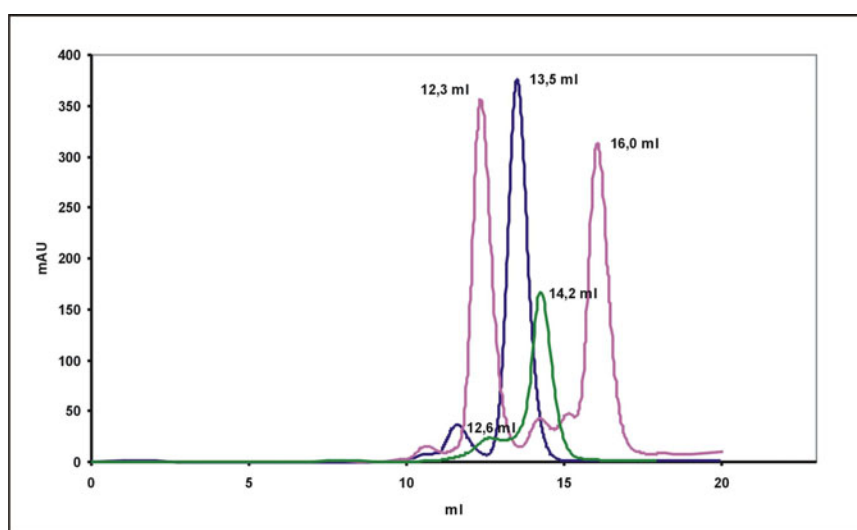
Figure 28 Determination of UGP oligomerisation status. Gelfiltration was used to determine the oligomerisation status of *L. major* UGP. The elution profiles of yeast alcohol dehydrogenase (12.3 ml, pink), bovine serume albumin (13.5 ml, blue), and bovine carbonic anhydrase (16.0 ml, pink) were used to calibrate the column. *L. major* UGP (14.2 ml) is shown in green.
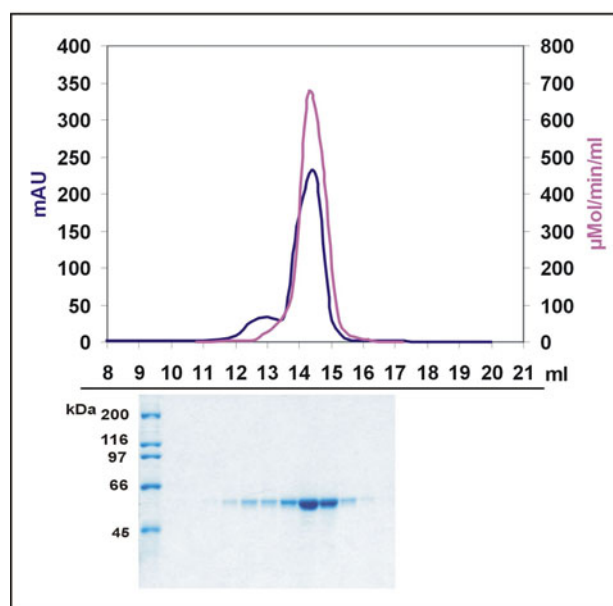
Figure 29 Determination of functional activity. To determine active fractions in the elution profile of the *L. major* UGP gelfiltration run (Figure 28), an activity test was carried out including all fractions. The primary y-axis shows the protein concentration and the secondary y-axis the *in vitro* activity of the forward reaction. The elution profile of the *L. major* UGP gelfiltration is indicated as blue line whereas the activity of the single fractions is shown as pink line. The fractions were analysed on a Roti-Blue stained SDS-PAGE.

In addition, a gelfiltration run including the substrates UTP and glucose-1-phosphate in the buffers was done. Again, the *L. major* UGP appeared as a monomer with the same elution profile as in Figure 28 (data not shown). No higher order oligomers could be detected in this experimental set up, indicating a clear difference to animal UGPs.

3.2.5 Crystallisation of *L. major* UGP

3.2.6 Determination of the minimal catalytically active unit

In crystallisation approaches, the rule is to determine the minimal active protein, to optimise protein expression and crystallisation. To reach this goal in the case of *L. major* UGP, N-and C-terminal truncations were carried out. The deletion mutants were tested for *in vivo* activity in the *E.coli* DEV6 *galU* mutant.

In the design of deletion mutants, sequence information from all known UGPs was included. Though the overall sequence homology of UGPs from plants, mammals and fungi is very high, the N-termini show no strong similarity (see Figure 16, Flores-Diaz *et al*., 1997) and may not be required for activity. Peng *et al*. (1993) identified a human liver clone truncated up to 43 amino acid residues at the N-terminus that was still able to complement the *E.coli galU* defect. This corresponds to amino acid 10 in the *L. major* UGP sequence. In contrast to the N-terminus, the C-terminus contained several con-

served residues but no functional data was available. However, as reported in 3.1.5, the UGP clone initially isolated in this study represented a C-terminally truncated form of the gene. The very C-terminal 15 amino acids were missing in the cDNA that was active both in Lec8 and *E.coli galU* complementation assays.

To predict a potential domain structure of the *L. major* UGP, a model based on the solved crystal structure of the human UAP (AGX1 and 2, Peneff *et al.,* 2001) using the program 3DPSSM (Kelly *et al.*, 2000) was generated. AGX is composed of three domains: an N-terminal domain, a C-terminal domain and a catalytic core domain including the pyrophosphorylase consensus motif and the binding pocket (Figure 30a). Though the sequence identity of the *L. major* UGP and AGX is only 17% (see Figure 16) and many gaps exist especially in the N- and C-terminal region, it may be possible that the *L. major* UGP exhibits a similar domain structure. Based on the model shown in Figure 30b, the potential N-terminal domain of the *L. major* UGP encompasses the amino acids 1-40. Therefore, one N-terminal truncation missing the first 38 amino acids was cloned. In a second construct, the first 69 amino acids were removed. The rational behind this truncation was to closely approximate the first very well conserved motif in the N-terminus, the pyrophosphorylase consensus motif, known to be required for activity.

The potential C-terminal domain comprises the amino acids 384 to 494 including a linker that connects the C-terminus to the core domain. However, the structure prediction program was not able to assign a structure to the last 47 amino acids. Therefore, these C-terminal residues were not included in Figure 30b. Two C-terminal truncations terminating the protein after amino acid 390 and 440, respectively, were designed (Figure 30). The corresponding cDNAs were cloned into the prokaryotic expression vector pET22b and were named pET-UGP-Δ38, pET-UGP-Δ69 and pET-UGP-Δ390–494, pET-UGP-Δ440-494, for the N-terminal and C-terminal truncations, respectively.
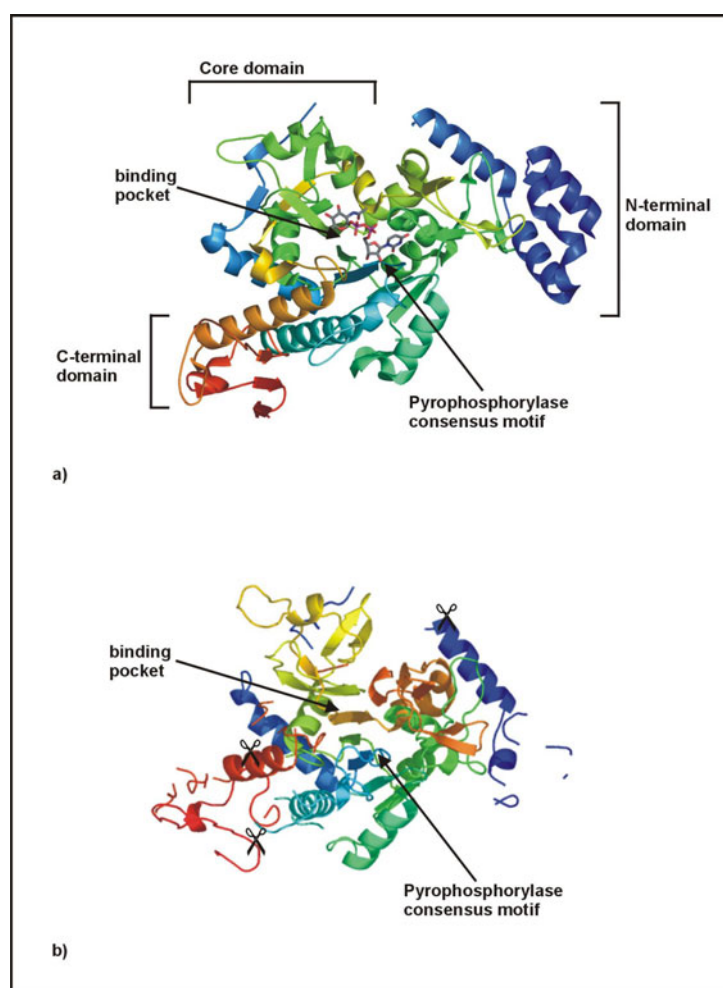
Figure 30 Predicted model of the *L. major* UGP. Based on the solved structure of the human UAP (AGX1) in complex with UDP-GlcNAc (a) a ribbon model has been build for the *L. major* UGP (program 3D-PSSM) (b). AGX consists of three domains an N-terminal, a C-terminal, and a core domain. The N- and C-terminal truncations of the *L. major* UGP are indicated by scissors. The mutant pET-UGP-Δ69 is not included in this figure, since the position is hidden in this presentation.

The constructs were transformed into *E.coli* DEV6 and tested for their *in vivo* activity on galactose containing MacConkey agar. The plasmid pET-UGP-His served as positive control in *E.coli* DEV6 complemention studies, visible by the growth of big red colonies (Figure 31f). Surprisingly, none of the truncated proteins was able to complement the *E.coli* DEV6 phenotype. These results indicated that deleted parts at either N- and C-terminus are necessary for functional activity of the UGP (Figure 31a-d). The empty vector pET22b was used as negative control (Figure 31e).

To exclude that the plasmids exhibited a lethal phenotype themselves, all constructs were transformed in *E.coli* DEV6 and cells were grown on glucose containing MacConkey agar. In this test system no lethal effects could be observed (data not shown).
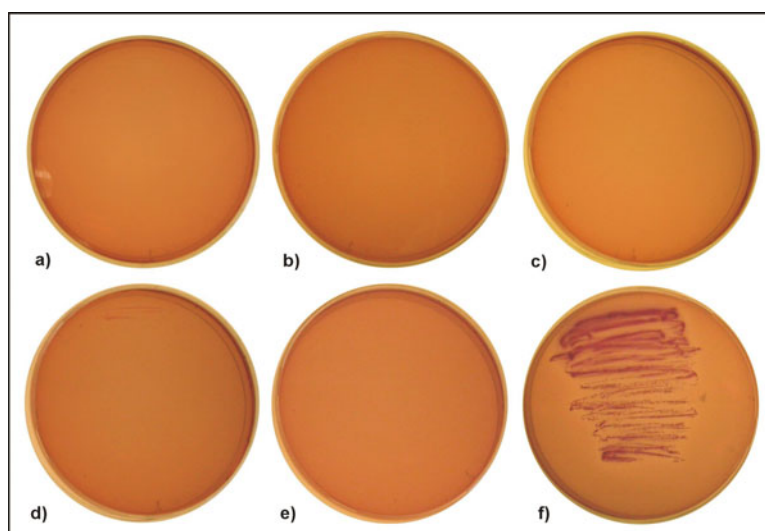
Figure 31 *In vivo* activity assay of the N- and C-terminal truncations. The constructs pET-UGP-Δ38 (a), pET-UGP-Δ69 (b),pET-UGP-Δ390−494 (c), pET-UGP-Δ440-494 (d), pET22b (e) and pET-UGP-His (f) were transformed into the *E.coli galU* mutant DEV6 and grown on 2% galactose and 1 mM IPTG containing MacConkey agar.

Since the expression in *E.coli* DEV6 was usually very low, the synthesis of stable proteins was confirmed in *E.coli* BL21(DE3). Soluble and insoluble protein fractions were prepared as described in 3.2.1. and fractions analysed by SDS-PAGE. The proteins were extended by C-terminal His-tags and could thus be identified in Western blot analysis using mAb α−pentaHis (Figure 32). Equal loading was confirmed by Roti-Blue staining (data not shown).
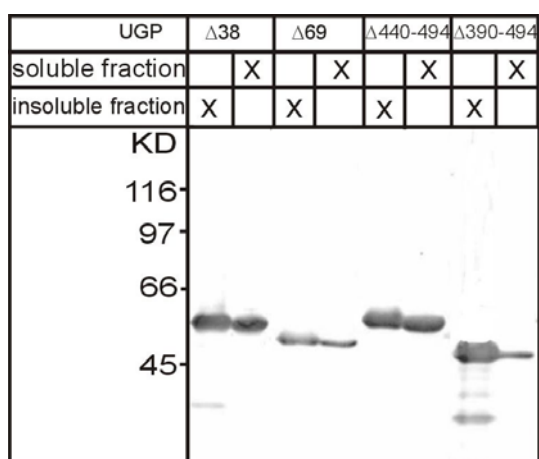
Figure 32 Expression control of the N- and C-terminal truncated UGPs. *E.coli* BL21(DE3) were used to express the truncated proteins cloned into the vectors pET-UGP-Δ38, pET-UGP-Δ69,pET-UGP-Δ390−494 and pET-UGP-Δ440-494. Expression was induced at an OD$_{600nm}$ of 0.6 with 1mM IPTG for 24 hours at 15°C. Cells were sonified and separated into soluble and insoluble fractions by centrifugation. The Western blotting was developed with mAb α−pentaHis.

The molecular masses of N-terminal truncated constructs were calculated to 53 kDa and 50 kDa. Protein bands of this size could be detected in the soluble and insoluble fractions as shown in Figure 32, lanes 1-4. UGP-Δ69 seemed to be less soluble and lower expressed than UDP-Δ38. In the case of the C-terminally truncated constructs UGP-Δ390–494 (50 kDa) was higher expressed and better soluble than UGP-Δ440-494 (46 kDa). Though there were differences in solubility of the different truncations, all cloned constructs allowed the expression of stable proteins, indicating that inactivity *in vivo* was not due to the absence of the proteins. In order to obtain more information on the functional domains of the *L major* UGP the decision was made to crystallise the full length protein.

3.2.7 Crystallisation of *L. major* UGP

As crystallisation may be hindered by flexible regions (e.g. epitope tags) within the protein, a construct bearing a thrombin cleavage site between the C-terminal His-tag and the UGP was cloned (pET22-UGP/thrombin-His). The expression, purification and activity testing of the His/thrombin-tagged UGP was the same as for His-tagged UGP described above. Purified fractions of the His-tagged, of the His/thrombin-tagged, and of the non modified UGP (after thrombin release of the His-tag) were used for crystallisation trials. These studies were carried out in collaboration with Dipl. Biochem.Thomas Steiner in the lab of Prof. Dr. Robert Huber, MPI for Biochemistry, Martinsried. In a first step, the crystallisation conditions were tested in a standard large scale approach.

Crystals were obtained for His- and His/thrombin-tagged UGP but these crystals did not diffract to a resolution sufficient for structure determination. Also after release of the His-tag no well diffracting crystals were obtained.

However, well-ordered crystals diffracting up to 2Å were obtained by adding the substrate UDP-glucose to the His/thrombin-tagged protein (Figure 33). The data set revealed that the crystal belonged to the monocline space group C2 (a= 88.11 Å, b= 80.2 Å, c= 138.11 Å, $\alpha = 90°$, $\beta = 90{,}46°$, $\gamma = 90°$). To solve the structure the multiwavelength anomalous dispersion phasing method using selenomethionine substituteded protein will be used. The selenomethionine labelled protein has already been produced and is currently used in crystallisation trials.
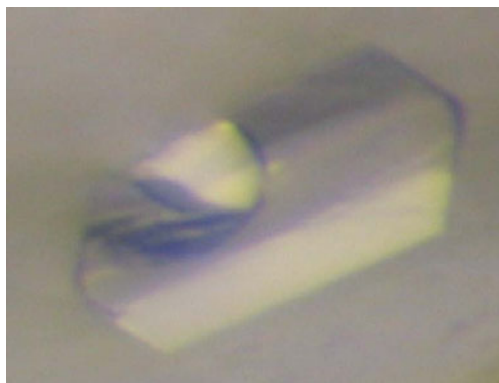
Figure 33 Crystal of His/thrombin-UGP. The crystal displayed was grown in the presence of UDP-glucose. The crystal diffracts up to 2 Å (picture supplied by Thomas Steiner)

3.2.8 Intracellular localisation of *L. major* UGP

The intracellular localisation of the *L. major* UGP was analysed by indirect immunofluorescence microscopy. CHO Lec8 cells were transiently transfected with pcDNAFL-*L. major*UGP expressing an N-terminally Flag-tagged enzyme. In addition, the plasmid peGFP-CI (Clontech) encoding the enhanced green fluorescent protein (eGFP) was transfected as a cytosolic and nuclear marker. The endogenous expressed proteins calnexin and mannosidase II were used to distinguish ER and Golgi localisation, respectively. 48 hours after transfection the cells were fixed, permeabilised and stained with the α–Flag M5 mAb and a α–mannosidase II or α– calnexin polyclonal serum. The secondary antibodies were coupled to Cy3 or Alexa 488 (Figure 34).

The fluorescence signal of *L. major* UGP colocalised with the cytosolic localised GFP signal. A nuclear localisation could be excluded (see Figure 34, GFP lane 3). This was also observed in the overlay with the ER marker calnexin. The fluorescence signal of the UGP is distributed within the whole cell and not restricted to the ER locus.
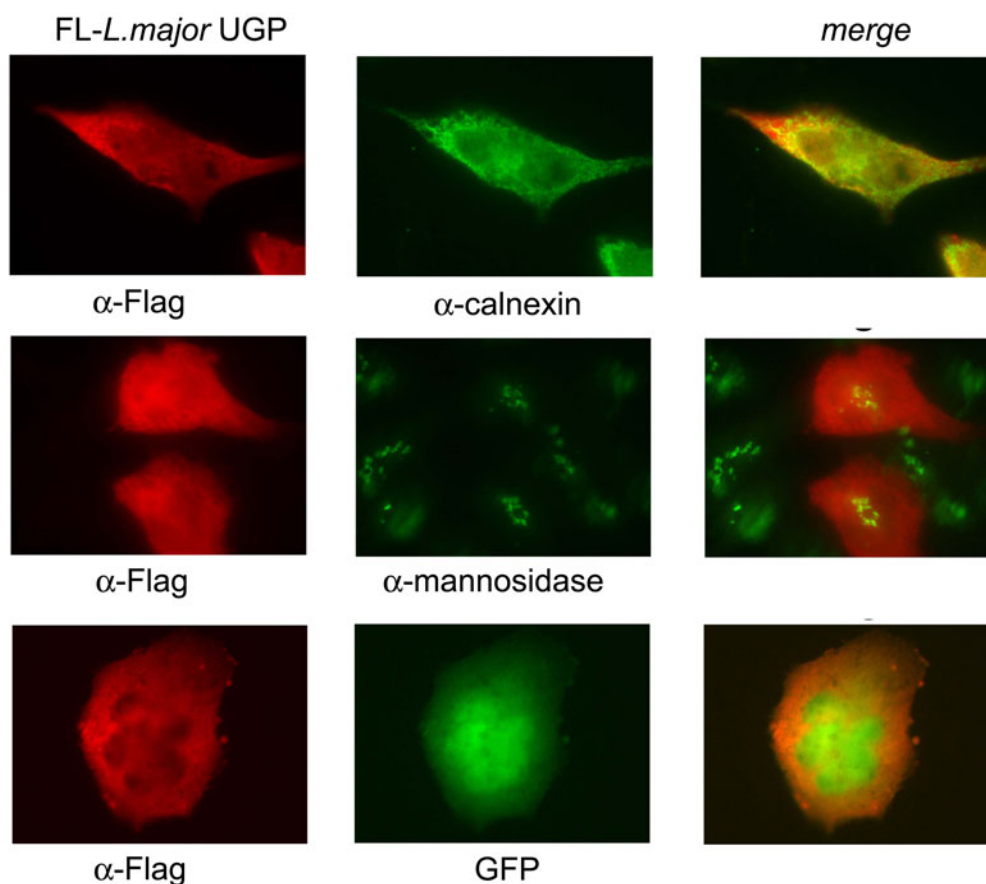
Figure 34 Intracellular localisation of *L. major* UGP. Indirect immunofluorescence labelling was used to display the intracellular localisation. The plasmids pcDNA3FL-*L. major*UGP and peGFP-CI were transfected into CHO Lec8 cells and the fixed cells permeabilised with Saponin. Endogenous calnexin and mannosidase II served as ER and Golgi marker, respectively. The intracellular localisation was analysed after 48 hours with the α–Flag mAb M5, α–calnexin and α–mannosidase II polyclonal serum, and Cy3- and Alexa488-conjugated secondary antibodies.

3.2.9 Production of a polyclonal serum directed against *L. major* UGP

So far, all characterisations were carried out with the recombinantly expressed epitope-tagged enzymes. In order to investigate endogenous *L. major* UGP, an antibody is required and under preparation. Aiming at generating a polyclonal antiserum five female New Zeeland rabbits, were immunized with an initial dosis of the purified UDP-glucose pyrophosphorylase and two boost injections have been followed after 3 and 7 weeks.

Titer development was tested in an ELISA (2.4.14) with serum samples taken 60 days after the first immunization. Therefore, microtiterplates were coated with the His-tagged UGP and incubated with serial dilutions of the sera (1:200 to 1:12800). As a positive control a α–pentaHis mAb and as a negative control serial dilutions of the preimmune sera were used. Signals were detected with the substrate ABTS after incubation with

HRP-coupled α–rabbit mAb or HRP-coupled α–mouse mAb for the positive control. A specific signal could be detected in the sera of all five rabbits with dilutions ranging from 1:3200 (rabbits #1, #2, #4) and 1:6400 (rabbits #3 and #5). Further boost injections are required to improve the antibody titre.

3.3 Generation and characterisation of a L. major *ugp gene deletion mutant*

The control of gene expression in *Trypanosomatids* differs from the mechanisms known in other eukaryotes. *Leishmania* genes contain no introns and are separated by short intergenic regions. The transcription is thought to occur in a polycistronic fashion and DNA sequences that usually mark promoters in other eukaryotes are absent (Borst *et al*., 1986, Kapler *et al*., 1990). However, the 5' and 3' untranslated regions are important for the correct transcription and processing into mature mRNA (de Lafaille *et al*., 1992, Flinn *et al.,* 1992). In addition, *Leishmania* are diploid unicellular organisms that lack a sexual cycle. To create a deletion mutant double targeted gene replacement has to be applied. Therefore, two independent selectable markers are used to replace both alleles of the complete endogenous gene locus by homologous recombination in successive rounds. For the proper transcription into polycistronic RNA, the untranslated regions are kept unaltered. This ensures not only the expression of the marker but also of surrounding genes, which is especially important in assigning a phenotype to a particular gene.

3.3.1 Determination of the *ugp* gene copy number in *L. major* 5ASKH

For a successful generation of a *ugp* gene deletion mutant, the gene copy number had to be determined. Genomic DNA from *L. major* 5ASKH (supplied by Joachim Clos, BNI Hamburg) was analysed by Southern Blotting. Therefore, the DNA was digested with the restriction enzymes *Nco*I, *Nco*I/*Bam*HI, *Blp*I, *Sac*I and *Sap*I. These digests allowed to determine the existence of different gene loci or multiple gene copies within the same locus. After transfer to a nitrocellulose membrane, the blot was hybridised with a Digoxigenin (DIG)-labelled *ugp* probe comprised of the complete open reading frame. The sizes of the expected signals assuming a single gene locus are depicted in Figure 35. The sequences of the 5' and 3' flanking regions were available from the *L. major* genome sequencing project (The Wellcome Trust Sanger Institute).
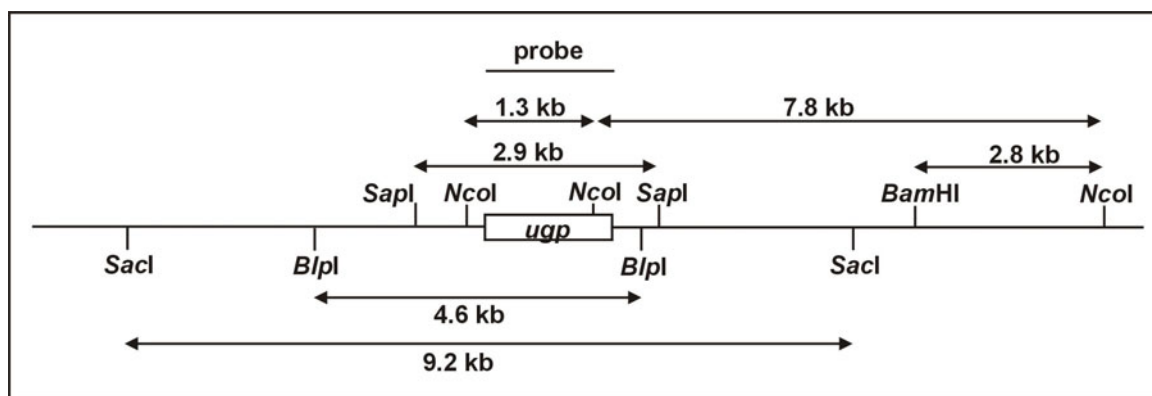
Figure 35 Schematic display of expected fragments in Southern blot analysis using the DIG-labelled *ugp* probe as shown.

Signals of about 4700 bp, 9200 bp and 2900 bp were obtained from DNA digested with *Blp*I, *Sac*I and *Sap*I, respectively, indicating a single *ugp* gene locus (Figure 36). The *Nco*I and *Nco*I/*Bam*HI digests confirmed this result. Since *Nco*I cuts once in the *ugp* sequence, two signals of about 7800 bp and 1300 bp were detected. The double digest using *Nco*I/*Bam*HI, reduced the 7800 bp fragement of the *Nco*I digest to a signal of about 5000 bp. No additional bands were visible. An unlabelled *ugp* PCR product of the complete coding sequence served as a positive control.
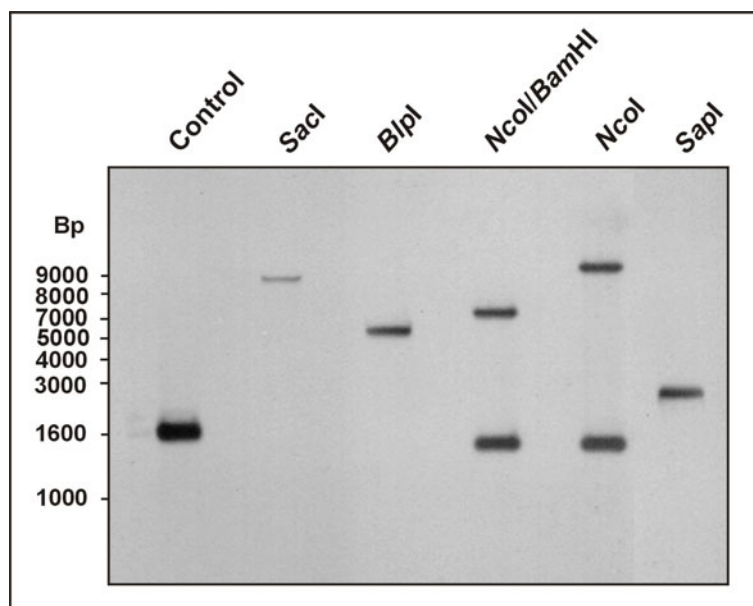
Figure 36 Southern Blot analysis of genomic *L. major* 5ASKH DNA. The DNA was digested with *Blp*I, *Sac*I, *Nco*I, *Nco*I/*Bam*HI and *Sap*I. The fragments were separated on a 0.7% agarose gel and transferred to a nitrocellulose membrane. The blot was hybridised with a DIG-labelled *ugp* probe. The control was unlabelled *ugp* PCR product.

3.3.2 Generation of a *L. major* gene deletion mutant

3.3.2.1 Cloning strategy

For gene replacement by homologous recombination the resistant markers hygromycin phosphotransferase (hyg), neomycin phosphotransferase (neo) and the phleomycin binding protein (phleo) were cloned between 1.5 kb of the 5' and 3' flanking regions of the *ugp* gene. As mentioned before, the sequence information was available from the *L. major* genome project (The Wellcome Trust Sanger Institute). The 5' and 3' region were amplified by PCR from the genomic *L. major* 5ASKH DNA using the primers ACM 54/ACM55 and ACM56/ACM57, respectively. The primers introduced a *Xba*I and *Bam*HI restriction site and a *Kpn*I and *Bam*HI restriction site at the 5' and 3' flanking region, respectively. These sites were used to subclone both fragments separately into the vector pcDNA3 (pcDNA3-5'FRs, pcDNA3-3'FRs). After sequencing, the *Bam*HI restriction site was used to fuse the flanking regions (pcDNA3-3'5'FRs) (Figure 38).

In addition, the above primers introduced a *Bsp*HI and *Nhe*I restriction site at the 3' end and 5' end of the 5' and 3' flanking region, respectively, to directly subclone the selectable markers from the vectors pCR2.1hyg, pCR2.1neo and pCR2.1phleo provided by Dr. Martin Wiese, BNI Hamburg. The *Bsp*HI site allowed the expression of the selectable markers from the same ATG start codon as the UGP, by altering only 2 bp of the 5' flanking region (Figure 37). The stop codon of the resistant markers was cloned in frame with the stop codon of the *ugp* gene separated by the *Nhe*I site. No mutations were made in the 3' untranslated region.

5' GGA GGT GAA G *TC* **ATG** A GGA TCC GCT AGC **TAG** GGG TCA CAA GCT 3'

                *Bsp*HI   *Bam*HI   *Nhe*I

Figure 37 Cloning region of the 5' and 3' flanking regions. The start and stop codon of the *ugp* gene are shown bold. The -1 and -2 positions were mutated from C to T and A to C to introduce the *Bsp*HI site depicted in italic.
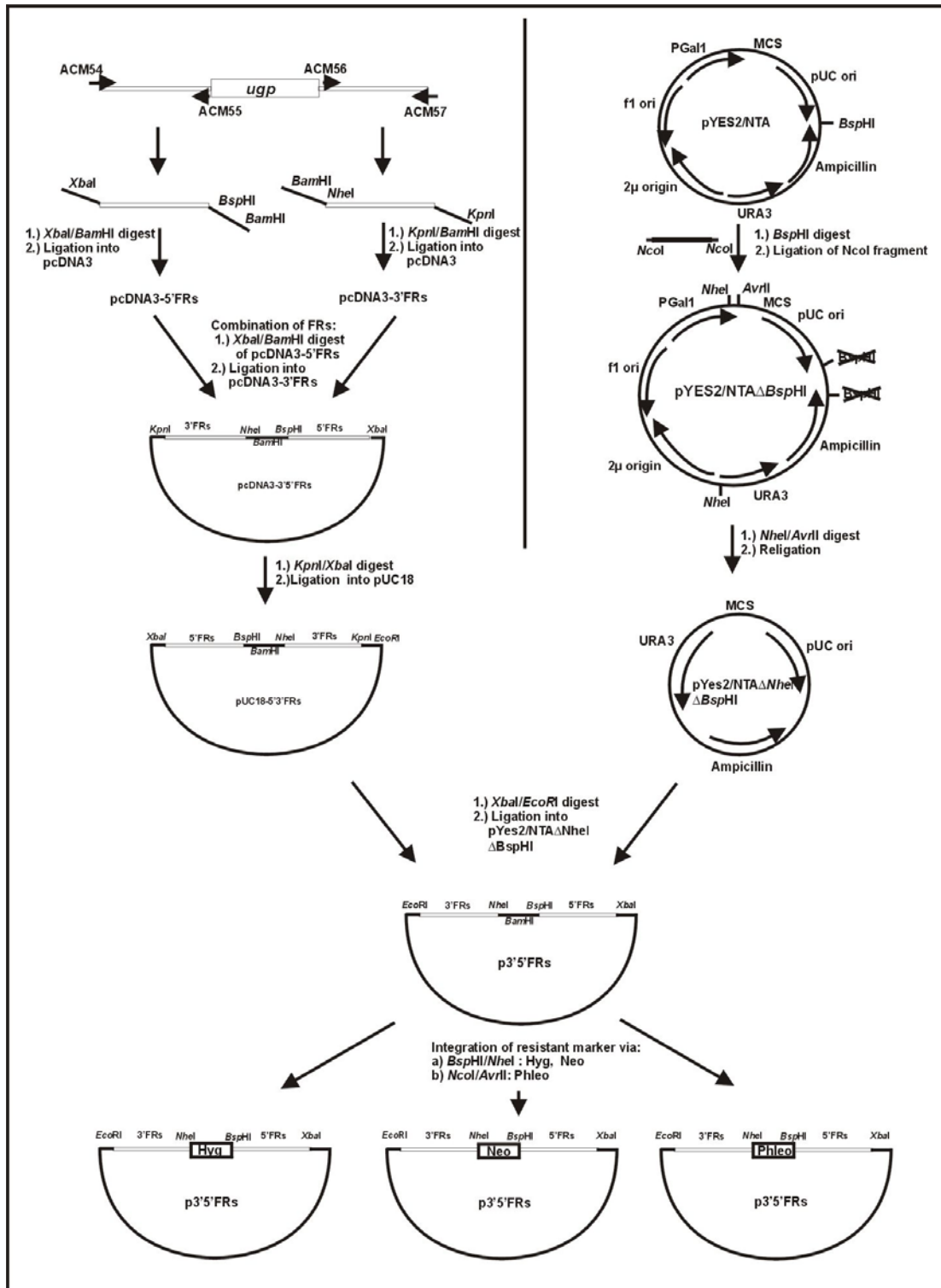
Figure 38 Cloning strategy to generate the *ugp* gene deletion constructs

In the next step, the backbone of the vector pYes2/NTA was chosen to create a new vector without *Bsp*HI and *Nhe*I restriction sites. *Nco*I sites ligate into *Bsp*HI sites by the loss of both restriction sites. The same is true for *Nhe*I and *Avr*II.

Therefore, the *Bsp*HI restriction site of pYes2/NTA was eliminated by the integration of a 900 bp *Nco*I fragment from the vector pcDNA3 resulting in the vector pYes2/NTAΔ*Bsp*HI. The digestion and relegation of pYes2/NTAΔ*Bsp*HI with *Nhe*I and *Avr*II destroyed the two remaining *Nhe*I restriction sites (Figure 38). The new vector was named pYes2/NTA Δ*Bsp*HI/Δ*Nhe*I . Unfortunately, the *Kpn*I site overlapped with the destroyed *Avr*II site and could not be used to directly subclone the fused 5' and 3' flanking region. The introduction of a suitable restriction site was achieved by subcloning the flanking regions into the vector puC18 (pUC18-5'3'FRs). After a *Xba*I/*Eco*RI restriction digest the flanking regions were ligated into pYes2/NTA Δ*Nhe*I/Δ*Bsp*HI (p3'5'FRs). In the last step, the hygromycin and neomycin resistant markers were subcloned between the 5' and 3' flanking regions using the *Bsp*HI and *Nhe*I restriction sites (p3'5'FRs-hyg, p3'5'FRs-neo). For the subcloning of the phleomycin resistant marker, the plasmid pCR2.1phleo and p5'3'FRs were digested with *Nco*I/*Avr*II and *Bsp*HI/*Nhe*I, respectively (p3'5'FRs-phleo). The ligation of the marker into p5'3'FRs resulted in the elimination of both restriction sites.

3.3.2.2   Targeted gene deletion of *L. major ugp*

The generation of the *L. major* knock out mutant was done in the lab of Dr. Martin Wiese, BNI Hamburg. Detailed transfection and selection protocols were kindly provided by Prof. Jonathan LeBowitz, Purdue University, West Lafayette, USA.

The hygromycin and phleomycin containing gene replacement cassettes were excised from the plasmids p5'3'FRs-hyg, p5'3'FRs-phleo by BsaAI digest resulting in fragments of 3.5 kb and 2.9 kb, respectively. The neomycin targeting construct was excised from the vector p5'3'FRs-neo by a *Kpn*I/BbvCI digest yielding a fragment of 3.1 kb.

The fragments were separated on an agarose gel and purified by gel extraction followed by ethanol precipitation (2.5.6.2 and 2.5.1).

Since the efficiency of the homologous recombination of the different markers varies depending on the *L. major* strain used, all three resistant markers were transfected in parallel experiments in the first round. Thus, wild-type *L. major* 5ASKH were transfected with 2 µg DNA by electroporation (2.3.2). The selection of the parasites was accomplished by growing the transfected parasites on agar plates containing the appropriate selective drug. In contrast to selection of transformants in solution, selection on plates permits isolation of clonal lines.

After 10 days of incubation at 26°C, colonies were visible on the agar plates. In the first round, more hygromycin than phleomycin resistant clones were obtained. This phenomenon was reproducible after repetition of the first round of transfection. This result suggested that the integration of the phleomycin resistant marker was more difficult than the hygromycin resistant marker. No colonies could be obtained using the neomycin targeting construct.

The colonies were transferred into liquid media and cultures were expanded to prepare genomic DNA and DMSO stocks (2.3.1 and 2.5.13). The DNA of the different clones were screened by PCR for the correct insertion of the resistance marker at the 5' and 3' end (see 2.5.12.2) and PCR-positive clones were subjected to Southern Blot analysis (2.5.14). In the following, figures one representative hygromycin and two representative phleomycin resistant clones are shown. These three clones were used in the consecutive round to generate homozygous mutants.

To confirm the integration into the right locus, a probe was designed that hybridized outside the region used for homologous recombination (5'UTR). The corresponding DNA sequence was subcloned into the vector pcR4-Topo and used for DIG-labelling (see 2.5.12.3).

The genomic DNA of the mutants and wild type was digested with *Blp*I, separated on an agarose gel and transferred to nitrocellulose. After hybridisation with the DIG-labelled 5'UTR probe, the wild type allele was detected at 4.6 kb in all samples (Figure 39). The hygromycin and phleomycin resistant mutants showed an additional band at 4.2 kb and 3.5 kb, respectively. These bands corresponded to the replaced *ugp* allele by the hygromycin and phleomycin cassettes and indicated successful replacement. In addition, a *Sph*I digest using the same probe also confirmed the correct insertions into the *ugp* gene locus (data not shown).
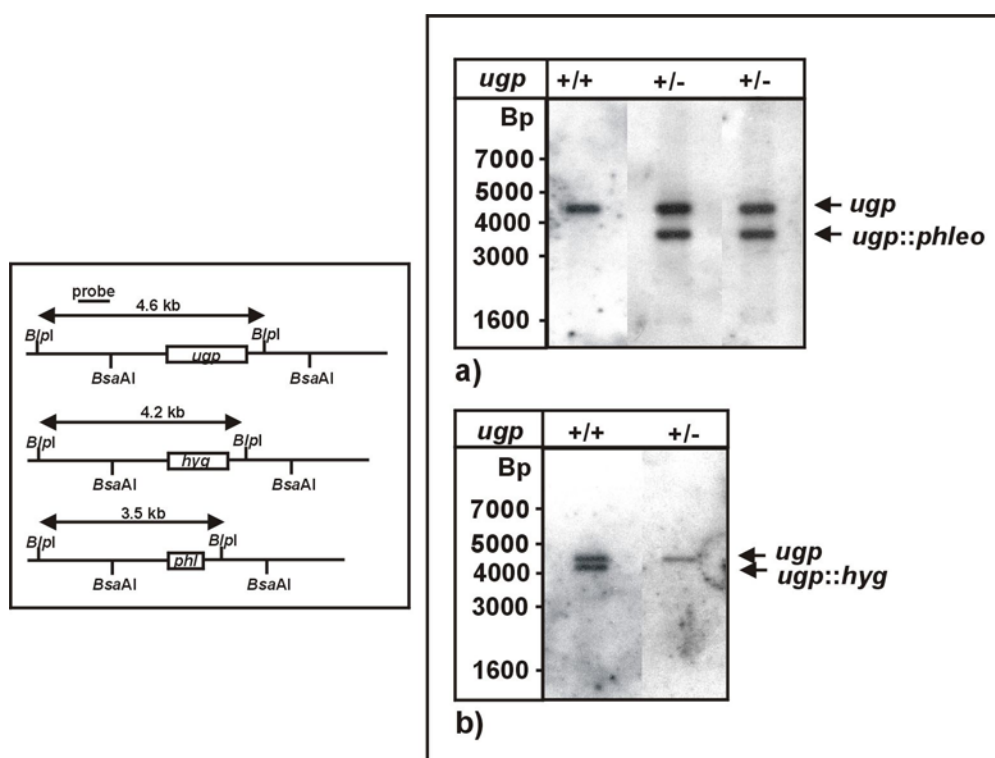
Figure 39 Southern Blot analysis of the heterozygous *ugp* mutants. Genomic DNA of a) phleomycin and b) hygromycin resistant clones was digested with *Blp*I, transferred to nitrocellulose and hybridized with a 5'UTR probe. The expected fragments are depicted on the left hand side. As a control wild type genomic DNA was treated in the same way.

To exclude random integration of the target construct, the genomic DNA was digested with *Sac*I and *Blp*I and hybridised with a DIG-labelled probe consisting of the complete coding sequence of the corresponding resistant marker. The signals detected for the phleomycin clones, 8.1 kb and 3.5 kb for the *Sac*I and *Blp*I digest, respectively, indicated a single integration into the genome at the *ugp* locus (Figure 40a). The same result was obtained for the hygromycin resistant clone, where fragments of 8.6 kb and 4.2 kb were visible (Figure 40b). The probes showed no unspecific hybridisation in wild type parasites.
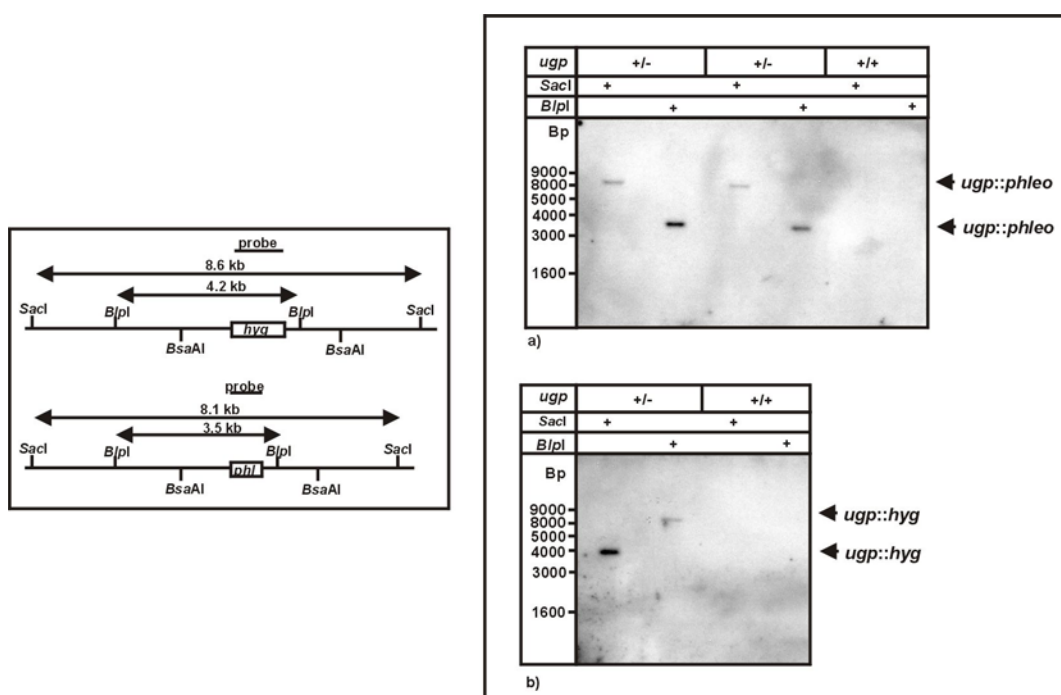
Figure 40 Determination of random integration by the targeting constructs. Genomic DNA of a) phleomycin, b) hygromycine resistant clones and of the wild type strain was digested with *Blp*I and *Sac*I and analysed by Southern blotting. The blots were hybridised with a DIG-labelled a) phleomycin and b) hygromycin probe. The expected fragments are shown on the left hand side.

Since the integration of the hygromycin targeting construct seemed to be preferred, two phleomycin resistant clones and just one hygromycin resistant were electroporated with the hygromycin and phleomycin targeting constructs in the second round, respectively. The neomycin targeting construct was not used any more.

Homozygous lines were obtained from both phleomycin resistant clones, but no clones could be obtained in the case of hygromycin resistant clone, confirming the result of the first round that integration of phleomycin in *L. major* 5ASKH is more difficult. The phleomycin/hygromycin resistant lines were expanded and genomic DNA as well as DMSO stocks were prepared.

As for the heterozygous mutants, PCR-positive clones were subjected to Southern blot analysis. For each heterozygous clone used in the second round, two representative homozygous clones are shown. The wild type and corresponding heterozygous clone was included in the analysis. The genomic DNA was digested with *Blp*I and after transfer to a nitrocellulose membrane, the correct insertion was confirmed by hybridisation with a DIG-labelled 5'UTR probe. The remaining wild type allele of the heterozygous phleomycin resistant clone was replaced with the hygromycin marker in the homozygous clones (Figure 41). The signals obtained for the homozygous clones corresponded to the size of the phleomycin (3.5 kb) and hygromycin (4.2 kb) resistant cassettes.
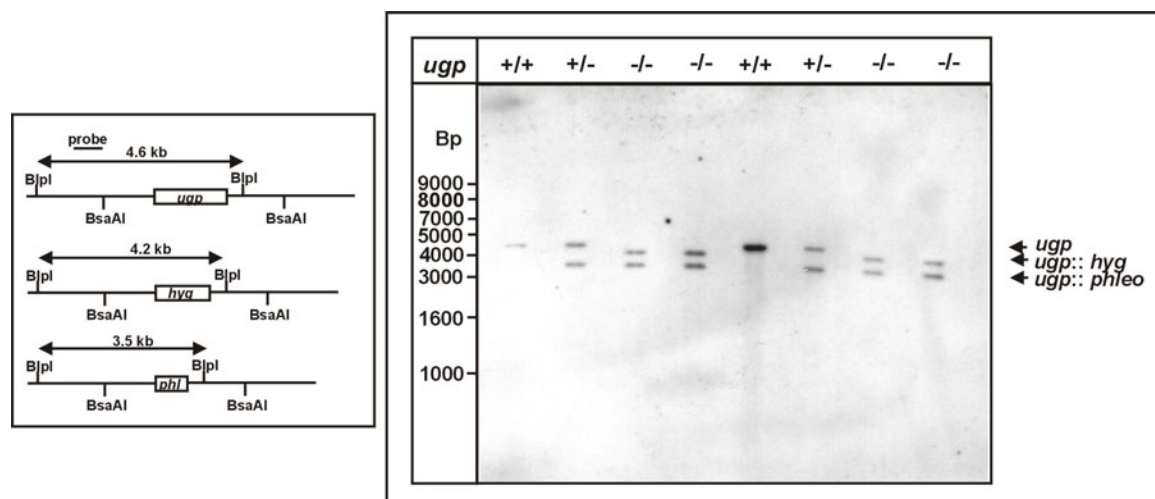
Figure 41 Southern Blot analysis of the homozygous *ugp* mutants. The homozygous *ugp* mutants, the corresponding heterozygous mutant and the wild type strain were transferred to nitrocellulose after *Blp*I digest and analysed with a DIG-labelled 5'UTR probe. On the left hand side the expected fragments are outlined.

The successful generation of *ugp* null mutants was confirmed by a Southern blot using the whole open reading frame of *ugp* as a probe. After *Sac*I digest, the signal intensity of the wild type alleles (9.2 kb) in the heterozygous clones was reduced compared to the wild type strain whereas no signal was detected for the homozygous clones (Figure 42).
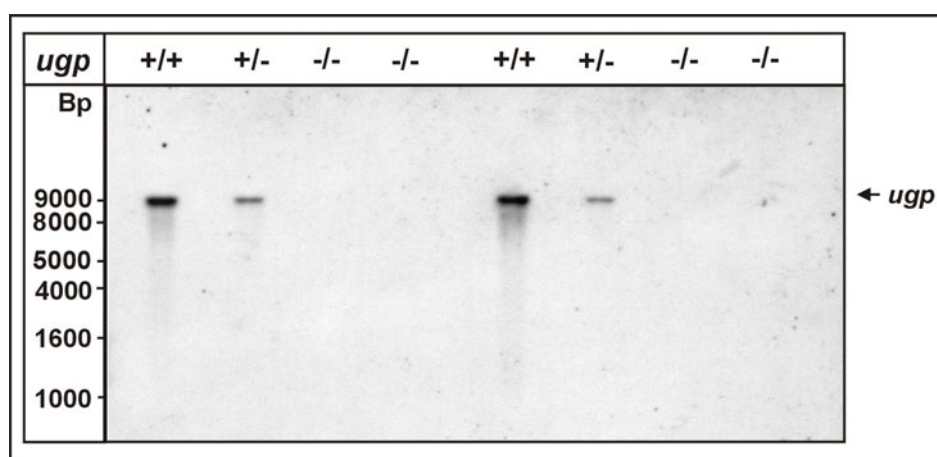
Figure 42 Confirmation of the gene deletion in the *ugp* locus. The hygromycin *ugp* mutants, the corresponding heterozygous mutant and the wild type strain were analysed by Southern blotting after *Sac*I digest using the complete coding sequence of the *ugp* gene as a probe.

In addition multiple insertions of the resistant markers in the second round were excluded by probing the clones with a DIG-labelled hygromycin probe after *Blp*I and *Sac*I digest and transfer to a nitrocellulose membrane (data not shown).

3.3.3 Charactersiation of the *ugp* knock out mutant

The deletion of the *ugp* gene was not lethal and the growth behaviour of homozygous and heterozygous clonal lines was normal compared to the parental wild type strain. In addition, no obvious differences in shape and size in the mutant lines could be detected using a light microscope.

3.3.3.1 Analysis of phosphoglycans

The major phosphoglycan on the cell surface of *L. major* is LPG. LPG consists of a GPI anchor joined to a glycan core and a large phosphoglycan domain of 15-30 Gal-Man-P repeating units (Figure 2). *L. major* also express proteophosphoglycans (PPGs), containing a phosphoglycan domain of Gal-Man-P repeating units, which is mainly secreted but also present on the cell surface (Foth *et al.*, 2002, see 1.2.1).

The synthesis of LPG and PPG requires the formation of UDP-glucose and UDP-galactose by the UDP-glucose pyrophosphorylase and thus should be hindered in the *ugp* mutants. In the following the phosphoglycan content of the *ugp* mutants was analysed.

3.3.3.2 *Analysis of phosphoglycans by immunofluorescence and immuno-fluorescence activated cell sorting (FACS)*

Leishmania wild type parasites, a heterozygous (*ugp* +/-) and two independent homozygous *ugp* mutant strains (*ugp* -/-, clone 1 and *ugp* -/-, clone 2) were analysed by immunoflourescence using the mAb WIC79.3 (Greenblatt *et al.*, 1983) and a Cy3-coupled secondary antibody (see 2.3.4). The mAb WIC79.3 recognizes the galactose substituted repeating unit of phosphoglycans. The nuclei were stained with DAPI and a 40x magnification was used to visualize the parasites.

As expected, the surface coat of wild type cells was strongly labelled. On the heterozygous *ugp* mutants the signal was less intense compared to the parental wild type strain. The homozygous parasites showed a drastically diminished signal (Figure 43). However they were not completely devoid of galactose substituted repeating units as can be seen using a two times longer exposure time than in Figure 43 (Figure 44). The same result was obtained using the mAb LT6 that recognizes unsubstituted Gal-Man-P repeats (data not shown).
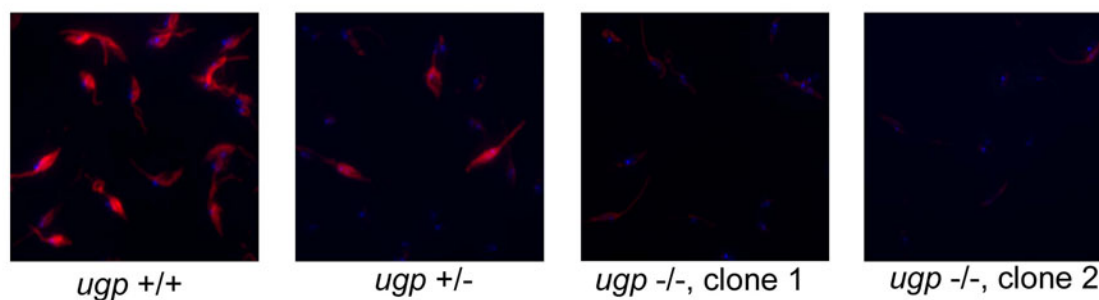
Figure 43 Detection of the phosphogylcans on the cell surface of *L. major* wild type and *ugp* het-erozygous and homozygous mutants. The parasites were fixed on poly-(L)-lysine coated glass slides and sequentially incubated with the mAb WIC79.3 and Cy3 coupled secondary antibody. Nuclei were stained with DAPI.
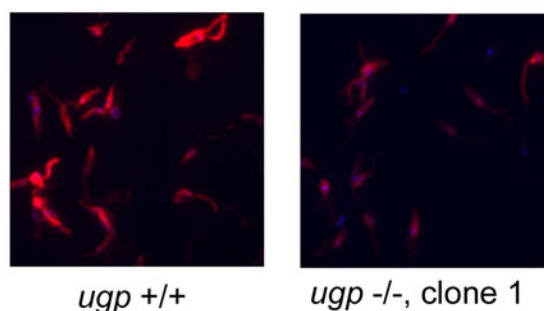
Figure 44 Intensified detection of phosphogylcans on the cell surface of *L. major* wild type and *ugp* heterozygous and homozygous mutants. In order to increase the signal observed in Figure 43 the exposure times were doubled in this experiment.

To quantify the phosphoglycan content of the homozygous lines, the parasites were analysed by FACS (2.3.3). Therefore, *Leishmania* wild type cells and homozygous *ugp* mutant cells were incubated with mAb WIC79.3 and FITC-conjugated secondary anti-body. Prior to the measurement, the parasites were fixed in paraformaldehyd. *L. major* wild type cells incubated only with secondary antibody were used as negative control (Figure 45). The analysis showed that the phosphoglycan content of the homozygous *ugp* mutants was about 100 fold decreased compared to wild type cells.
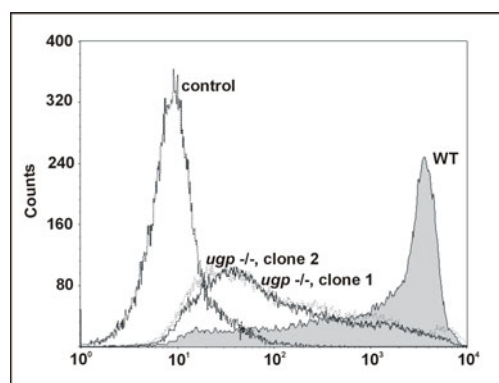
Figure 45 FACS analysis of the homozygous *ugp* mutants and wild type parasites. Cells were stained with the mAb WIC79.3 followed by FITC-coupled secondary antibody. 50 000 fixed parasites were counted per experiment.

Though the cells were all grown in the same culture, they can be in slightly different stages with a varying number of the phosphoglycan repeating unit (see introduction). Since this is the epitope recognized by the mAb WIC79.3 and LT6, the cell populations were not homogeneously stained in the immunofluorescence and FACS analysis.

3.3.3.3 *Western Blot analysis of LPG*

LPG was solubilised in lysis buffer containing 0.1%TritonX-100 followed by sonification (see 2.4.9.1). The protein concentration of the soluble fractions was determined by a BCA assay and equal amounts of the lysates from the wild type and *ugp* mutants strains were separated on a gradient SDS-PAGE (2.4.2). The Western Blot was analysed with the mAb WIC 79.3 and ECL detection (Figure 46a). Due to microheterogenicity of the chain length, LPG appears as a diffuse distending signal between 100 and 30 kDa. In the heterozygous line the LPG content is drastically reduced compared to the parental wild type strain. However, there was still a LPG signal present in the two independent homozygous lines (lanes 3 and 4) though it is less intense compared to the heterozygous and wild type strain. Equal loading was confirmed by Ponceau S staining of the membrane (data not shown) and by Roti-Blue staining of a second gel (Figure 46b). This result confirmed the data obtained from immunofluorescence and FACS analysis. Though the *ugp* gene was missing, the mutants were still able to produce UDP-galactose.
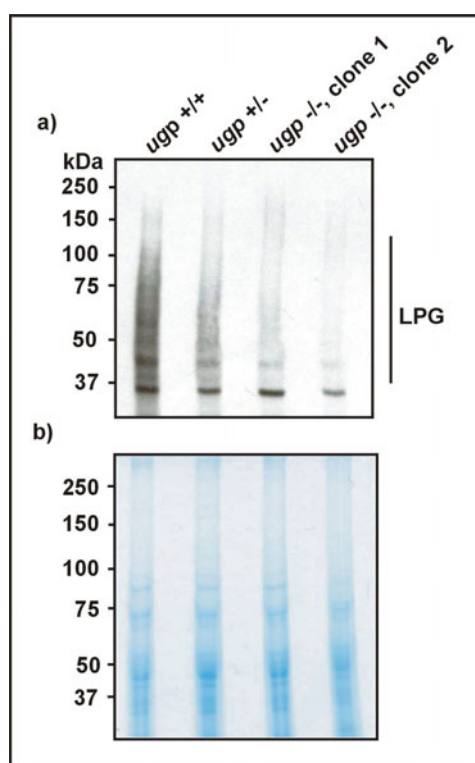
Figure 46 Detection of LPG by Western blotting. a) Lysates of wild type, *ugp* heterozygous and two independent strains of homozygous parasites were separated on a gradient SDS-PAGE and after Western blotting were analysed with the mAB WIC79.3 and ECL detection. b) A second gel was stained with Roti Blue to confirm equal loading.

3.3.3.4 Measurement of UDP-glucose pyrophosphorylase activity in the *ugp* mutants

The UGP activity of the *ugp* mutants was determined in an *in vitro* activity assay. The activity was measured by a coupled $NADH+H^+$ producing reaction with the UDP-glucose dehydrogenase. The $NADH+H^+$ production was monitored at OD_{340nm} in a spectrophotometer and used to calculate activity (see 3.2.2).

Parasites of the wild type strain and the mutant strains were suspended in assay buffer (50 mM Tris/HCl, pH 8. 10 mM $MgCl_2$) and sonified. Lysis was confirmed using a light microscope and the protein concentration determined by a BCA test (2.4.9.2). In the soluble fraction of the wild type strain an activity of 0.41 µmol/min per mg protein was measured whereas in the heterozygous *ugp* sample the activity was reduced by half to 0.24 µmol/min per mg protein. However, the two homozygous lines (*ugp* -/-, clone 1, *ugp* -/-, clone 2) tested clearly showed a residual UGP activity of 0.04 and 0.06 µmol/min per mg protein, respectively (fig. 40).

The existence of a second $NADH+H^+$ producing reaction in the lysates itself was analysed by an activity measurement without the coupling enzyme UDP-glucose dehydrogenase. No activity could be detected in these controls.
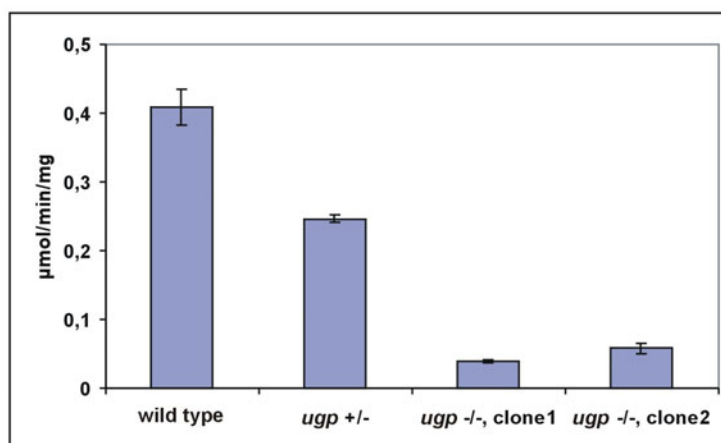
Figure 47 *In vitro* UGP activity of wild type and *ugp* mutants. The cells were lysed by sonification and the activity of the forward reaction analysed by a coupled enzyme assay. NAD^+ reduction was measured in a spectrophotometer and the linear rates used to calculate activity based on its extinction coefficient.

3.3.3.5 Experimental infection of mice with the *ugp* mutants

The influence of the *ugp* deletion on infectivity was determined in a mouse infection model. The virulence of the parasites was assessed following inoculation in footpads of female Balb/c mice. The parental wild type line, two clonal heterozygous and 4 clonal homozygous lines were grown to late logarithmic phase and 10^7 parasites per mouse were injected. Each group consisted of five mice. The lesion formation was monitored by comparing the thickness of the infected and uninfected footpad with a Vernier calliper. The footpads were measured every 7 days over a period of 10 weeks.

Lesion formation of the wild type strain occurred 3 weeks after inoculation and progressed steadily (Figure 48). In contrast the homozygous lines showed a delayed lesion formation and swelling occurred 5 weeks after inoculation. Interestingly infection with the heterozygous mutants produced a time course that was exactly between the wild type and homozygous lines. This data suggest a gene doses effect.

The *in vivo* infection model indicated that the *ugp* mutants are attenuated for virulence in mice.
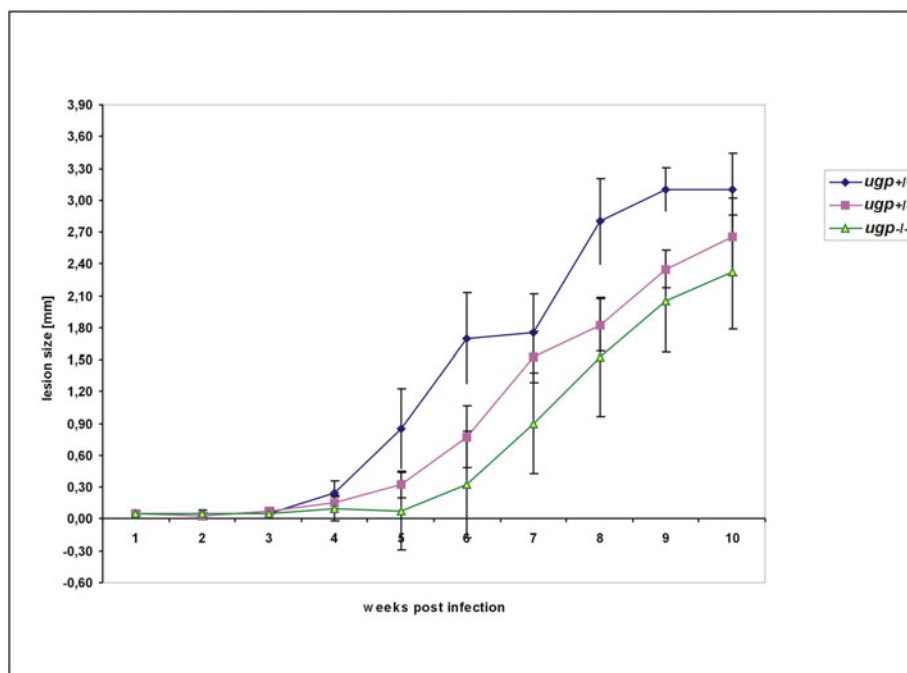
Figure 48 *In vivo* **testing of virulence.** The time course of lesion formation after infection of Balb/c mice with *L. major* wild type (blue line), heterozygous (pink line), and homozygous (green line) *ugp* mutant strains was monitored by measuring swelling of footpad. After infection of female Balb/c mice the infected and uninfected footpads were measured once a week over 10 weeks. The median size difference (+/- MAD) of the infected and uninfected footpad was plotted against the weeks post infection. Two heterozygous and four homozygous mutant clones were tested. For each clone 5 animals were infected.

4 Discussion

4.1 Identification of the L. major *UDP-glucose pyrophosphory-lase*

In this study, a functional active UDP-glucose pyrophosphorylase (UGP) from *L. major* was identified and biochemically characterised. The enzyme catalyses the reversible reaction of glucose-1 phosphate and UTP to UDP-glucose and pyrophosphate (see Figure 5). The enzyme represents a key position in the galactose metabolism allowing the entry of galactose-1 phosphate into glycolysis in organisms that utilize the Leloir pathway (see 1.4.1). In addition, UDP-glucose is a direct and indirect precursor of a number of nucleotide sugars, like UDP-glucuronic acid, UDP-xylose and UDP-rhamnose (Kleczkowski *et al.,*1994).

Most surprisingly, the *L. major* enzyme was able to reconstitute the wild type phenotype after transfection into Lec8 cell, a CHO cell line defective in the UDP-galactose transporter (Deutscher *et al.,* 1986). This cell line was used before to isolate functionally active UDP-galactose transporters from a cDNA library by complementation cloning (Bakker *et al.,* 2004). Although, an identical cloning strategy was applied to isolate the UDP-galactose transporter from an *L. major* cDNA library, this approach resulted in the identification of the UGP. In fact, the cloning of this gene cannot be explained by potential artefacts caused by the applied staining techniques because different detection systems including the use of two antibodies and different colour reactions were used. Moreover, the absence of cross-reactions with the secondary antibody was guaranteed. Thus, the complementation seen in CHO Lec8 cells by the *L. major* UGP was real and most likely can be explained by the characteristics of the cell line as will be discussed below.

The UGP-mRNA must be highly expressed in procyclic promastigote parasites because the corresponding cDNA was present in 64 out of 86 pools of the cDNA library derived from this organism (see 3.1.7). This observation is in line with the fact that procyclic promastigote parasites upregulate the expression of galactose containing phosphoglycans which requires the expression of enzymes involved in the galactose metabolism (reviewed in Naderer *et al.,* 2004). Since the UGP plays a critical role in the galactose metabolism, the high expression level provides strong indication for the central function of the enzyme in promastigote *L. major* parasites.

The initially selected complementing cDNA pool did not contain a complete UGP clone. The full length cDNA could be isolated based on homology to a sequence fragment identified in the genome data base (The Wellcome Trust Sanger Institute and see 3.1.5.1). Comparative complementation testings carried out with the truncated and full

length cDNA did not reveal any significant differences, indicating, that the terminal 15 amino acids are dispensable for the formation of the active enzyme.

UGPs have been identified from a number of prokaryotic and eukaryotic organisms, but no significant sequence homology can be observed between prokaryotic and eukaryotic UGPs. Thus, the motif $XLXGGXGTXXGX_4K$, called the pyrophosphorylase consensus motif, highly conserved in all eukaryotic UGPs including *L. major* and in various eukaryotic UDP-GlcNAc/GalNAc pyrophosphorylases (UAP) is absent in the prokaryotic UGPs, although, surprisingly, a similar motif ($XLXXGXGTX_7K$) exists in the bacterial UAP (Peneff *et al.,* 2001).

If aligned to the human, yeast and plant homologous, the *L. major* UGP shows an amino acid sequence identity of 37% to 40% (3.1.5.2). Conservation is focused to amino acid stretches 15-20 residues in length and largely concentrated in the C-terminal part of the protein (Figure 16). The function of the conserved motifs is not clear yet. Since, no eukaryotic UGP has been crystallised so far, the available data on the human UAP (AGX) was used to predict the three dimensional structure of the *L. major* enzyme (Figure 30).

Despite this high identity, the UGP activity was confirmed *in vivo* and *in vitro*. The *in vivo* activity was analysed by the complementation of the *E.coli galU* mutant. Due to a defect in the *ugp* the *E.coli galU* mutant is not able to metabolise galactose (Sundararajan *et al.,* 1962). The growth on agar, containing galactose as the only carbohydrate source is abolished. The transformation of the *L. major* UGP restored the wild type situation and confirmed activity *in vivo* (see 3.2.3). In addition, the epitope-tagged *L. major* UGP was recombinantly expressed in *E.coli* BL21 (DE3) and purified by affinity chromatography (see 3.2.1). In a one step purification using a C-terminal His-tag a purity of about 95% and a yield of about 20 mg per litre culture was obtained. Interestingly, an N-terminal StrepII-tag was not accessible for purification though an N-terminal Flag-tag could be used in indirect immunofluorescence (see 3.2.8).

The activity of the purified enzyme was analysed in the forward (fwd.) and reverse (rev.) reaction by coupled enzymatic reactions (see 3.2.2.). The maximum velocities were determined to be $V_{max,fwd}$ = 3347 µmol/min per mg protein and $V_{max,rev.}$ = 2316 µmol/min per mg protein indicating a reversible activity *in vitro*.

4.1.1 Characterisation of the galactose background in CHO Lec8 cells

As mentioned in chapter 3.1.1, Lec8 cells were found to be not completely devoid of galactose on their cell surface though they have been proven to lack a functional UDP-galactose transporter. In immunocytochemistry, a basal galactose expression on the cell

surface of the CHO Lec8 cell line CHOP8 could be detected. The background of positive cells could neither be depleted by cultivating the cells in the presence of the sialic acid binding lectin WGA (wheat germ agglutinin) nor by incubation with the galactose binding lectins European mistletoe or Ricinus communis agglutinin (RIC) (see 3.1.1.1). The classification of a glycosylation defective CHO cell line into a certain complementation group is based on its resistance or sensitivity to a series of certain plant lectins (Lec-mutants, Stanley, 1984). However, lectin resistances or sensitivities are relative values and are reported as fold resistance/sensitivity compared to the parental cell line. Though the CHO Lec8 cell line is a 100 fold more resistant to WGA and 2 fold more resistant to RIC than wild type cells, this does not ensure that the cells are completely devoid of galactose or sialic acid.

To gain deeper insight into the galactosylation capacity of Lec8 cells, three additional cell lines exhibiting the *lec8* defect (Lec3.2.8, Lec4.8.7A and the commercially available Lec8(3D)) were investigated. These mutants were chosen, because an earlier study in the laboratory (Oelmann *et al.,* 2001) had confirmed the absence of a functional UDP-galactose transporter. As described in paragraph 3.1.6, these cell lines are still able to express galactosylated and sialylated glycans on the cell surface. In addition, the FACS analysis demonstrated that all cells in the population show a residual presence of sialylation and negates the possibility that the background transport of UDP-galactose is due to single revertants.

Revertants were known to occur during the cultivation of the CHO Lec32 cell line lacking a functional CMP-*N*-acetylneuraminic acid synthetase (CMP-sialic acid synthetase, see PhD thesis, Anja Münster 1999 and Münster *et al*., 1998). This enzyme catalyses the formation of CMP-sialic acid (Neu5Ac) and PP_i from Neu5Ac and CTP and is located in the nucleus. The reason for this unusual intracellular localisation has been investigated for more than 30 years but is still an enigma. The loss of CMP-sialic acid synthetase activity results in the absence of sialic acid on the cell surface. The molecular basis for the revertation of this cell line is not understood, but may be related to a putative second function of this enzyme in the nucleus rather than the requirement of sialic acid on the cell surface. Support for this speculation arises from the fact that another asialo mutant shows a stable phenotype. This cell line of the complementation group Lec2 lacks a functional CMP-sialic acid transporter (Deutscher *et al.,* 1984). The second unknown function of the CMP-sialic acid synthetase may result in the activation of the second allele that is usually inactivated by methylation in CHO cells (Holliday *et al.,*1990). The existence of revertants in the case of the CHO Lec8 cells was rather unlikely since the appearance of positive cells was not increased during the time of cultivation. In addition,

a clear complementation could be detected even with the basal level of UDP-galactose transport. This could also account for a lower expression of the second allele but most likely, Oelmann *et al.,* (2001) would have detected this functional mRNA transcript in the detailed characterisation of the CHO Lec8 cells (see PhD thesis Stefan Oelmann and Oelmann *et al.,* 2001). Taken together, these findings suggest another reason for the basal galactose expression in CHO Lec8 cells. As mentioned in 3.1.5 the possibility exists that other nucleotide sugar transporters are able to transport UDP-galactose though with a lower efficiency. Until now, four multi-substrate nucleotide sugar transporters have been described. These include a *C.elegans* transporter transporting UDP-glucuronic acid (UDP-GlcA), UDP-N-acteylglucosamine (UDP-GlcNAc) and UDP-galactose (UDP-Gal) (Bernisone *et al.,* 2001), a humane UDP-glucuronic acid/UDP-N-acteylgalactosamine transporter (Muraoka *et al.,* 2001), and a *Drosophila* transporter called fringe connection that transports UDP-GlcA, UDP-GlcNAc, UDP-GalNAc, UDP-glucose(UDP-Glc) and UDP-xylose (UDP-Xyl) (Goto *et al.,* 2001,Selva *et al.,* 2001). Martinez-Duncker *et al.* (2002) suggested that all these transporters are able to transport UDP-GlcA, UDP-GalNAc, UDP-Xyl, UDP-Gal, UDP-GlcNAc, and UDP-Glc but probably with different efficiency. Another example is the human UDP-galactose transporter that also transports UDP-GlcNAc (Segawa *et al.,* 2002) and the LPG2 transporter from *L.donovanii* that transports GDP-mannose, GDP-arabinose and GDP-fucose (Hong *et al.,* 2000). Thus, broader substrate recognition is not restricted to UDP-sugar transporters.

Worthwhile to mention at this point is that a basal galactose transport activity has also been demonstrated in the Ricinus communis agglutinin resistant MDCKII (Mardi-Darby canine kidney strain II, Brandli *et al.,* 1988) cells that also lack a functional UDP-galactose transporter. All this data point towards the existence of a second transport system for UDP-galactose.

4.1.2 Characterisation of the complementing activity of UDP-glucose pyrophsphorylases

The efficiency of the UDP-galactose transport by a potential second nucleotide sugar transporter in CHO Lec8 cells is lower compared to the transport activity of the UDP-galactose transporter itself. This is shown by the high expression of galactose on the cell surface upon transfection with a plasmid encoding a functional UDP-galactose transporter (see 3.1.3, Figure 12 and 3.1.4, Figure 13). Nevertheless, an increase of the UDP-galactose concentration in the cytosol might augment the UDP-galactose transport by a

multi-substrate transporter. By overexpression of the *L. major* UGP, elevated levels of UDP-galactose could be obtained, since UDP-glucose can be converted to UDP-galactose by the two enzymes UDP-galactose-4-epimerase and galactose-1 phosphate uridyltransferase (see 1.3.1.1).

Similarly, a GDP-fucose transport defect observed in a fibroblast cell line derived from a Turkish patient with a leukocyte adhesion deficiency type II (LADII) (Lübke *et al.,* 1999) could be complemented by increasing the intracellular level of GDP-fucose. In addition, oral administration of fucose restored the fucosylation deficiency in the patient (Marquardt *et al.,* 1999), who is mentally retarded and lacks fucosylated glycoproteins. This also includes the selectin ligands, which are essential for the intact immune system (Etzioni *et al.,* 1992, Becker *et al.,* 1999). Lübke *et al.* (1999) could show that in the patient's fibroblasts the high affinity transport of UDP-fucose into the Golgi apparatus was deficient, but a low level transport for GDP-fucose still occurred. The defect in the GDP-fucose transport protein was confirmed by complementation cloning (Lühn *et al.,* 2001, Lübke *et al.,* 2001) and the analysis of the patient's GDP-fucose transporter identified a homozygous point mutation in the inactive protein. This suggests that like in CHO Lec8 cells, the basic GDP-fucose transport can be enhanced by raising the substrate level. Indeed, Lühn *et al.,* (2001) identified a second *C. elegans* GDP-fucose transporter that showed a low complementing activity in the LADII fibroblasts.

Another possible explanation is that the UGP directly or indirectly interacts with a nucleotide sugar transporter and influences substrate specificity or transport efficiency. UGPs are usually found in the cytoplasm. However, in some plants, UGP activity was associated with membrane fractions (Simcox *et al.,* 1977, Nishimura *et al.,* 1979) and in cat liver about 10% of the UGPase activity was found to be associated with Golgi membranes (Persat *et al.,* 1983). Indirect immunofluorescence of the *L. major* UGP showed a distribution of the protein within the whole cell indicating a cytosolic and/or ER localisation. In this kind of experiment, no association with the Golgi apparatus could be detected (see 3.2.8). However, a more detailed analysis is necessary to answer the question whether low amounts of the *L. major* UGP are also associated to the Golgi membrane and there could interact with nucleotide sugar transporters. In addition, the intracellular localisation of the UGP in the parasite itself will be analysed. Since the expression of tagged proteins in *Leishmania* is difficult, antibodies are required to study the endogenous protein. Towards this goal, a polyclonal serum is currently prepared (see 3.2.9) by using the purified recombinant protein for immunization. In addition, the detection of the endogenous protein is preferable, to develop a detailed picture of the natural situation.

In contrast to the *L. major* UGP, the humane muscle UGPs were not able to complement the CHO Lec8 cells. A possible explanation might be differences in the structural and kinetic properties of UGPs despite their high sequence homology or in protein stability. This will be discussed in more detail in the following chapters.

Unfortunately, the UDP-galactose transporter could not be identified in the remaining UGP negative pools and is masked by the signal of this enzyme. A potential way to clone the transporter would be to subdivide more pools of the library until a complementing subpool without UGP cDNA can be identified. This strategy is however, labour intensive and has a high risk to fail. Another option is the generation of a cDNA library from the *ugp* gene deletion *L. major* mutant (see 3.3). This work is still in progress.

4.2 Structural and functional characterisation of the L. major UGP

4.2.1 Structural analysis of a potential *L. major* UGP core domain

A structural homology search in the PDB database and the use of the program 3D-PSSM (Kelley *et al.,* 2000) revealed a model of the *L. major* UGP based on the solved structure of the humane UDP-GlcNAc/GalNAc pyrophosphorylase (AGX1 and 2, Peneff *et al.,* 2001). The structure of AGX1 and the splice variant AGX2 were solved in complex with the nucleotide sugars UDP-GlcNAc and UDP-GalNAc. Though the sequence identity is rather low (17%, see Figure 16) and this structure could not be used to solve the phase problem of the obtained *L. major* UGP crystal data set (see 3.2.7), some structural features seem to be conserved. AGX1 and 2 are composed of three domains: a large central domain and clearly discernible N- and C-terminal domains. The central domain contains the catalytic site and in its centre binds the nucleotide sugar in a deep pocket. The binding of the nucleotide part of the nucleotide sugar involves the first have of the core domain including the pyrophosphorylase consensus motif (see Figure 30). The second half of the core stabilizes the sugar ring. Though there are many gaps, it may be that the fold of the central domain of AGX1 and *L. major* UGP are conserved. In Figure 30, the position of a potential binding pocket as well as the position of the pyrophos-phorylase consensus motif is shown. Still the prediction of residues involved in the catalytic mechanisms of the *L. major* UGP can not be made, since the corresponding data of AGX1 and 2 are preliminary and need further confirmation.

4.2.2 The N- and C-terminal domain and the oligomerisation state of UGP

The N-terminus of AGX1 contacts a four stranded antiparallele ß-sheet of the core domain. In the model of the *L. major* UGP, the structure prediction of this domain comprises many gaps except for one alpha helix that also seems to contact the core domain. According to this model, the N-terminal domain of the *L. major* enzyme is comprised of the amino acids 1-40. A truncation of the first 38 amino acid generated an inactive protein (see 3.2.6). This indicates that either the contact of the alpha helix to the core domain or additional interactions of the N-terminus that are not included in this model, are important for activity or stability of the protein. The influence on activity seems more likely, since the N-terminus of AGX1 locates on top of the active site pocket and is believed to regulate activity (Peneff *et al.,* 2001). The truncated UGP was stably expressed in *E.coli* BL21(DE3) suggesting the formation of an intact folded protein. In contrast, truncation of the first 69 residues of the N-terminus- including a part of the core domain- seems to interfere with protein stability. Though protein of the expected size was expressed in *E.coli* BL21(DE3), a comparatively high amount was detected in the insoluble fraction.

The C-terminus of AGX1 and AGX2 is connected via an alpha helix to the core domain and is involved in the subunit interaction. As mentioned above, AGX2 is a splice variant of AGX1. Both sequences are identical except for a 17 amino acid insertion in the C-terminus in the case of AGX2. The site of this insertion contributes to the subunit interaction in the AGX1 dimers and reaches into the active site pocket of the second molecule. Furthermore, this part provides additional binding sites for the nucleotide sugar. In AGX2 the structure of this part of the C-terminus was disordered and could not be traced. Interestingly, AGX2 was found to be a monomer in gelfiltration experiments whereas AGX1 was dimeric. By diluting AGX1 into the nanomolar range or by increasing the salt concentration, dissociation into monomers was observed (Peneff *et al.,* 2001). The question whether the dimer or monomer is the physiological relevant form and whether the dimeric form is catalytically active remains to be answered.

The oligomerisation status of the *L. major* UGP was analysed by gelfiltration experiments and revealed the monomer as active species even at high protein concentrations (see 3.2.4). Unfortunately, the C-terminus of the *L. major* UGP was very poorly predicted by 3D-PSSM and the last 44 amino acids are not included in the model. Based on these findings, it is possible that the *L. major* UGP C-terminus comprises a different structure. However, the truncation of the last 38 and 69 residues revealed a stably expressed, but inactive protein indicating an influence of the C-terminus on the catalytic activity. In

addition, some parts of the C-terminus might also be important for the stability of the protein, since the expression of UGP-Δ380-494 increased the level of non soluble protein.

Though the existence of a small fraction of *L. major* UGP dimers can not be excluded by size exclusion chromatography, higher oligomeric structures could not be detected. Peaks mimicking higher organized protein fractions were also observed for the standard proteins and are believed to represent unspecific protein aggregates. The addition of the substrates UTP and glucose-1 phosphate to the buffers confirmed the monomeric nature of the *L. major* UGP. Dissociation from dimers into monomers to achieve an open confirmation of the active state could not be observed. This mechanism was suggested for the barley UGP that was found to be a mixture of oligomers with the monomer as active species (Martz *et al.,* 2002). Mutant analysis of this enzyme revealed that a higher polymerisation capacity reduced the maximum velocity in activity assays. Thus, it was postulated that deoligomersiation has a critical impact upon catalysis and may be the rate-limiting step. Other eukaryotic UGPs, e.g. the human, calf and rabbit liver UGPs are suggested to occur as octamer *in vivo* though also lower oligomeric forms could be detected (Turnquist *et al.,* 1974) and the enzyme from potato tuber exists as monomer and dimer (Sowokinos *et al.,* 1993). The crystal structure obtained for AGX1 and 2 and the data obtained from the barley enzyme suggest a potential role of oligomersiation in the regulation of activity and will be discussed further in the next chapter.

The crystal structure of the *L. major* UGP shell soon be resolved and will reveal whether C- and/or N-terminus participate in the formation of the active enzyme or in mediating subunit interaction.

## 4.2.3 Kinetic comparison of UDP-glucose pyrophosphorylases

Despite their high homology, eukaryotic UGPs differ in their kinetic characteristics. To compare the kinetic data of the *L. major* UGP with the data available from the human (Duggleby *et al.,* 1996), potato (Sowokinos *et al.,* 1993), and barley (Elling *et al.,* 1996) UGPs, the purified *L. major* UGP was used to determine the K_m values in an *in vitro* activity assay for both the forward and reverse reaction (see table 2). The enzyme displayed a Michaelis Menten kinetic towards all substrates. Compared to the kinetic data published by Chang *et al.,* (1995), the *L. major* UGP showed a higher affinity to the substrates UTP (K_m = 917 µM) and glucose-1 phosphate (K_m = 404 µM) than the human muscle form 2, whereas the K_m values of the human muscle form 1 (UTP: K_m = 301 µM, glucose-1 phosphate: K_m = 207 µM) were in about the same range. In the reverse reaction, the human forms showed a higher affinity for UDP-glucose (63 µM and 41 µM, for

muscle form 2 and 1 respectively) than the *Leishmania* enzyme. The K_m value for pyro-phosphate was determined only for the human muscle form 2 (384 µM) and was about a factor of 1.9 higher than for the *L. major* UGP (Duggleby *et al.,* 1996).

Substrate	muscle form 1	muscle form 2	lacZ/liver	potato tuber	barley	*L. major*
glucose-1 phosphate	207	404	174	80-68	74	192
UTP	301	917	692	180-530	93	70
UDP-glucose	41	63	55	140	191	104
PP	sigmoid	384	172	130	172	200

Table 2 Comparison of the UGP K_m values for the human muscle form 1 and 2, for the human lacZ/liver fusion enzyme, for the barley and *L. major* enzyme. The enzyme from potato tuber exhibits a complex kinetic towards glucose-1 phosphate and UTP, depicted by two K_m values for each substrate.

Surprisingly, the muscle form 1 showed sigmoid kinetics with respect to pyrophosphate. As mentioned in 3.1.8, the amino acid sequences of the two human muscle enzymes are identical except that muscle form 1 contains a N-terminal extension of 11 amino acids (Figure 49). The N-terminal elongation is the result of alternative splicing. Duggleby *et al.* (1996) assigned the kinetic difference in regard to the pyrophosphate to the difference in the N-terminal region. The influence of the N-terminus on the kinetics was also observed using the humane liver UGP (Duggleby *et al.,* 1996). The human liver enzyme differs in only 6 amino acid positions from the human muscle form 1 and shows also the elongated N-terminus (Figure 49).
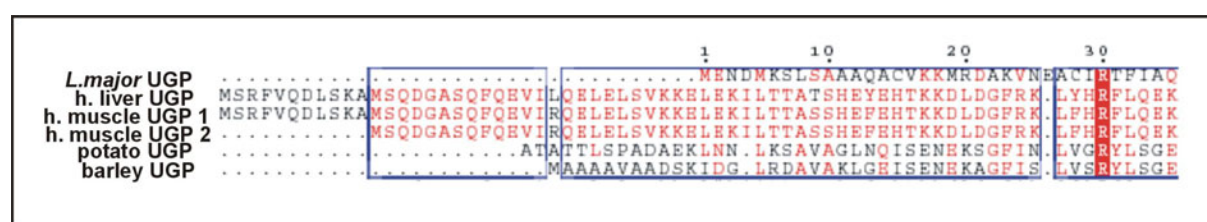
Figure 49 Primary sequence alignment of the N-terminal regions of UGPs. The N-termini of the enzymes isolated from human liver (Peng *et al.,* 1993), human muscle (Duggelby *et al.,* 1996), *L. major* (this study), potato (Sowokinos *et al.,*1993) and barley (Eimert *et al.,* 1996) are aligned. Conserved amino acids are highlighted with a red background, amino acids that are conserved in two out of the three sequences are coloured in red, stretches of conserved residues are boxed in blue.

The liver enzyme exhibited a complex kinetic towards pyrophosphate. However, after the replacement of the first nine residues by lacZ the protein revealed not longer kinetic anomalies and followed a Michaelis Menten kinetic with respect to all substrates. Dug-gleby *et al.,*(1996) proposed, that the oligomeric status could account for the complex

kinetics of the enzyme, since it was reported that the human liver UGP is an octamer in nature (Turnquist *et al.,* 1974). A potential explanation is the existence of different rate constants for catalysis when one or all active sites are occupied (Duggleby *et al.,* 1996) or for the deoligomerisaton into active monomers as suggested by Martz *et al.* (2002). In either case, the N-terminus could be involved in subunit interaction though a direct proof, for example by gelfiltration studies with the lacZ fusion enzyme or the muscle enzyme, does not yet exist. The *L. major* enzyme exhibits a simple Michaelis Menten kinetic towards all substrates and has the monomer as active species. This would be in agreement with Duggleby *et al.* (1996) suggesting that a complex kinetic is coupled to oligomerisation events.   Another explanation on how the N-terminus of the UGP could influence the kinetics is based on the solved crystal structure of AGX1. As mentioned above, the N-terminal domain is located on top of one site of the active site pocket and might regulate activity (Peneff *et al.,* 2001). The N-terminus of the *L. major* UGP is 24 amino acids shorter compared to the human muscle form 2 (Figure 49) and does not seem to hinder the binding of the substrates to the catalytic pocket as indicated by the kinetic data.

Though these data suggest that the N-terminus influences the kinetic properties, there may be other regions of the proteins involved in regulating oligomersiation and/or activity. An example is the potato UGP that exhibits a shorter N-terminus than the human muscle forms (Figure 42 and 16), has still the ability to form dimers and shows a complex kinetic behaviour in regard to UTP and glucose-1 phosphate (Sowokinos *et al.,* 1993). The barley enzyme has about the same length as the potato enzyme (Figure 42 and 16) but forms a mixture of oligomers with the monomer as active species and exhibits simple Michaelis Menten kinetics with regard to all substrates (Elling *et al.,* 1996). As mentioned above, a mutant barley UGP showed a higher order of oligomersiation and a reduced V_{max} suggesting that the transition between oligomer- and monomer state has an impact on activity. Interestingly, the mutation was not introduced at the N-terminus of the enzyme but in the core domain C-terminal of the pyrophosphorylase consensus motif.

The data suggest that regulation of the UGP activity is complex. This is also supported by the finding that alternative splicing of pyrophosphorylases as in the cases of AGX and the human muscle UGPs leads to an alteration in the enzymatic properties even though rather small changes within the sequence occur. Unfortunately, the oligomeric difference between AGX1 as monomer and AGX2 as dimer could not be measured in the activity assays used by Peneff *et al.* (2001), since nanomolar concentration ranges are used in their assay. As mentioned above, both AGX forms are monomers under these conditions and show similar kinetics despite the observed structural difference (Peneff *et al.,* 2001). However, other studies suggested that AGX1 prefers GalNAc-1 phosphate and AGX2

GlcNAc-1 phosphate as substrate indicating an influence of the splicing differences on substrate specificity (Wang-Gillam *et al.,* 1998).

Since rather small sequence differences can exhibit changes in the kinetic behaviour and/or activity of the UGPs, this may also explain why the human muscle UGPs are not able to complement the CHO Lec8 phenotype though the sequence homology to the *L. major* UGP is about 53%. However, more kinetic and functional data has to be collected to get a complete data set for all isolated UGPs. This would include the purification of the corresponding enzymes, kinetic analysis and studies on the oligomerisation status. In addition, the crystal structure of the *L. major* UGP should provide insight into the regulation of the enzymatic activity.

4.3 Generation and characterisation of a L. major *UGP gene deletion mutant*

Essential for the parasites survival in the hostile environment of the sand fly vector and the mammalian host are various surface glycoconjugates, which collectively form a dense cell surface, the glycocalyx (Pimenta *et al.,* 1991). The major surface glucoconjugates are the GPI-anchored glycoproteins, the lipophosphoglycan (LPG), free GPI glycolipids (GIPLs) and proteophosphoglycans (PPGs) (McConville, 2002, Descoteaux *et al.,* 1999). Thus, the enzymes involved in the biosynthesis of the parasite glycocalyx provide interesting targets for therapeutic drugs and were intensively investigated (see introduction). Essential for the biosynthesis of glycoconjugates is the activation of the monosaccharides as nucleotide sugars. The formation of two activated sugars, UDP-glucose and UDP-galactose, is dependent on the activity of the UGP. To investigate the role of the UGP in the parasite, an *ugp* gene deletion mutant was generated. The cloning strategy was influenced by the fact that *Leishmania* contain no introns and that transcription occurs in a polycistronic fashion (Stiles *et al.,* 1999, Stein *et al.,* 1990). In addition, consensus elements that are characteristic for eukaryotic promoters are absent. Thus, the complete open reading frame of the targeted gene was replaced by the coding sequence of the resistant markers leaving the 5' and 3' untranslated regions unaltered to allow the correct splicing and polyadenylation of the marker. *L. major* is a diploid asexual parasite and requires two consecutive rounds of homologous recombination to create a null mutant of a particular gene.

In the case of the *L. major ugp*, it was not possible to precisely determine the start and end positions of the neighbouring genes by sequence analysis. Therefore, it was important to introduce no point mutation in the flanking regions used for homologous recombi-

nation. Since the *L. major ugp* is a single copy gene (see 3.3.1), two rounds of targeted gene replacement resulted in the exchange of the complete *ugp* open reading frame by hygromycin and phleomycin resistant markers. However, the insertion of hygromycin was preferred compared to the insertion of the phleomycin resistant marker. It might be possible that the size of the DNA influences the polycistronic gene transcription giving advantage to the hygromycin resistant marker, which with 1000 bp closely apporoximates the size of the *ugp* gene (1400 bp). The phleomycin resistant gene has a size of only 400 bp.

Using the *L. major* 5ASKH, it was not possible to obtain neomycin resistant clones. Since, other laboratories (Clos *et al.,* BNI Hamburg) also had difficulties introducing a neomycin resistant cassette, this phenomenon might be due to some unknown peculiarities of the selected *L. major* strain.

In addition, the generation of the gene deletion mutant was extremely influenced by the amount and quality of the cDNA as high amounts of the targeting fragments resulted in multiple false insertions into the genome. This was also reported by Cruz *et al.* (1990 and 1991) who established the technique of the double targeted gene replacement for creating null mutants in *L. major.*

The correct insertion of the resistant markers was confirmed by PCR and Southern Blot analysis. Since *L. major* loose their virulence in culture, it was extremely important to work with freshly isolated parasites and to process as fast as possible. In addition, the parental wild type strain, was treated and cultivated in the same way as the mutants to allow the direct comparison of the results in the following experiments.

4.3.1 Charaterisation of *L. major ugp* deletion mutants

The obtained clones showed normal growth in culture compared to the wild type strain indicating that the UGP is not required for growth under the applied cultivation conditions. Unfortunately, an increased sensitivity to galactose as observed for the *E.coli galU* mutant, could not be tested, because of the complex nutrient requirements of these parasites in culture. However, the deletion of this enzyme should not only effect the assembly of the major macromolecule LPG in the promastigote surface glycocalyx but also the generation of the type-2 free GIPLs, the GPI-anchored and secreted PPGs as well as glucoslyated N-glycans (see Figure 3).

In order to obtain a first insight into the consequences of the *ugp* gene deletion, the LPG and surface bound PPGs were analysed by indirect immunofluorescence. Since galactosylation requires the formation of UDP-galactose and therefore the availability of UDP-glucose, the mutants should have been devoid of the Gal-Man-P repeating unit characteristic for LPG and PPGs. This epitope was displayed by the antibodies used in im-

munofluoresence. By comparing the parental wild type strain with the *ugp* mutants a reduction of the signal intensity was observed in the heterozygous clones. However, in the case of the homozygous clones a residual signal could be detected especially if exposure times were extended (3.3.4). This result was confirmed in FACS analysis and also in Western blotting using whole cell lysates to detect LPG. Since two independent homozygous mutant lines were tested, this result was not an artefact of a single clone. A cross reactivity of the antibody seemed unlikely as two different antibodies showed the same result although it might be possible, that the *ugp* gene deletion induces the expression of other surface compounds, which mimic the epitope recognized by these antibodies.

However, using the UGP *in vitro* activity assay, a residual activity was measurable in the lysates of the homozygous mutants confirming the results obtained in immunofluoresence, FACS and Western blot analysis. Since, the mutant is a complete deletion of the *ugp* gene locus as could be shown by Southern blot analysis and since no other *ugp* homolog could be found in the database of the *L. major* genome project, it is likely that an alternative pathway exist, or that other pyrophosphorylases synthesize UDP-glucose. Since the major activity was deleted in the *ugp* mutant, this potential enzyme might exhibit only a low but sufficient affinity for glucose-1 phosphate. Cross reactivity has been demonstrated also for the *L. major* UGP-glucose pyrophosphorylase, which activates galactose-1 phosphate and UTP to UDP-galactose and PP_i. Though this activity might not be significant under physiological conditions, it was postulated that it is sufficient to metabolise galactose in galactosemic patients (Isselbacher *et al.,* 1957). Galactosemia is caused by a defect in the enzyme galactose-1 phosphate uridyltransferase. The accumulation of galactose leads to the formation of toxic products like galactitol resulting in mentally retarded patients (see 1.4.1).

It is also possible that an alternative, compensatory galactose-activating pathway exists. Compensatory mechanisms were already reported in the context of other gene deletion mutants. As mentioned in 1.2.2.4, the alkyldihydroxyacetonephosphate synthase (ADS1) gene deletion mutant was still able to express the GPI-anchored protein GP63 at wild type level though the GPI-anchor synthesis should have been abolished (Zufferey *et al.,* 2003). Thus, sufficient GPI synthesis occurred to exhibit protein anchoring whereas no detectable levels of LPG and GIPLs were present. This suggested that alternative pathways exist that produce protein anchor precursors. Alternatively, modified GPI-anchors may be used to substitute for the missing activity. In addition, this mutant contained a novel and yet unidentified lipid that is postulated to have a compensatory effect for the loss of the glycolipids and renders the parasite virulent though at reduced levels (Zufferey *et al.,* 2003).

Compensatory effects were also observed in the *L. major* LGP2 mutant lacking the GDP-mannose transporter gene. Though this mutant had lost virulence, some parasites could be reisolated from the site of injection several months after infection. The recovered mutants do not synthesize phosphoglycans, but can replicate in macrophages (Späth *et al.,* 2003). This property is similar to *L .mexicana* as these parasites do not require LPG or PPGs for infectivity (Ilg *et al.,* 2001, see introduction). In *L .mexicana* the metacyclic promastigotes resemble the amastigote stage that lack LPG and synthesize only low level of PPGs. Thus, other metabolic pathways may be upregulated in *L. mexicana* and the *L. major* LPG2 mutant that facilitate alternative mechanisms to infect the mammalian host.

As no compensatory effects were reported in the bacteria (Chang et l, 1996, Mollerach *et al.,* 1998) and yeast (Daran *et al.,* 1995) *ugp* gene deletion mutants, this feature is unique to the *L. major ugp* mutant and might also indicate the importance of these structures for virulence. It will be interesting to investigate the observed galactose activation in this mutant, since it reflects an alternative pathway to the one described by Leloir.

To further investigate, whether the residual galactose content on the *ugp* mutant surface is mainly associated with LPG, the proteophosphoglycans and the GIPLs are going to be analysed in more detail. In addition, analysis will be carried out to identify whether the LPG structure of the mutant is altered. The reduced level of UDP-galactose may change the length or composition of the glycoconjugates.

4.3.2 Test of virulence in a mice infection model

The virulence of the *ugp* gene deletion mutant was assessed by the lesion formation of Balb/c mice after inoculation with the parasites. The lesion formation was measured over a time of 10 weeks. This initial experiment showed that the *ugp* gene deletion mutant exhibits attenuated virulence in mice. The inoculum of 10^7 parasite per mouse was relatively high and thus, the reduced infectivity indicates a strong effect of the *ugp* deletion. Lower doses are known to accentuate the differences between mutant and wild type parasites and result in a delayed appearance of lesions (Späth *et al.,* 2000). In the case of the *L. major* LGP1 (galactofuranosyl transferase) mutant, the inoculation of saturating doses resulted in the minimization and even elimination of the differences between wild type and mutant parasites whereas lower doses of about 10^6 parasites per inoculum showed a significant delayed lesion formation (Späth *et al.,* 2000). In nature, infected sand flys transmit only a small number of parasites (less than a 100) into the mammalian host (Warburg *et al.,* 1986) and thus, a decreased infectivity could already have a strong impact on the resistance to the parasites. However, the inoculation of such a low number

of parasites by a syringe into mice would not cause a lesion. One possible explanation is the advantage of salvia in establishing the infection in the mammalian host (Solbach and Laskay, 2000).

The loss of virulence in *L. major* seems more likely by affecting more than one group of glycocojungates since compensatory mechanisms occur (Naderer *et al.,* 2004, see above). For example, the deletion of LPG alone, achieved by the knock out LPG1, resulted in a reduced virulence in mouse and macrophage infection assays whereas parasites without LPG and PPGs as in the case of the GDP-mannose transporter (LPG2) deletion, were rapidly killed in macrophages and did not form lesions in the mouse infection model (Späth *et al.,* 2000, Bogdan *et al.,* 2000). However, as mentioned above, a few parasites of the LPG2 mutant survived, may be by infecting other cells of the host (Naderer *et al.,* 2004, Rittig *et al.,* 2000).

The *ugp* gene deletion should have abolished the galactose metabolism and effected the synthesis of various glycoconjugates (see above). However, residual galactose residues were detected on the surface of the mutants, most likely explaining the reduced but not complete loss of virulence in the mouse model. Whether this phenotype is more severe than phenotypes described for other mutants so far, will be investigated by the use of lower inoculum doses in the mouse model.

In addition, to the reduced galactose content of the glycoconjugates on the mutant cell surface, the reduced lesion formation of the *ugp* gene could also be a consequence of the hindered energy metabolism. Though the growth of the parasites in culture was identical to wild type cells, the altered nutrient availability and endocrine situation in the mouse could inhibit the growth of the parasite. Thus, the nature of the delayed lesion formation has to be investigated in more detail using macrophage infection models. In these kinds of experiments, one can distinguish whether the mutant phenotype is due to an inhibited invasion, reduced proliferation within the cells or is facilitated by the survival of a few parasites within the initial phase of macrophage infection.

4.4 Outlook

Leishmaniasis currently affects over 12 million people worldwide. Since there are no specific drugs or vaccination strategies available, the goal is to identify and validate potential drug targets. Enzymes that are involved in the biosynthesis of the *Leishmania* glycoconjuagtes were intensively investigated within the last years. The UDP-glucose pyrophosphorylase (UGP) provides an interesting target since it is a key enzyme for the synthesis of UDP-glucose and UDP-galactose that serve as sugar donors in glycoconju- gates biosynthesis. The deletion of *ugp* in *L. major* resulted in a reduced virulence in a

mice infection model indicating an important role of UGP in the infection process. Further studies will include a more detailed investigation of the infection mechanism in mice and macrophage and the analysis of the remaining glycoconjugates in the mutant.

Though the mutant was not completely avirulent in this model, which may be due to the residual galactose-containing glycoconjugates, the reduced virulence might be sufficient to hinder *Leishmania* infection in nature. The investigation of this hypothesis would require the identification of a specific *L. major* UGP inhibitor. Despite the high sequence homology to the mammalian counterparts, the enzymes differ in their enzymatic behaviour. The observed differences will be further investigated by the production of the corresponding recombinant protein and biochemical characterisation including kinetic analysis. In addition, the crystal structure of the *L. major* UGP that is currently solved by Thomas Steiner (MPI Martinsried) could be used for *in silico* predictions of potential inhibitors.

5 References

Abeijon C, Robbins P W, Hirschberg C B. Molecular cloning of the Golgi apparatus uridine diphosphate-N-acetylglucosamine transporter from *Kluyveromyces lactis*. Proc Natl Acad Sci U S A 1996; (93): 5963-5968.

Alexander J, Russell D G. The interaction of *Leishmania* species with macrophages. Adv Parasitol 1992; (31): 175-254.

Aoki K, Sun-Wada G H, Segawa H, Yoshioka S, Ishida N, Kawakita M. Expression and activity of chimeric molecules between human UDP-galactose transporter and CMP-sialic acid transporter. J Biochem (Tokyo) 1999; (126): 940-950.

Bakker H, Routier F, Oelmann S, Jordi W, Lommen A, Gerardy-Schahn R, Bosch D. Molecular cloning of two Arabidopsis UDP-galactose transporters by complementation of a deficient chinese hamster ovary cell line. Glycobiology 2004.

Bates P A, Hermes I, Dwyer D M. Golgi-mediated post-translational processing of secretory acid phosphatase by *Leishmania donovani* promastigotes. Mol Biochem Parasitol 1990; (39): 247-255.

Becker D J, Lowe J B. Leukocyte adhesion deficiency type II. Biochim Biophys Acta 1999; (1455): 193-204.

Berninsone P, Hwang H Y, Zemtseva I, Horvitz H R, Hirschberg C B. SQV-7, a protein involved in Caenorhabditis elegans epithelial invagination and early embryogenesis, transports UDP-glucuronic acid, UDP-N- acetylgalactosamine, and UDP-galactose. Proc Natl Acad Sci U S A 2001; (98): 3738-3743.

Berninsone P M, Hirschberg C B. Nucleotide sugar transporters of the Golgi apparatus. Curr Opin Struct Biol 2000; (10): 542-547.

Bogdan C, Donhauser N, Doring R, Rollinghoff M, Diefenbach A, Rittig M G. Fibroblasts as host cells in latent leishmaniosis. J Exp Med 2000; (191): 2121-2130.

Borst P. Discontinuous transcription and antigenic variation in trypanosomes. Annu Rev Biochem 1986; (55): 701-732.

Brandli A W, Hansson G C, Rodriguez-Boulan E, Simons K. A polarized epithelial cell mutant deficient in translocation of UDP-galactose into the Golgi complex. J Biol Chem 1988; (263): 16283-16290.

Brown L M, Burbach B J, McKenzie B A, Connell G J. A cis-acting A-U sequence element induces kinetoplastid U-insertions. J Biol Chem 1999; (274): 6295-6304.

Capasso J M, Hirschberg C B. Mechanisms of glycosylation and sulfation in the Golgi apparatus: evidence for nucleotide sugar/nucleoside monophosphate and nucleotide sulfate/nucleoside monophosphate antiports in the Golgi apparatus membrane. Proc Natl Acad Sci U S A 1984; (81): 7051-7055.

Chang H Y, Lee J H, Deng W L, Fu T F, Peng H L. Virulence and outer membrane properties of a galU mutant of *Klebsiella pneumoniae* CG43. Microb Pathog 1996; (20): 255-261.

Chang H Y, Peng H L, Chao Y C, Duggleby R G. The importance of conserved residues in human liver UDPglucose pyrophosphorylase. Eur J Biochem 1996; (236): 723-728.

Coburn CM, Otteman KM, McNeely T, Turco SJ, Beverley SM. Stable DNA transfection of a wide range of trypanosomatids. Mol Biochem Parasitol 1991;(46 1): 169-179

Croft S L, Coombs G H. *Leishmania*sis--current chemotherapy and recent advances in the search for novel drugs. Trends Parasitol 2003; (19): 502-508.

Cruz A, Beverley SM, Gene replacemtn in parasitic protozoa. Nature 1990; (348): 171-173

Cruz A, Coburn CM, Beverley SM. Double targeted gene replacement for creating null mutants. PNAS 1991, (88): 7170-7174

Cummings L, Warren CE, Granovsky M, Dennis JW. Antisense and sense cDNA expression cloning ugins autonomously replicating vectors and toxic lectin selection. BBRC 1993; (195): 814-822

Daran J M, Dallies N, Thines-Sempoux D, Paquet V, Francois J. Genetic and biochemical characterization of the UGP1 gene encoding the UDP-glucose pyrophosphorylase from *Saccharomyces cerevisiae*. Eur J Biochem 1995; (233): 520-530.

Descoteaux A, Luo Y, Turco S J, Beverley S M. A specialized pathway affecting virulence glycoconjugates of *Leishmania*. Science 1995; (269): 1869-1872.

Descoteaux A, Turco S J. Glycoconjugates in *Leishmania* infectivity. Biochim Biophys Acta 1999; (1455): 341-352.

Desjardins M, Descoteaux A. Inhibition of phagolysosomal biogenesis by the *Leishmania* lipophosphoglycan. J Exp Med 1997; (185): 2061-2068.

Deutscher S L, Nuwayhid N, Stanley P, Briles E I, Hirschberg C B. Translocation across Golgi vesicle membranes: a CHO glycosylation mutant deficient in CMP-sialic acid transport. Cell 1984; (39): 295-299.

Deutscher S L, Hirschberg C B. Mechanism of galactosylation in the Golgi apparatus. A Chinese hamster ovary cell mutant deficient in translocation of UDP-galactose across Golgi vesicle membranes. J Biol Chem 1986; (261): 96-100.

Duggleby R G, Chao Y C, Huang J G, Peng H L, Chang H Y. Sequence differences between human muscle and liver cDNAs for UDPglucose pyrophosphorylase and kinetic properties of the recombinant enzymes expressed in Escherichia coli. Eur J Biochem 1996; (235): 173-179.

Eckhardt M, Muhlenhoff M, Bethe A, Gerardy-Schahn R. Expression cloning of the Golgi CMP-sialic acid transporter. Proc Natl Acad Sci U S A 1996; (93): 7572-7576.

Eckhardt M, Gerardy-Schahn R. Molecular cloning of the hamster CMP-sialic acid transporter. Eur J Biochem 1997; (248): 187-192.

Eckhardt M, Gotza B, Gerardy-Schahn R. Membrane topology of the mammalian CMP-sialic acid transporter. J Biol Chem 1999; (274): 8779-8787.

Eimert K, Villand P, Kilian A, Kleczkowski L A. Cloning and characterization of several cDNAs for UDP-glucose pyrophosphorylase from barley (Hordeum vulgare) tissues. Gene 1996; (170): 227-232.

Elling L, Kula M R. Purification of UDP-glucose pyrophosphorylase from germinated barley (malt). J Biotechnol 1994; (34): 157-163.

Etzioni A, Frydman M, Pollack S, Avidor I, Phillips M L, Paulson J C, Gershoni-Baruch R. Brief report: recurrent severe infections caused by a novel leukocyte adhesion deficiency. N Engl J Med 1992; (327): 1789-1792.

Flinn H M, Smith D F. Genomic organisation and expression of a differentially-regulated gene family from *Leishmania major.* Nucleic Acids Res 1992; (20): 755-762.

Flores-Diaz M, Alape-Giron A, Persson B, Pollesello P, Moos M, Eichel-Streiber C, Thelestam M, Florin I. Cellular UDP-glucose deficiency caused by a single point mutation in the UDP-glucose pyrophosphorylase gene. J Biol Chem 1997; (272): 23784-23791.

Foth B, Piani A, Curtis J M, Ilg T, McConville M, Handman E. *Leishmania major* proteophosphoglycans exist as membrane-bound and soluble forms and localise to the cell membrane, the flagellar pocket and the lysosome. Int J Parasitol 2002; (32): 1701-1708.

Gao X D, Dean N. Distinct protein domains of the yeast Golgi GDP-mannose transporter mediate oligomer assembly and export from the endoplasmic reticulum. J Biol Chem 2000; (275): 17718-17727.

Gao X D, Nishikawa A, Dean N. Identification of a conserved motif in the yeast golgi GDP-mannose transporter required for binding to nucleotide sugar. J Biol Chem 2001; (276): 4424-4432.

Genevaux P, Bauda P, DuBow M S, Oudega B. Identification of Tn10 insertions in the rfaG, rfaP, and galU genes involved in lipopolysaccharide core biosynthesis that affect Escherichia coli adhesion. Arch Microbiol 1999; (172): 1-8.

Genevaux P, Bauda P, DuBow M S, Oudega B. Identification of Tn10 insertions in the dsbA gene affecting Escherichia coli biofilm formation. FEMS Microbiol Lett 1999; (173): 403-409.

Gerardy-Schahn R, Oelmann S, Bakker H. Nucleotide sugar transporters: biological and functional aspects. Biochimie 2001; (83): 775-782.

Goto S, Taniguchi M, Muraoka M, Toyoda H, Sado Y, Kawakita M, Hayashi S. UDP-sugar transporter implicated in glycosylation and processing of Notch. Nat Cell Biol 2001; (3): 816-822.

Greenblatt C L, Slutzky G M, de Ibarra A A, Snary D. Monoclonal antibodies for serotyping *Leishmania* strains. J Clin Microbiol 1983; (18): 191-193.

Guha-Niyogi A, Sullivan D R, Turco S J. Glycoconjugate structures of parasitic protozoa. Glycobiology 2001; (11): 45R-59R.

Holliday R, Ho T. Evidence for allelic exclusion in Chinese hamster ovary cells. New Biol 1990; (2): 719-726.

Hong K, Ma D, Beverley S M, Turco S J. The *Leishmania* GDP-mannose transporter is an autonomous, multi-specific, hexameric complex of LPG2 subunits. Biochemistry 2000; (39): 2013-2022.

Ilg T, Overath P, Ferguson M A, Rutherford T, Campbell D G, McConville M J. O- and N-glycosylation of the *Leishmania mexicana*-secreted acid phosphatase. Characterization of a new class of phosphoserine-linked glycans. J Biol Chem 1994; (269): 24073-24081.

Ilg T, Stierhof Y D, Craik D, Simpson R, Handman E, Bacic A. Purification and structural characterization of a filamentous, mucin-like proteophosphoglycan secreted by *Leishmania* parasites. J Biol Chem 1996; (271): 21583-21596.

Ilg T, Handman E, Stierhof Y D. Proteophosphoglycans from *Leishmania* promastigotes and amastigotes. Biochem Soc Trans 1999; (27): 518-525.

Ilg T, Montgomery J, Stierhof Y D, Handman E. Molecular cloning and characterization of a novel repeat-containing *Leishmania major* gene, ppg1, that encodes a membrane-associated form of proteophosphoglycan with a putative glycosylphosphatidylinositol anchor. J Biol Chem 1999; (274): 31410-31420.

Ilg T. Proteophosphoglycans of *Leishmania*. Parasitol Today 2000; (16): 489-497. (a)

Ilg T. Lipophosphoglycan is not required for infection of macrophages or mice by *Leishmania mexicana*. EMBO J 2000; (19): 1953-1962. (b)

Ilg T, Demar M, Harbecke D. Phosphoglycan repeat-deficient *Leishmania mexicana* parasites remain infectious to macrophages and mice. J Biol Chem 2001; (276): 4988-4997.

Ilgoutz S C, Mullin K A, Southwell B R, McConville M J. Glycosylphosphatidylinositol biosynthetic enzymes are localized to a stable tubular subcompartment of the endoplasmic reticulum in *Leishmania mexicana*. EMBO J 1999; (18): 3643-3654.

Ishida N, Miura N, Yoshioka S, Kawakita M. Molecular cloning and characterization of a novel isoform of the human UDP-galactose transporter, and of related complementary DNAs belonging to the nucleotide-sugar transporter gene family. J Biochem (Tokyo) 1996; (120): 1074-1078.

Ishida N, Yoshioka S, Chiba Y, Takeuchi M, Kawakita M. Molecular cloning and functional expression of the human Golgi UDP-N-acetylglucosamine transporter. J Biochem (Tokyo) 1999; (126): 68-77.

Ishida N, Yoshioka S, Iida M, Sudo K, Miura N, Aoki K, Kawakita M. Indispensability of transmembrane domains of Golgi UDP-galactose transporter as revealed by analysis of genetic defects in UDP-galactose transporter-deficient murine had-1 mutant cell lines and construction of deletion mutants. J Biochem (Tokyo) 1999; (126): 1107-1117.

Jaffe C L, Perez L, Schnur L F. Lipophosphoglycan and secreted acid phosphatase of *Leishmania tropica* share species-specific epitopes. Mol Biochem Parasitol 1990; (41): 233-240.

Joshi P B, Sacks D L, Modi G, McMaster W R. Targeted gene deletion of *Leishmania major* genes encoding developmental stage-specific leishmanolysin (GP63). Mol Microbiol 1998; (27): 519-530.

Kapler G M, Coburn C M, Beverley S M. Stable transfection of the human parasite *Leishmania major* delineates a 30-kilobase region sufficient for extrachromosomal replication and expression. Mol Cell Biol 1990; (10): 1084-1094.

Katsube T, Kazuta Y, Tanizawa K, Fukui T. Expression in *Escherichia coli* of UDP-glucose pyrophosphorylase cDNA from potato tuber and functional assessment of the five lysyl residues located at the substrate-binding site. Biochemistry 1991; (30): 8546-8551.

Kazuta Y, Tanizawa K, Fukui T. Comparative affinity labeling with reactive UDP-glucose analogues: possible locations of five lysyl residues around the substrate bound to potato tuber UDP-glucose pyrophosphorylase. J Biochem (Tokyo) 1991; (110): 708-713.

Kazuta Y, Omura Y, Tagaya M, Nakano K, Fukui T. Identification of lysyl residues located at the substrate-binding site in UDP-glucose pyrophosphorylase from potato tuber: affinity labeling with uridine di- and triphosphopyridoxals. Biochemistry 1991; (30): 8541-8545.

Kelly LA, MacCallum RM, Sternberg MJE, Enhanced genome annotation using structural profiles in the program 3D-PSSM, J Mol Biol 2000; (299, 2): 499-520

Kevil CH, Walsh L, Laroux S, Kalogerist T, Grisham MB, Alexander JS, An improved, rapid Northern protocol. BBRC 1997; (238): 277-279

Kim H, Wu C A, Kim D Y, Han Y H, Ha S C, Kim C S, Suh S W, Kim K K. Crystallization and preliminary X-ray crystallographic study of UDP-glucose pyrophosphorylase (UGPase) from *Helicobacter pylori*. Acta Crystallogr D Biol Crystallogr 2004; (60): 1447-1449.

Kleczkowski LA, Glucose activation and metabolism through UDP-glucose pyrophosphorylase in plants, Phytochemistry 1994; (37): 1507-1515.

Kleczkowski L A, Geisler M, Ciereszko I, Johansson H. UDP-glucose pyrophosphorylase. An old protein with new tricks. Plant Physiol 2004; (134): 912-918.

Klein C, Gopfert U, Goehring N, Stierhof Y D, Ilg T. Proteophosphoglycans of *Leishmania mexicana*. Identification, purification, structural and ultrastructural characterization of the secreted promastigote proteophosphoglycan pPPG2, a stage-specific glycoisoform of amastigote aPPG. Biochem J 1999; (344 Pt 3): 775-786.

Konishi Y, Tanizawa K, Muroya S, Fukui T. Molecular cloning, nucleotide sequencing, and affinity labeling of bovine liver UDP-glucose pyrophosphorylase. J Biochem (Tokyo) 1993; (114): 61-68.

Konishi Y, Tanizawa K, Muroya S, Fukui T. Molecular cloning, nucleotide sequencing, and affinity labeling of bovine liver UDP-glucose pyrophosphorylase. J Biochem (Tokyo) 1993; (114): 61-68.

de Lafaille MAC, Laban A, Wirth DF. Gene expression in *Leishmania* : Analysis of essential 5'DNA sequences. Proc. Natl. Acad. Sci. USA 1992; (89): 2703-2707

Lai K, Elsas L J. Overexpression of human UDP-glucose pyrophosphorylase rescues galactose-1-phosphate uridyltransferase-deficient yeast. Biochem Biophys Res Commun 2000; (271): 392-400.

Lerner E A, Ribeiro J M, Nelson R J, Lerner M R. Isolation of maxadilan, a potent vasodilatory peptide from the salivary glands of the sand fly *Lutzomyia longipalpis*. J Biol Chem 1991; (266): 11234-11236.

Levine S, Illett T A, Hagman E, Hansen R G. Uridine diphosphate glucose pyrophosphorylase. II. J Biol Chem 1969; (244): 5729-5734.

Lubke T, Marquardt T, von Figura K, Korner C. A new type of carbohydrate-deficient glycoprotein syndrome due to a decreased import of GDP-fucose into the golgi. J Biol Chem 1999; (274): 25986-25989.

Lubke T, Marquardt T, Etzioni A, Hartmann E, von Figura K, Korner C. Complementation cloning identifies CDG-IIc, a new type of congenital disorders of glycosylation, as a GDP-fucose transporter deficiency. Nat Genet 2001; (28): 73-76.

Luhn K, Wild M K, Eckhardt M, Gerardy-Schahn R, Vestweber D. The gene defective in leukocyte adhesion deficiency II encodes a putative GDP-fucose transporter. Nat Genet 2001; (28): 69-72.

Martinez-Duncker I, Mollicone R, Codogno P, Oriol R. The nucleotide-sugar transporter family: a phylogenetic approach. Biochimie 2003; (85): 245-260.

Martz F, Wilczynska M, Kleczkowski L A. Oligomerization status, with the monomer as active species, defines catalytic efficiency of UDP-glucose pyrophosphorylase. Biochem J 2002; (367): 295-300.

McConville M J. Glycosylated-phosphatidylinositols as virulence factors in *Leishmania*. Cell Biol Int Rep 1991; (15): 779-798.

McConville M J, Turco S J, Ferguson M A, Sacks D L. Developmental modification of lipophosphoglycan during the differentiation of *Leishmania major* promastigotes to an infectious stage. EMBO J 1992; (11): 3593-3600.

McConville M J, Collidge T A, Ferguson M A, Schneider P. The glycoinositol phospholipids of *Leishmania mexicana* promastigotes. Evidence for the presence of three distinct pathways of glycolipid biosynthesis. J Biol Chem 1993; (268): 15595-15604.

McConville M J, Ferguson M A. The structure, biosynthesis and function of glycosylated phosphatidylinositols in the parasitic protozoa and higher eukaryotes. Biochem J 1993; (294 (Pt 2)): 305-324.

McConville M J, Mullin K A, Ilgoutz S C, Teasdale R D. Secretory pathway of trypanosomatid parasites. Microbiol Mol Biol Rev 2002; (66): 122-154.

McCoy J J, Beetham J K, Ochs D E, Donelson J E, Wilson M E. Regulatory sequences and a novel gene in the msp (GP63) gene cluster of *Leishmania chagasi*. Mol Biochem Parasitol 1998; (95): 251-265.

McGwire B S, Chang K P. Posttranslational regulation of a *Leishmania* HEXXH metalloprotease (gp63). The effects of site-specific mutagenesis of catalytic, zinc binding, N-glycosylation, and glycosyl phosphatidylinositol addition sites on N-terminal end cleavage, intracellular stability, and extracellular exit. J Biol Chem 1996; (271): 7903-7909.

McNeely T B, Rosen G, Londner M V, Turco S J. Inhibitory effects on protein kinase C activity by lipophosphoglycan fragments and glycosylphosphatidylinositol antigens of the protozoan parasite *Leishmania*. Biochem J 1989; (259): 601-604.

Medina-Acosta E, Karess R E, Schwartz H, Russell D G. The promastigote surface protease (gp63) of *Leishmania* is expressed but differentially processed and localized in the amastigote stage. Mol Biochem Parasitol 1989; (37): 263-273.

Miura N, Ishida N, Hoshino M, Yamauchi M, Hara T, Ayusawa D, Kawakita M. Human UDP-galactose translocator: molecular cloning of a complementary DNA that complements the genetic defect of a mutant cell line deficient in UDP-galactose translocator. J Biochem (Tokyo) 1996; (120): 236-241.

Mollerach M, Lopez R, Garcia E. Characterization of the galU gene of *Streptococcus pneumoniae* encoding a uridine diphosphoglucose pyrophosphorylase: a gene essential for capsular polysaccharide biosynthesis. J Exp Med 1998; (188): 2047-2056.

Molthoff J, Competent cells of *E.coli*. Gene 1990; (96):23-28

Moss J M, Reid G E, Mullin K A, Zawadzki J L, Simpson R J, McConville M J. Characterization of a novel GDP-mannose:Serine-protein mannose-1-phosphotransferase from *Leishmania mexicana*. J Biol Chem 1999; (274): 6678-6688.

Mosser D M, Rosenthal L A. *Leishmania*-macrophage interactions: multiple receptors, multiple ligands and diverse cellular responses. Semin Cell Biol 1993; (4): 315-322.

Munster A K, Eckhardt M, Potvin B, Muhlenhoff M, Stanley P, Gerardy-Schahn R. Mammalian cytidine 5'-monophosphate N-acetylneuraminic acid synthetase: a nuclear protein with evolutionarily conserved structural motifs. Proc Natl Acad Sci U S A 1998; (95): 9140-9145.

Munster A K. Klonierung und molekulare Charakterisierung der murinen CMP-N-Acetylneuaminsäure-Synthase, 1999, Dissertation, Universität Hannover

Muraoka M, Kawakita M, Ishida N. Molecular characterization of human UDP-glucuronic acid/UDP-N-acetylgalactosamine transporter, a novel nucleotide sugar transporter with dual substrate specificity. FEBS Lett 2001; (495): 87-93.

Naderer T, Vince J E, McConville M J. Surface determinants of *Leishmania* parasites and their role in infectivity in the mammalian host. Curr Mol Med 2004; (4): 649-665.

Nakano K, Omura Y, Tagaya M, Fukui T. UDP-glucose pyrophosphorylase from potato tuber: purification and characterization. J Biochem (Tokyo) 1989; (106): 528-532.

Oelmann S, Stanley P, Gerardy-Schahn R. Point mutations identified in Lec8 Chinese hamster ovary glycosylation mutants that inactivate both the UDP-galactose and CMP-sialic acid transporters. J Biol Chem 2001; (276): 26291-26300.

Oelmann S. Molekulare Analyse von CHO-Zellen der Komplementationsgruppe Lec8: Ableitung von Struktur-Funktions-Beziehungen für den UDP-Galactose Transporter, 2001, Dissertation, Universität Hannover

Pan F, Jackson M, Ma Y, McNeil M. Cell wall core galactofuran synthesis is essential for growth of mycobacteria. J Bacteriol 2001; (183): 3991-3998.

Parodi A J. N-glycosylation in trypanosomatid protozoa. Glycobiology 1993; (3): 193-199.

Peneff C, Ferrari P, Charrier V, Taburet Y, Monnier C, Zamboni V, Winter J, Harnois M, Fassy F, Bourne Y. Crystal structures of two human pyrophosphorylase isoforms in complexes with UDPGlc(Gal)NAc: role of the alternatively spliced insert in the enzyme oligomeric assembly and active site architecture. EMBO J 2001; (20): 6191-6202.

Peng H L, Chang H Y. Cloning of a human liver UDP-glucose pyrophosphorylase cDNA by complementation of the bacterial *galU* mutation. FEBS Lett 1993; (329): 153-158.

Persat F, Azzar G, Martel M B, Got R. Properties of uridine diphosphate glucose pyrophosphorylase from Golgi apparatus of liver. Biochim Biophys Acta 1983; (749): 329-332.

Pimenta P F, Saraiva E M, Sacks D L. The comparative fine structure and surface glycoconjugate expression of three life stages of *Leishmania major*. Exp Parasitol 1991; (72): 191-204.

Pimenta P F, Turco S J, McConville M J, Lawyer P G, Perkins P V, Sacks D L. Stage-specific adhesion of *Leishmania* promastigotes to the sandfly midgut. Science 1992; (256): 1812-1815.

Pimenta P F, Saraiva E M, Rowton E, Modi G B, Garraway L A, Beverley S M, Turco S J, Sacks D L. Evidence that the vectorial competence of phlebotomine sand flies for different species of *Leishmania* is controlled by structural polymorphisms in the surface lipophosphoglycan. Proc Natl Acad Sci U S A 1994; (91): 9155-9159.

Proudfoot L, Schneider P, Ferguson M A, McConville M J. Biosynthesis of the glycolipid anchor of lipophosphoglycan and the structurally related glycoinositolphospholipids from *Leishmania major*. Biochem J 1995; (308 (Pt 1)): 45-55.

Puentes S M, Da Silva R P, Sacks D L, Hammer C H, Joiner K A. Serum resistance of metacyclic stage *Leishmania major* promastigotes is due to release of C5b-9. J Immunol 1990; (145): 4311-4316.

Ralton J E, McConville M J. Delineation of three pathways of glycosylphosphatidylinositol biosynthesis in *Leishmania mexicana*. Precursors from different pathways are assembled on distinct pools of phosphatidylinositol and undergo fatty acid remodeling. J Biol Chem 1998; (273): 4245-4257.

Ralton J E, Mullin K A, McConville M J. Intracellular trafficking of glycosylphosphatidylinositol (GPI)-anchored proteins and free GPIs in *Leishmania mexicana*. Biochem J 2002; (363): 365-375.

Ralton J E, Naderer T, Piraino H L, Bashtannyk T A, Callaghan J M, McConville M J. Evidence that intracellular beta1-2 mannan is a virulence factor in *Leishmania* parasites. J Biol Chem 2003; (278): 40757-40763.

Rittig M G, Bogdan C. *Leishmania*-host-cell interaction: complexities and alternative views. Parasitol Today 2000; (16): 292-297.

Robinson A, Beverley SM. Improvements in transfection efficiency and test of RNA interference (RNAi) approaches in the protozoan parasite *Leishmania*. Mol Bio Parasitol 2003; (128): 217-228

Sacks D L. Metacyclogenesis in *Leishmania* promastigotes. Exp Parasitol 1989; (69): 100-103.

Sacks D L, Pimenta P F, McConville M J, Schneider P, Turco S J. Stage-specific binding of *Leishmania donovani* to the sand fly vector midgut is regulated by conformational changes in the abundant surface lipophosphoglycan. J Exp Med 1995; (181): 685-697.

Sacks D L, Modi G, Rowton E, Spath G, Epstein L, Turco S J, Beverley S M. The role of phosphoglycans in *Leishmania*-sand fly interactions. Proc Natl Acad Sci U S A 2000; (97): 406-411.

Segawa H, Kawakita M, Ishida N. Human and Drosophila UDP-galactose transporters transport UDP-N-acetylgalactosamine in addition to UDP-galactose. Eur J Biochem 2002; (269): 128-138.

Selva E M, Hong K, Baeg G H, Beverley S M, Turco S J, Perrimon N, Hacker U. Dual role of the fringe connection gene in both heparan sulphate and fringe-dependent signalling events. Nat Cell Biol 2001; (3): 809-815.

Sowokinos J R, Spychalla J P, Desborough S L. Pyrophosphorylases in Solanum tuberosum (IV. Purification, Tissue Localization, and Physicochemical Properties of UDP-Glucose Pyrophosphorylase). Plant Physiol 1993; (101): 1073-1080.

Spath G F, Epstein L, Leader B, Singer S M, Avila H A, Turco S J, Beverley S M. Lipophosphoglycan is a virulence factor distinct from related glycoconjugates in the protozoan parasite *Leishmania major*. Proc Natl Acad Sci U S A 2000; (97): 9258-9263.

Spath G F, Lye L F, Segawa H, Sacks D L, Turco S J, Beverley S M. Persistence without pathology in phosphoglycan-deficient *Leishmania major*. Science 2003; (301): 1241-1243.

Spath G F, Garraway L A, Turco S J, Beverley S M. The role(s) of lipophosphoglycan (LPG) in the establishment of *Leishmania major* infections in mammalian hosts. Proc Natl Acad Sci U S A 2003; (100): 9536-9541.

Spath G F, Lye L F, Segawa H, Sacks D L, Turco S J, Beverley S M. Persistence without pathology in phosphoglycan-deficient *Leishmania major*. Science 2003; (301): 1241-1243.

Stanley P, Siminovitch L. Complementation between mutants of CHO cells resistant to a variety of plant lectins. Somatic Cell Genet 1977; (3): 391-405.

Stanley P. Selection of specific wheat germ agglutinin-resistant (WgaR) phenotypes from Chinese hamster ovary cell populations containing numerous lecR genotypes. Mol Cell Biol 1981; (1): 687-696.

Stanley P. Glycosylation mutants of animal cells. Annu Rev Genet 1984; (18): 525-552.

Stiles J K, Hicock P I, Kong L, Xue L, Meade J C. *Leishmania donovani* proton translocating P-type adenosine triphosphatases LDH1A and LDH1B: trans-splicing and polyadenylation of transcripts in amastigotes and promastigotes. Mol Biochem Parasitol 1999; (103): 105-109.

SUNDARARAJAN T A, RAPIN A M, KALCKAR H M. Biochemical observations on *E. coli* mutants defective in uridine diphosphoglucose. Proc Natl Acad Sci U S A 1962; (48): 2187-2193.

Tachado S D, Gerold P, Schwarz R, Novakovic S, McConville M, Schofield L. Signal transduction in macrophages by glycosylphosphatidylinositols of Plasmodium, Trypanosoma, and *Leishmania*: activation of protein tyrosine kinases and protein kinase C by inositolglycan and diacylglycerol moieties. Proc Natl Acad Sci U S A 1997; (94): 4022-4027.

Terayama K, Oka S, Seiki T, Miki Y, Nakamura A, Kozutsumi Y, Takio K, Kawasaki T. Cloning and functional expression of a novel glucuronyltransferase involved in the biosynthesis of the carbohydrate epitope HNK-1. Proc Natl Acad Sci U S A 1997; (94): 6093-6098.

Theodos C M, Ribeiro J M, Titus R G. Analysis of enhancing effect of sand fly saliva on *Leishmania* infection in mice. Infect Immun 1991; (59): 1592-1598.

Turco S J, Descoteaux A. The lipophosphoglycan of *Leishmania* parasites. Annu Rev Microbiol 1992; (46): 65-94.

Turco S J. The lipophosphoglycan of *Leishmania*. Subcell Biochem 1992; (18): 73-97.

Turco S J, Spath G F, Beverley S M. Is lipophosphoglycan a virulence factor? A surprising diversity between *Leishmania* species. Trends Parasitol 2001; (17): 223-226.

Turnquist R L, Gillett T A, Hansen R G. Uridine diphosphate glucose pyrophosphorylase. Crystallization and properties of the enzyme from rabbit liver and species comparisons. J Biol Chem 1974; (249): 7695-7700.

Turnquist R L, Turnquist M M, Bachmann R C, Hansen R G. Uridine diphosphate glucose pyrophosphorylase: differential heat inactivation and further characterization of human liver enzyme. Biochim Biophys Acta 1974; (364): 59-67.

Wang-Gillam A, Pastuszak I, Elbein A D. A 17-amino acid insert changes UDP-N-acetylhexosamine pyrophosphorylase specificity from UDP-GalNAc to UDP-GlcNAc. J Biol Chem 1998; (273): 27055-27057.

The Wellcome Trust Sanger Institute, http://www.sanger.ac.uk

World Health Organisation, http://www.who.int/health-topics/*Leishmania*sis.htm

Zhang K, Barron T, Turco S J, Beverley S M. The LPG1 gene family of *Leishmania major*. Mol Biochem Parasitol 2004; (136): 11-23.

Zufferey R, Allen S, Barron T, Sullivan D R, Denny P W, Almeida I C, Smith D F, Turco S J, Ferguson M A, Beverley S M. Ether phospholipids and glycosylinositolphospholipids are not required for amastigote virulence or for inhibition of macrophage activation by *Leishmania major*. J Biol Chem 2003; (278): 44708-44718.

6 Abbreviations

α–	Anti-
ABTS	2,2'-Azino-di-(3-ethylenbethiazolin-sulphate)
AP	Alkaline phosphatase
APS	Ammonium peroxidisulphate
ATP	Adenosine triphosphate
BCA	Bichionic acid
BCIP	5-Brom-4-chlor-3-indolyl-phosphate
bp	Base pairs
BSA	Bovine serum albumin
CMP	Cytidine 5'-monophosphat
Da	Dalton
DMEM	'Dulbecco's Modified Eagle's medium'
DMF	Dimethylformamide
DMSO	Dimethylsulfoxide
DNA	Desoxyribonucleic acid
DTT	Dithiothreito
EDTA	Ethylendiamine-N,N,N',N'-tetraacetic acid
ELISA	Enzyme linked immono sorbant assay
IPTG	Isopropyl-beta-D-thiogalactopyranoside
kb	kilobase
kDa	Kilodalton
L.major/mexicana/donovani	*Leishmania major/mexicana/donovani*
LB	Luria-Bertani
mAb	Monoclonal antibody
NBT	Nitrotetrazolium-blue chloride
NCAM	Neural cell adhesion molelcule
Neu5Ac	5-*N*-acetyl-neuraminic acid
OD	Optical density
PAGE	Polyacrylamide gelelectrophoresis
PBS	Phosphate buffered saline
PCR	Polymerase chain reaction
PMSF	Phenylmethansulfonylflouride
polySia	Polysialic acid
RT	Room temperature
SDS	Sodium dodecyl-sulphate
TEMED	N,N,N',N'-Tetramethyl-ethylendiamin
TRIS	Tris(hydroxymethyl)-aminomethan)
UDP	Uridin 5'-diphosphate
UDP-gal	UDP-galactose
UDP-glc	UDP-glucose
UDP-glcA	UDP-glucuronic acid
UDP-glcNAc/galNAc	UDP-*N*-acetylglucosmanie/galactosamine
UDP-xyl	UDP-xylose
UGP	UDP-glucose pyrophosphorylase

7 Lebenslauf und Publikationsliste

Name	Anne-Christin Lamerz, geb. Mackensen
Adresse	Aegidiendamm 9 30169 Hannover
E-mail	Lamerz.Anne-Christin@mh-hannover.de
Geburtsdatum, -ort	25.12.1974, Bad Gandersheim
Staatangehörigkeit	Deutsch

Schule

1981-1985	Grundschule Bad Gandersheim
1985-1987	Orientierungsstufe Bad Gandersheim
1987-1994	Roswitha-Gymnasium Bad Gandersheim
Juni 1994	Abitur

Hochschulstudium

1995-2001	Studium der Biochemie an der Universität Hannover
2000/ 2001	Diplomarbeit in der Arbeitsgruppe von Prof. Michael Martin, Abteilung Pharmakologie, Medizinische Hochschule Hannover • „Molekulare Mechanismem der IRAK-Aktivierung: Charakterisierung der Phosphorylierungsschritte auf Aminosäureebene" , Fortsetzung der Arbeit bis 31.12.2001
15.01.2001	Diplom im Fach Biochemie

Promotion

Seit 2002	Promotion in der Arbeitsgruppe von Prof. Rita Gerardy-Schahn, Abteilung Zelluläre Chemie, Zentrum Biochemie, Medizinische Hochschule Hannover

Auslandsaufenthalte

1994-1995	Au pair in Kanada
1998-1999	Studienaufenthalt an der Purdue University, West Lafayette, Indiana, USA, gefördert durch die Fulbright Kommission

Publikationsliste

Wissenschaftliche Veröffentlichungen:

'Sequential autophosphorylation steps in the interleukin-1 receptor-associated kinase-1 regulate its availability as an adapter in interleukin-1 signaling', J Biol Chem. 2004; 279(7):5227-36.**,** Kollewe C*, **Mackensen AC***, Neumann D*, Knop J, Cao P, Li S, Wesche H, Martin MU. (equally contributing first authors)

Posterpräsentationen:

02.11.2000 -04.11.2000
Millenium Meeting der Gesellschaft für Signal Transduktion: Signal Transduction-Receptors, Mediators and Genes, Berlin
Topic: 'Domain mapping of the Interleukin-1 receptor associated kinase IRAK: The death domain is essential for the interaction of IRAK with the receptor complex and IL-1 signaling', Knop J., **Mackensen A.C.**, Neumann, D., Martin, M.U.

26.09.2001-29.09.2001
Annual Meeting of the German Society of Immunology, Dresden
Topic: 'Molecular mechanisms of IRAK-1 activation: Threonin 387 is a critical amino acid in the autophosphorylation of IRAK-1', **Mackensen A.C**., Wesche H., Kollewe C., Martin M.U.

20.09. 2003-24.09.2003
ELSO/GBM Tagung, Dresden
Topic: 'Cloning and Characterisation of a UDP-Glucose Pyrophosphorylase from *Leishmania major',* **Mackensen A.C.**, Bakker H., Routier F, Gerardy-Schahn R

20.09. 2003-24.09.2003
ELSO/GBM Tagung, Dresden
Topic: 'Drosophila Melanogaster: Identification of the sialic acid activating enzyme CMP-*N*-acetylneuramic acid synthetase',* Ritz V., **Mackensen A.C.**, Weinhold B., Gerardy-Schahn R., Münster-Kühnel A.K.

17.11.2004-20.11.2004
Joint Meeting of the Society for Glycobiology and the Japanese Society of Carbohydrate Research, Honolulu
Topic: 'Leishmania major UDP-galactopyranose mutase: characterisation and validation of a potential drug target, Kleczka B., **Lamerz A.C.**, Bakker H., Wiese M., Gerardy-Schahn R., Routier F.H.

8 Erklärung

Hiermit versichere ich an Eides statt, dass ich die vorliegende Dissertation selbständig und nur unter Verwendung der angegebenen Quellen und Hilfsmittel angefertigt habe. Außerdem versichere ich an Eides statt, dass die zugrunde liegenden Ergebnisse nicht für eine andere Prüfungsarbeit verwendet worden sind.

Hannover, 16.12.2004

Danksagung